SUPPLEMENTARY MATERIAL

Achyranbidens A - C: Three new compounds from *Achyranthes bidentata* Blume

Nguyen Thi Mai[a], Bui Thi Mai Anh[a], Vu Thi Xuan[a], Hoang Thi Tuyet Lan[a,*], Duong Thi Hai Yen[b], Bui Huu Tai[b,c], Nguyen Xuan Nhiem[b,c], and Phan Van Kiem[b,c*]

[a]*Faculty of Basic Sciences, University of Transport and Communications, Cau Giay, Lang Thuong, Dong Da, Hanoi, Vietnam*

[b]*Department of Structural Research, Institute of Marine Biochemistry, Vietnam Academy of Science and Technology, 18 Hoang Quoc Viet, Cau Giay, Hanoi, Vietnam*

[c]*Faculty of Chemistry, Graduate University of Science and Technology, Vietnam Academy of Science and Technology, 18 Hoang Quoc Viet, Cau Giay, Hanoi, Vietnam*

*Corresponding authors:

Phan Van Kiem, Prof. Ph.D.

Department of Structural Research, Institute of Marine Biochemistry, Vietnam Academy of Science and Technology, 18 Hoang Quoc Viet, Cau Giay, Hanoi, Vietnam

Tel.: +84-4-3791-7053 Fax: +84-4-3791-7054 E-mail: phankiem@yahoo.com

Hoang Thi Tuyet Lan, Prof. Ph.D.

Faculty of Basic Sciences, University of Transport and Communications, Cau Giay, Lang Thuong, Dong Da, Hanoi, Vietnam

Tel.: +84-9-1261-2167 E-mail: lanhtt@utc.edu.vn

ABSTRACT

Phytochemical study on the roots of *Achyranthes bidentata* Blume led to the isolation of sixteen compounds including three new ones (**1**-**3**). Their chemical structures were determined as oleanolic acid 28-*O*-*β*-D-glucopyranoside-3-*O*-[*β*-D-glucopyranosyl-(1→3)-*β*-D-galactopyranoside) (**1**), methyl (8*Z*,11*Z*)-5,6,7-trihydroxytetradeca-8,11-dienoate (**2**), methyl (6*E*,11*Z*)-5,8,9-trihydroxytetradeca-6,11-dienoate (**3**), fulgidic acid (**4**), (9*E*,11*E*)-13-oxooctadeca-9,11-dienoic acid (**5**), (9*Z*,11*E*,15*Z*)-13-hydroxyoctadeca-9,11,15-trienoic acid (**6**)**,** oleanolic acid 28-*O*-*β*-D-glucopyranoside-3-*O*-*α*-L-rhamnopyranosyl-(1→4)-*β*-D-glucuronopyranoside (**7**), oleanolic acid 28-*O*-*β*-D-glucopyranoside-3-*O*-*β*-D-glucopyranosyl-(1→2)-[*α*-L-rhamnopyranosyl-(1→3)]-*β*-D-glucuronopyranoside (**8**), oleanolic acid 3-*O*-*β*-D-glucopyranosyl-(1→2)-[*α*-L-rhamnopyranosyl-(1→3)]-*β*-D-glucuronopyranoside (**9**), oleanolic acid 3-*O*-*α*-L-rhamnopyranosyl-(1→3)-*β*-D-glucuronopyranoside (**10**), blumenol C glucoside (**11**), citroside A (**12**), 6*S*,9*S*-roseoside (**13**), ginsenoside Rg1 (**14**), 20-hydroxyecdysone (**15**), and benzyl *α*-L-rhamnopyranosyl-(1→6)]-*β*-D-glucopyranoside (**16**) by spectroscopic analysis. Compounds **1**, **7** and **11**-**16** inhibited NO production in LPS-activated RAW264.7 cells with IC_{50} values in the range from 28.03 to 54.23 µM (positive control, L-NMMA: IC_{50} = 35.52 µM). Compounds **14** and **15** showed anti *α*-glucosidase activity with IC_{50} values of 176.24 and 156.92 µM, respectively, compared with the positive control, acarbose, IC_{50} = 160.99 µM.

Keywords: *Achyranthes bidentata*, Amaranthaceae, achyranbiden A, achyranbiden B, achyranbiden C, NO production inhibitory activity, antidiabetic activity.

Content

Experimental

General

The IR spectra were recorded on a Spectrum Two FT-IR spectrometer. The optical rotations were measured on a Jasco P2000-polarimeter. The HR-ESI-MS was measured on an Agilent 6530 Accurate Mass Q-TOF LC/MS. The NMR spectra were recorded on a Bruker 600 MHz spectrometer. The preparative HPLC were run on an Agilent-1100 system including quaternary pump, DAD detector, autosampler, and preparative HPLC column YMC J'sphere ODS-H80 (4 µm, 20 × 250 mm). Isocratic mobile phase with the flow rate of 3 mL/min was used in pre-HPLC. The compound was monitored at wavelengths of 205, 230, 254, and 280 nm. Flash column chromatography was run using silica gel, reversed phase C-18, and diaion HP-20 resins as stationary phase. Thin layer chromatography was carried out on pre-coated silica gel 60 F_{254} and RP-18 F_{254S} plates. The spots were detected by spraying with aqueous solution of H_2SO_4 5% followed by heating with a heat gun.

Nitric oxide assay

The RAW264.7 cells were received from Perugia University, Italy and were maintained in DMEM containing 10% FBS, 2 mM L-glutamine, 10 mM HEPES and 1 mM sodium pyruvate. The cells were dispensed into a 96-well plate (2×10^5 cells/well) and incubated at 37°C in a humidified atmosphere (5% CO_2 and 95% air). After 24 h incubation, the culture medium was replaced with DMEM without FBS and continuously incubated for 3 h. The cells were treated with either compounds or vehicle solution and then stimulated with LPS (1 µg/mL) in the next 2 h. After an additional 24 h incubation, the cell culture medium (100 µL) was mixed with an equal volume of Griess reagent (Promega, Fitchburg, WI, USA) for 10 min and the absorbance was read at 540 nm. The amount of nitrite, an indicator of NO production in the medium, was obtained from a standard curve, which was constructed by $NaNO_2$ serial dilution. N^G-monomethyl-L-arginine acetate salt (L-NMMA) was used as a positive control. Cell viability was determined by adding 10 µL MTT solution (5 mg/mL) and incubating for 4 h. Formazan crystals were dissolved in 50 µL of DMSO. Absorbance was read at 540 nm and compared with the vehicle group. Experiments were performed in triplicate and data are expressed as the mean ± standard deviation. Statistical analysis was performed using GraphPad Prism software.

References:

Bernardes NR, Heggdorne-Araújo M, Borges IF, Almeida FM, Amaral EP, Lasunskaia EB, Muzitano MF, Oliveira DB. 2014. Nitric oxide production, inhibitory, antioxidant and

antimycobacterial activities of the fruits extract and flavonoid content of *Schinus terebinthifolius*. Rev. Bras. Farmacogn. 24(6):644-650.

Cheenpracha S, Park EJ, Rostama B, Pezzuto JM, Chang LC. 2010. Inhibition of nitric oxide (NO) production in lipopolysaccharide (LPS)-activated murine macrophage RAW 264.7 cells by the norsesterterpene peroxide, epimuqubilin A. Marine drugs. 8(3):429-437.

Combet S, Balligand JL, Lameire N, Goffin E, Devuyst O. 2000. A specific method for measurement of nitric oxide synthase enzymatic activity in peritoneal biopsies. Kidney Int. 57(1):332-338.

Liao H, Banbury L, Liang H, Wang X, Lu X, Wu J. 2014. Effect of honghua (*Flos Carthami*) on nitric oxide production in RAW 264.7 cells and *α*-glucosidase activity. J. Tradit. Chin. Med. 34(3):362-368.

Tsai PJ, Tsai TH, Yu CH, Ho SC. 2007. Comparison of NO-scavenging and NO-suppressing activities of different herbal teas with those of green tea. Food Chem. 103: 181-187.

α-Glucosidase inhibitory assay

The *α*-glucosidase (G0660-750UN, Sigma-Aldrich, St. Louis, MO) enzyme inhibition assay was performed according to the previously described method.[20] The sample solution (20 µL, dissolved in dimethyl sulfoxide (DMSO) and buffer) and 0.5 U/mL *α*-glucosidase (40 µL) were mixed in 100 µL of 0.1 M phosphate buffer (pH 7.0). After 5 min pre-incubation, 5 mM *p*-nitrophenyl-*α*-D-glucopyranoside solution (40 µL) was added, and the solution was incubated at 37 ^{o}C for 30 min. The absorbance of released 4-nitrophenol was measured at 405 nm by using a microplate reader (Molecular Devices, Sunnyvale, CA).

Reference

Trang DT, Yen DTH, Tai BH, Doan VV, Yen PH, Quang TH, Nhiem NX, Minh CV, Kiem PV, Cuong NT, Anh LT, Hoai NT, Tai BH, Doan VV, Yen PH, Quang TH, Nhiem NX, Minh CV, Kiem PV. 2021. Pregnane glycosides from *Gymnema inodorum* and their α-glucosidase inhibitory activity. Nat Prod Res. 35(13):2157-2163.

Acid hydrolysis and confirmation of monosaccharide

Compound **1** (8.0 mg) was separately dissolved in 1.0 M HCl (dioxane–H_2O, 1:1, v/v, 1.0 mL) and heated to 80 °C in a water bath for 3 h. The acidic solution was dried under N_2 overnight. After extraction with $CHCl_3$, the aqueous layer was dried using N_2 to give aqueous residue. This aqueous residue was separated by silica gel CC eluting with CH_2Cl_2–EtOH (10:1, v/v) and then further fractionated by RP-18 CC using a solvent gradient of EtOH–H_2O (6:4, 7:3, and 8:2, v/v) to give the saccharide. The specific rotations ($[\alpha]_D^{25}$) of sugars were determined after dissolving in H_2O for 24h and compared to the literature (lit): D-glucose (1.5 mg): found +49.0 (*c* 0.1, H_2O), lit +48.0 (Abe et al. 1999); D-galactose (0.9 mg): found +46.5 (*c* 0.1, H_2O), lit 45.0 (Voutquenne-Nazabadioko et al. 2013).

References

Abe F, Okabe H, Yamauchi T, Honda K, Hayashi N. 1999. Pregnane glycosides from *Marsdenia tomentosa*. Chem Pharm Bull. 47(6):869–875.

Voutquenne-Nazabadioko L, Gevrenova R, Borie N, Borie N, Harakat D, Sayagh C, Weng A, Thakur M, Zaharieva M, Henry M. 2013. Triterpenoid saponins from the roots of *Gypsophila trichotoma* Wender. Phytochemistry. 90:114-127.

Table S1. ^{1}H and ^{13}C NMR spectroscopic data for compound **1** in CD_3OD.

Pos.	δ_C	δ_H (mult., *J*, Hz)	Pos.	δ_C	δ_H (mult., *J*, Hz)
1	39.8	0.10 (m)/1.63 (m)	27	26.3	1.18 (s)
2	27.0	1.70 (m)/1.95 (m)	28	178.1	-
3	90.7	3.21 (dd, 12.0, 4.2)	29	33.5	0.93 (s)
4	40.2	-	30	24.0	0.95 (s)
5	57.1	0.78 (d, 11.0)	3-*O*-gal		
(6	19.4	1.41 (m)/1.56 (m)	1′	106.8	4.36 (d, 7.8)
7	34.0	1.33 (m)/1.50 (m)	2′	72.2	3.71 (dd, 9.0, 7.8)
8	40.7	-	3′	84.7	3.62 (dd, 9.0, 3.0)
9	49.0	1.59 (m)	4′	69.6	4.10 (br d, 3.0)
10	37.9	-	5′	75.9	3.53 (m)
11	24.6	1.90 (m)	6′	62.4	3.72*/3.85*
12	123.8	5.27 (t, 3.6)	3′- *O*-glc		
13	144.9	-	1″	105.6	4.57 (d, 7.8)
14	42.9	-	2″	75.4	3.31 (dd, 9.0, 7.8)
15	28.9	1.10 (m)/1.82 (m)	3″	77.7	3.32 (dd, 9.0, 9.0)
16	24.0	1.72 (m)/2.06 (td, 13.5, 3.5)	4″	71.3	3.35 (dd, 9.0, 9.0)
17	48.0	-	5″	77.9	3.37 (m)
18	42.6	2.87 (dd, 13.5, 3.5)	6″	62.3	3.72*/3.85*
19	47.2	1.17 (m)/1.73 (t, 13.5)	28-*O*-glc		
20	31.5	-	1‴	95.7	5.40 (d, 7.8)
21	34.9	1.23 (m)/1.41 (m)	2‴	73.9	3.33 (dd, 9.0, 7.8)
22	33.2	1.63 (m)/1.75 (m)	3‴	78.3	3.42 (dd, 9.0, 9.0)
23	28.4	1.08 (s)	4‴	71.2	3.70 (dd, 9.0, 9.0)
24	16.6	0.86 (s)	5‴	78.7	3.37 (m)
25	16.0	0.98 (s)	6‴	62.4	3.72*/3.85*
26	17.8	0.82 (s)			

Gal: *β*-D-galactopyranosyl, glc: *β*-D-glucopyranosyl, NMR data were assigned by HSQC, HMBC, ^{1}H-^{1}H COSY, NOESY spectra, *overlapped signals.

Table S2. ^{1}H and ^{13}C NMR spectroscopic data for compounds **2** and **3** in $CDCl_3$.

Pos.	δ_C	δ_H **(mult., *J*, Hz)**	δ_C	δ_H **(mult., *J*, Hz)**
1	174.2	-	175.8	-
2	33.7	2.37 (dt, 1.8, 6.6)	34.7	2.36 (t, 7.8)
3	20.9	1.70 (m)/1.78 (m)	22.1	1.69 (m)/1.75 (m)
4	33.8	1.55 (m)/1.64 (m)	37.6	1.57 (m)
5	71.3	3.62 (m)	72.6	4.16 (dd, 6.6, 5.0)
6	75.8	3.30 (br d, 5.0)	136.2	5.84 (dd, 15.6, 5.0)
7	69.4	4.56 (dd, 8.4, 5.0)	131.4	5.76 (dd, 15.6, 6.0)
8	128.4	5.49 (dd, 10.2, 8.4)	75.7	4.01 (dd, 6.0, 5.4)
9	133.5	5.63 (dt, 10.2, 7.2)	75.9	3.53 (m)
10	26.2	2.87 (m)/2.92 (m)	31.6	2.26 (m)/2.31 (m)
11	126.2	5.30 (dt, 10.2, 7.2)	126.4	5.38 (dt, 10.2, 7.0)
12	132.8	5.41 (dt, 10.2, 7.2)	134.4	5.57 (dt, 10.2, 7.0)
13	20.6	2.08 (m)	21.7	2.06 (m)
14	14.2	0.98 (t, 7.2)	14.6	0.98 (t, 7.2)
OCH_3	51.6	3.67 (s)	52.0	3.67 (s)

NMR data were assigned by HSQC, HMBC, ^{1}H-^{1}H COSY, NOESY spectra

Table S3. Inhibitory activity of compounds **1-16** on NO production in the LPS-activated RAW264.7 cells

Compounds	IC_{50} (μM)	Cell viability (%)
1	42.84 ± 3.17	97.64
2	> 100	100.00
3	> 100	99.34
4	> 100	95.45
5	> 100	98.15
6	> 100	97.36
7	42.25 ± 3.32	91.44
8	> 100	86.34
9	> 100	100.00
10	> 100	97.23
11	39.70 ± 2.68	96.97
12	33.54 ± 2.47	98.65
13	29.28 ± 2.89	91.66
14	54.23 ± 3.48	97.36
15	28.37 ± 2.13	90.83
16	28.03 ± 2.20	96.04
L-NMMA[a]	35.52 ± 2.98	100.00

[a)]Positive control. Results are presented as the mean values ± SD obtained from three independent.

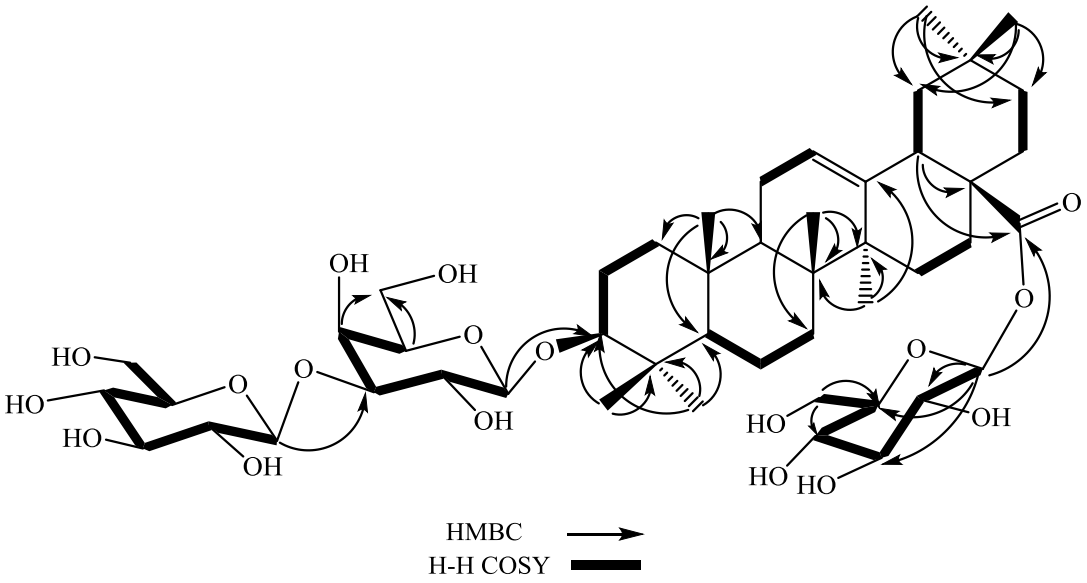

Figure S1. Important HMBC and COSY correlations of compound **1**

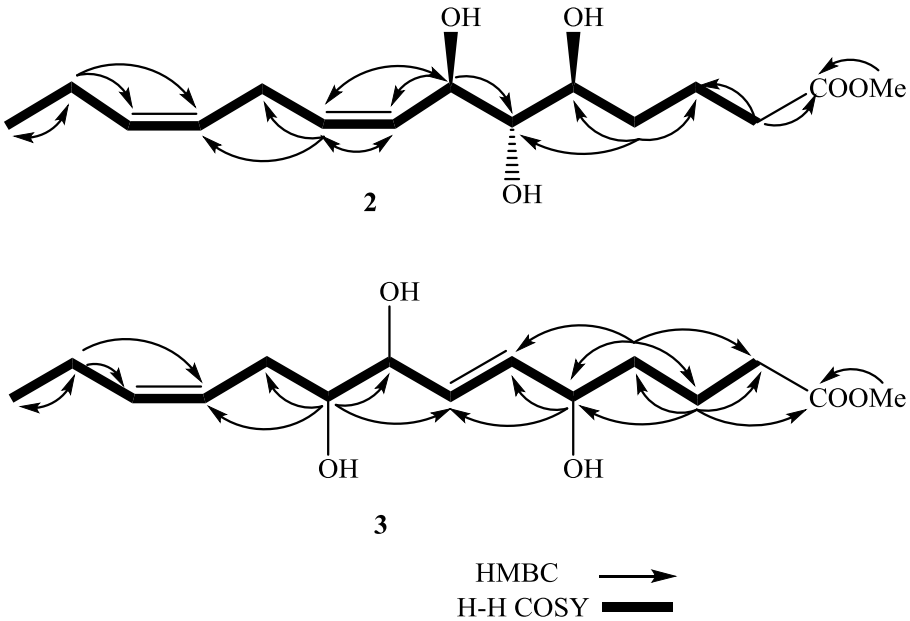

Figure S2. Important HMBC and COSY correlations of compounds **2** and **3**

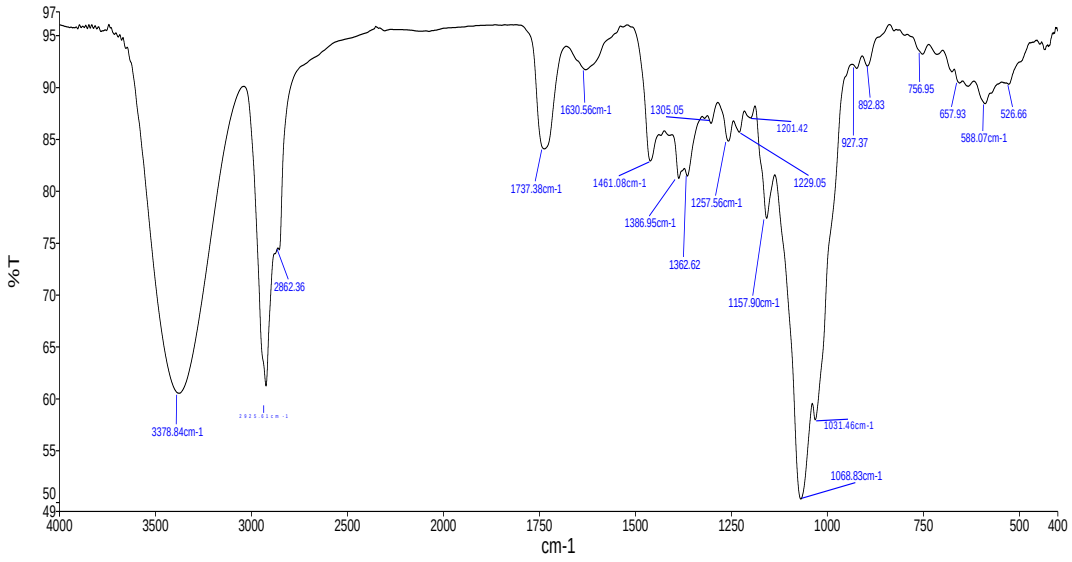

Figure S3. IR spectrum of compound **1**

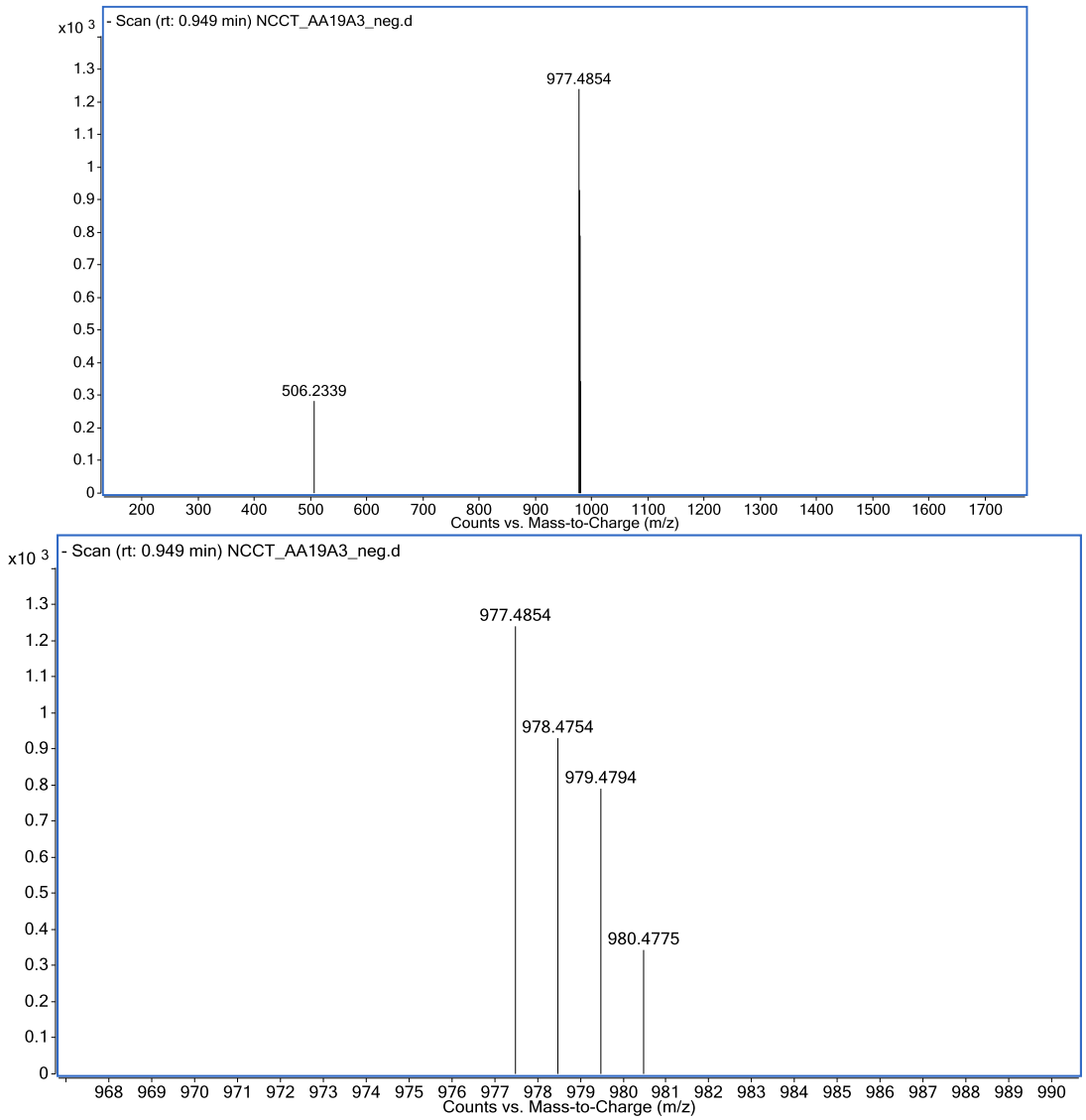

Figure S4. HR-ESI-MS of compound **1**

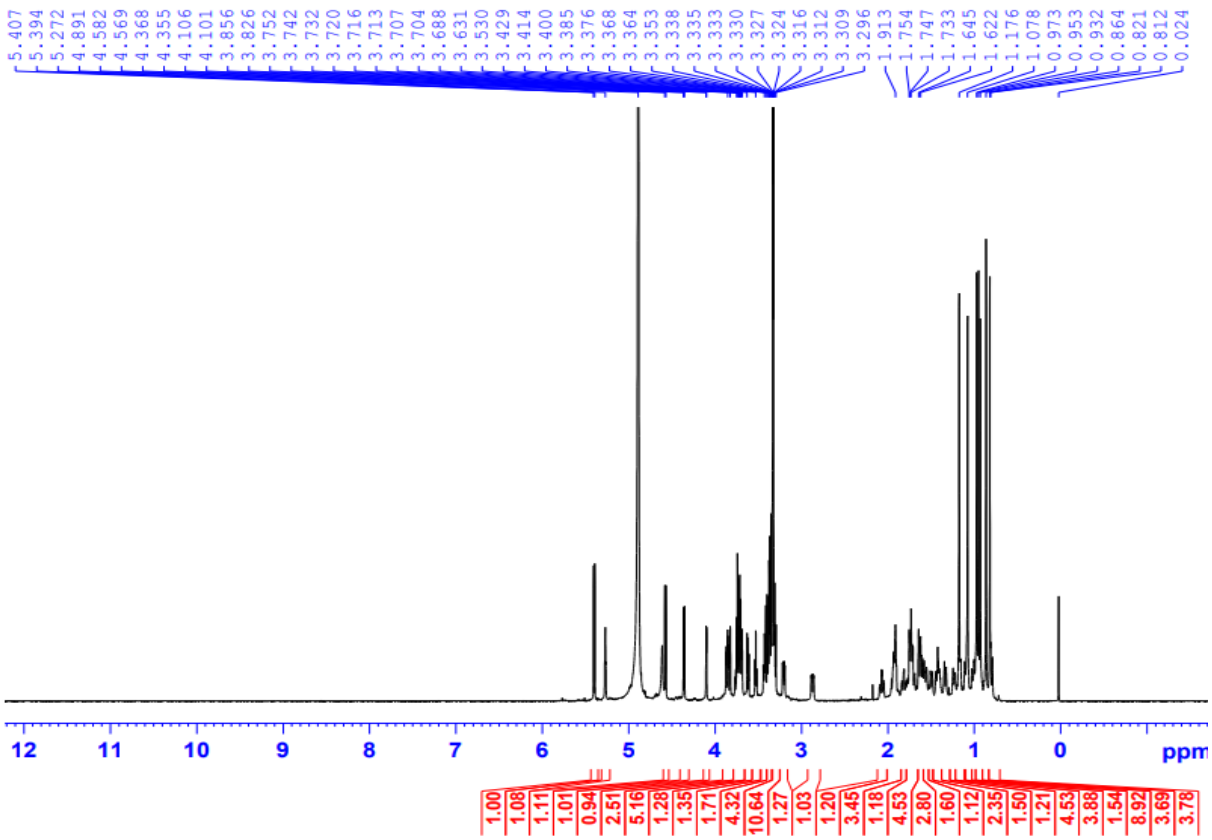

Figure S5. ^{1}H-NMR spectrum of compound **1**

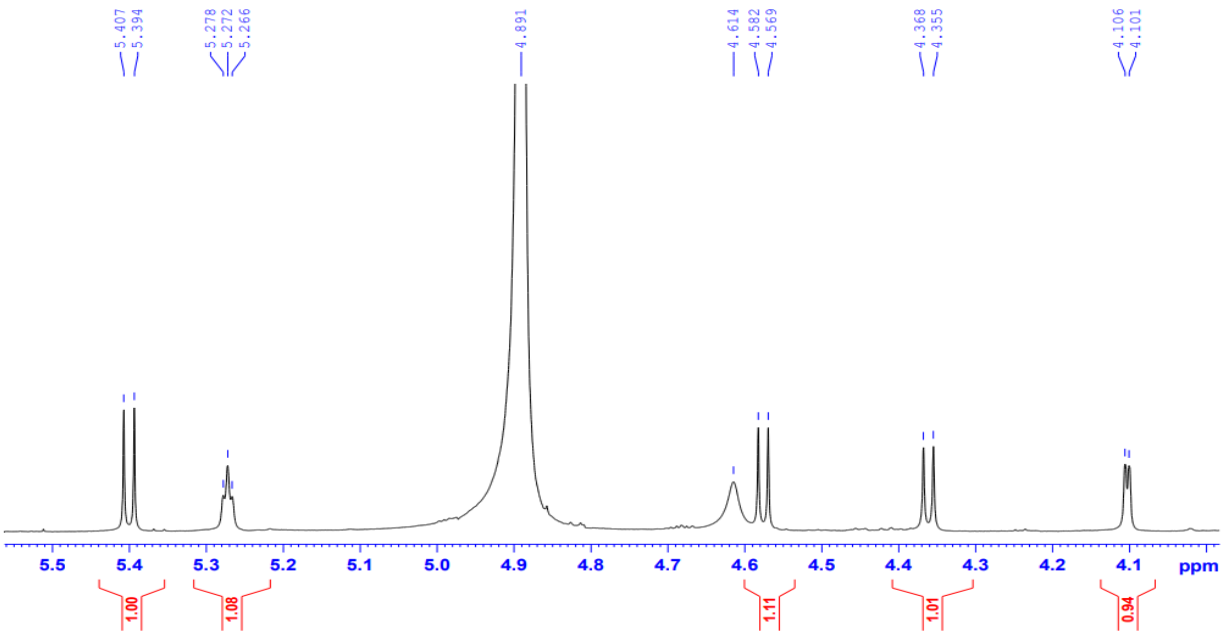

Figure S6. Extended ^{1}H-NMR spectrum of compound **1**

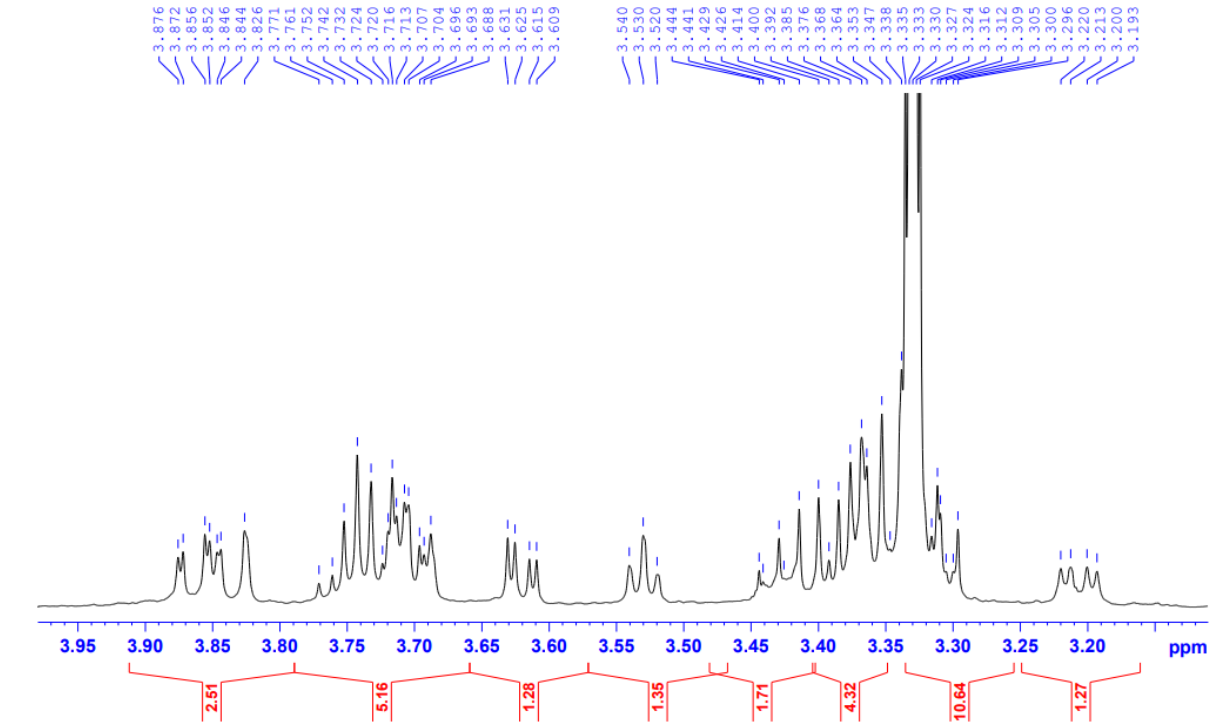

Figure S7. Extended [1]H-NMR spectrum of compound **1**

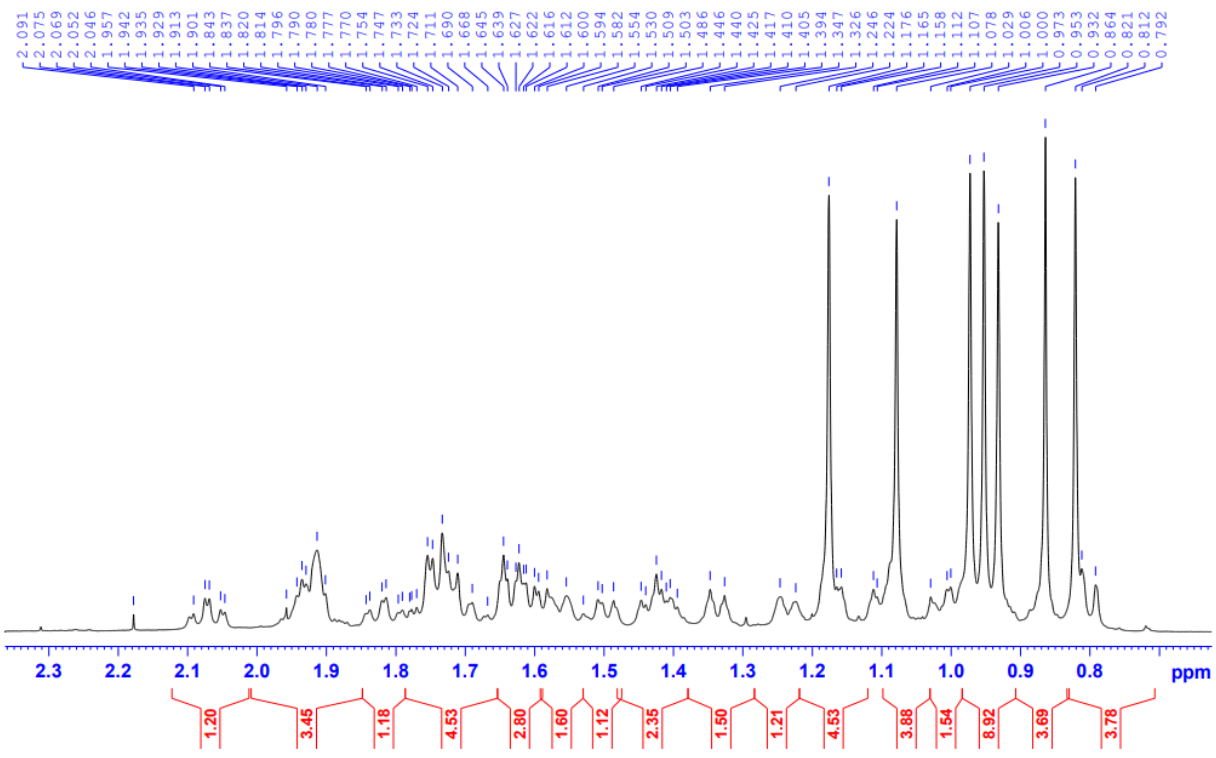

Figure S8. Extended [1]H-NMR spectrum of compound **1**

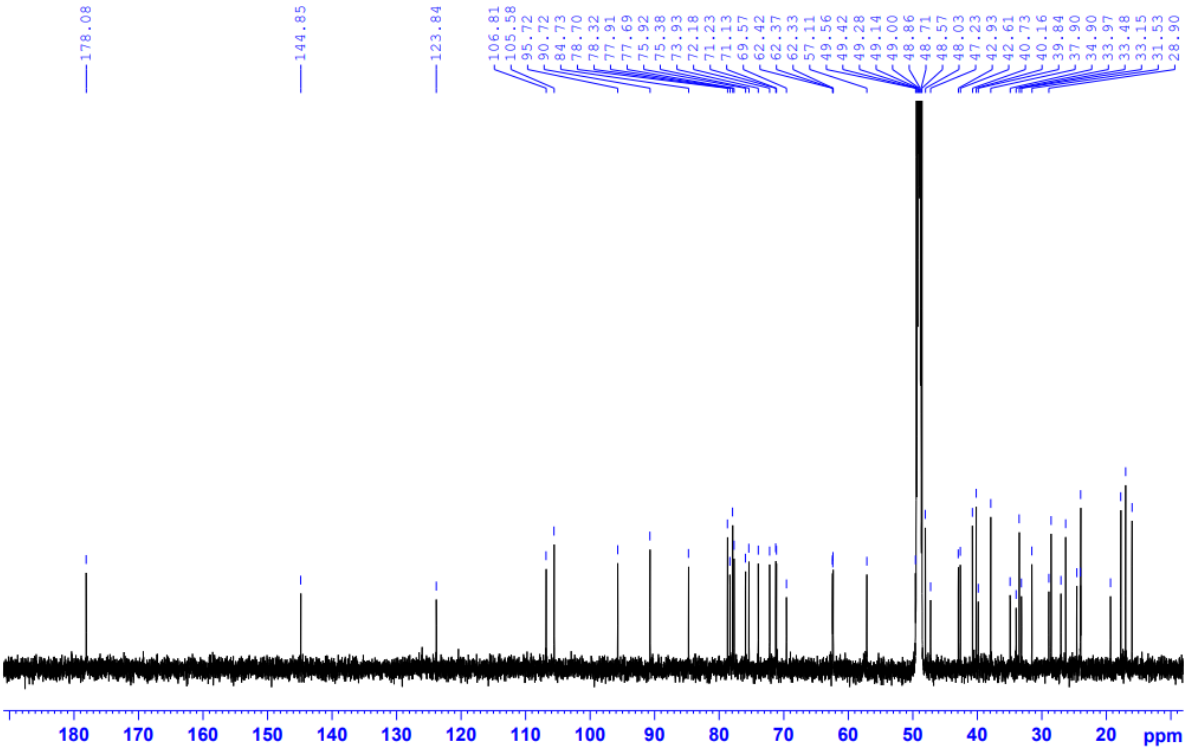

Figure S9. ^{13}C-NMR spectrum of compound **1**

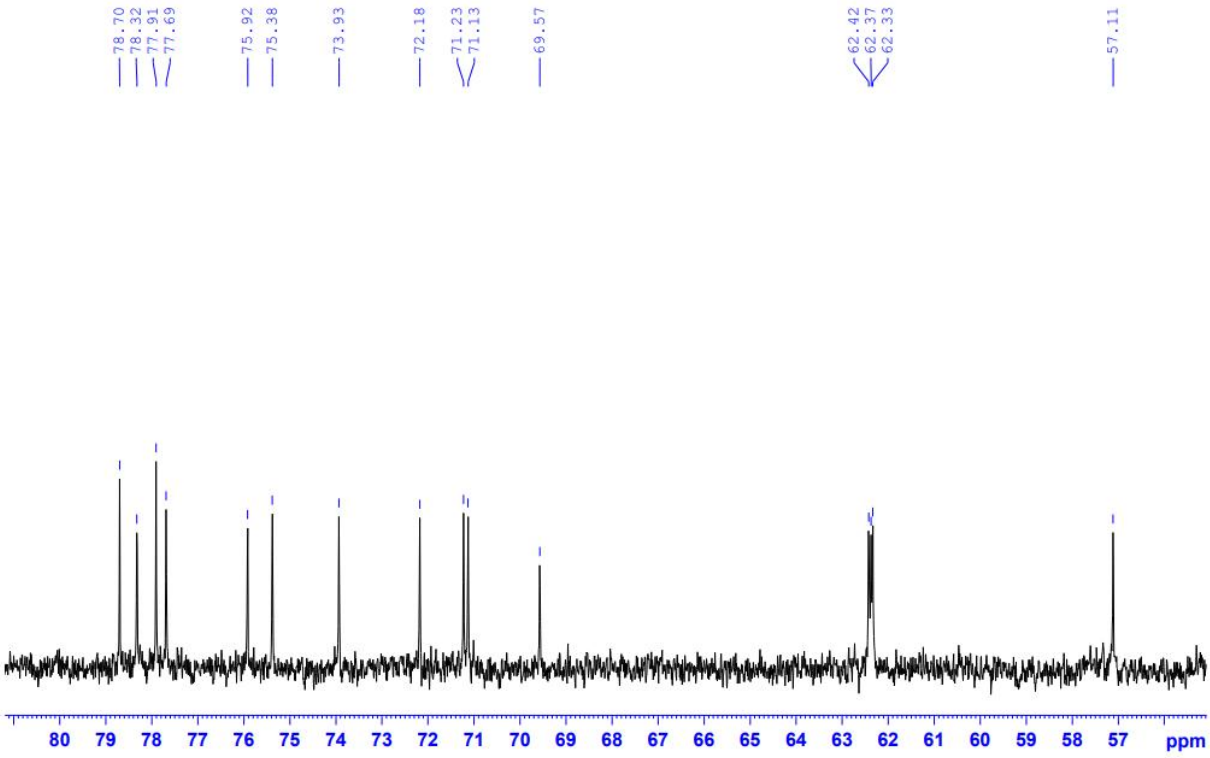

Figure S10 Extended ^{13}C-NMR spectrum of compound **1**

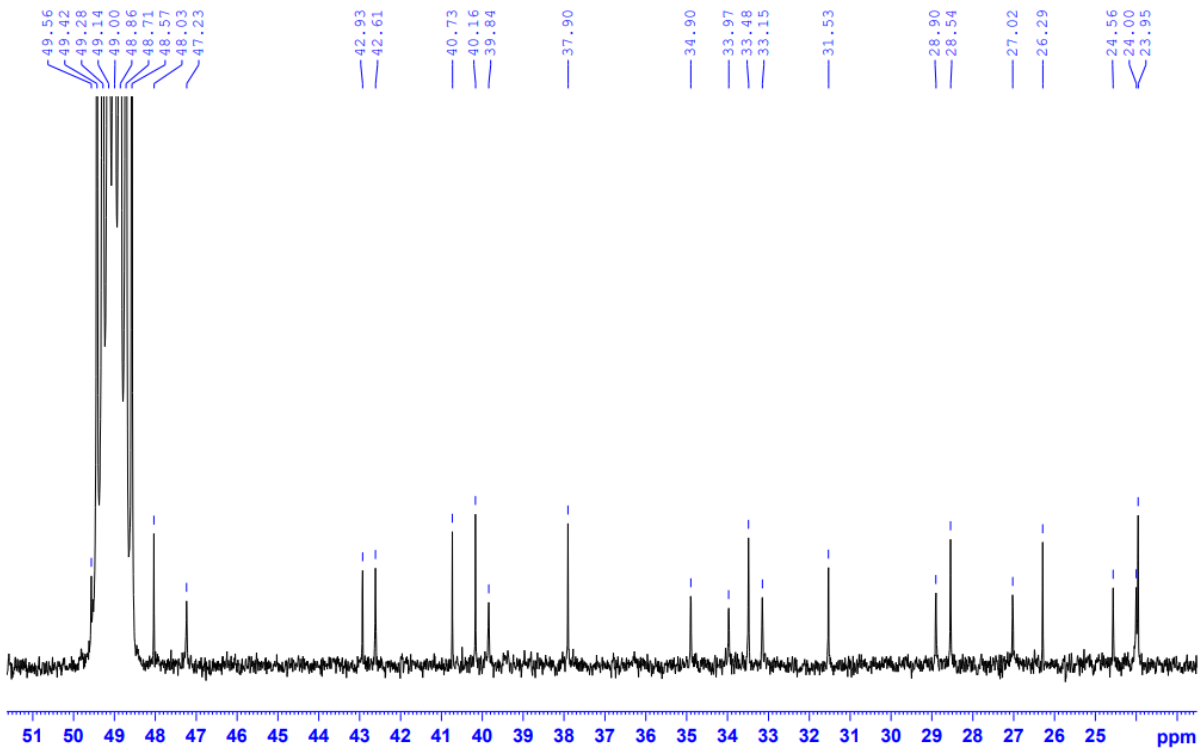

Figure S11. Extended ^{13}C-NMR spectrum of compound **1**

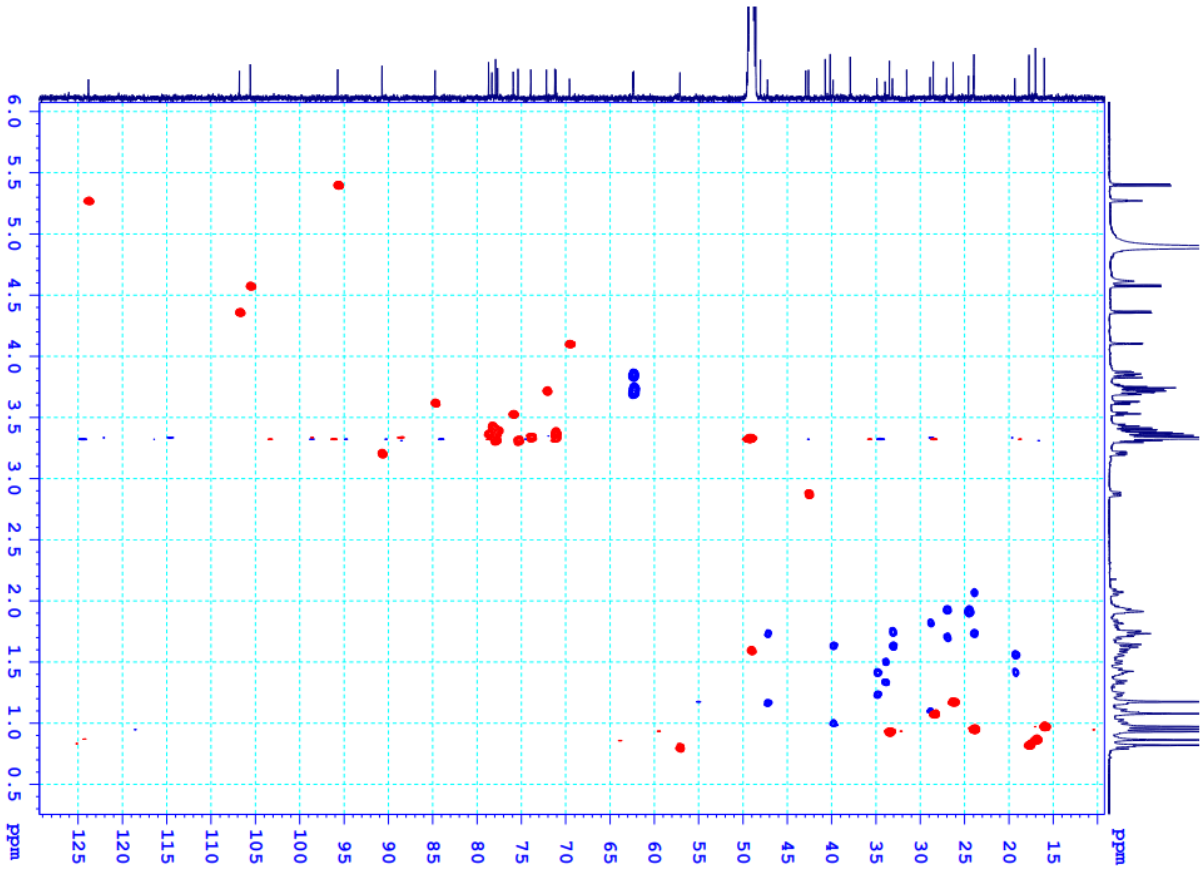

Figure S12. HSQC spectrum of compound **1**

c

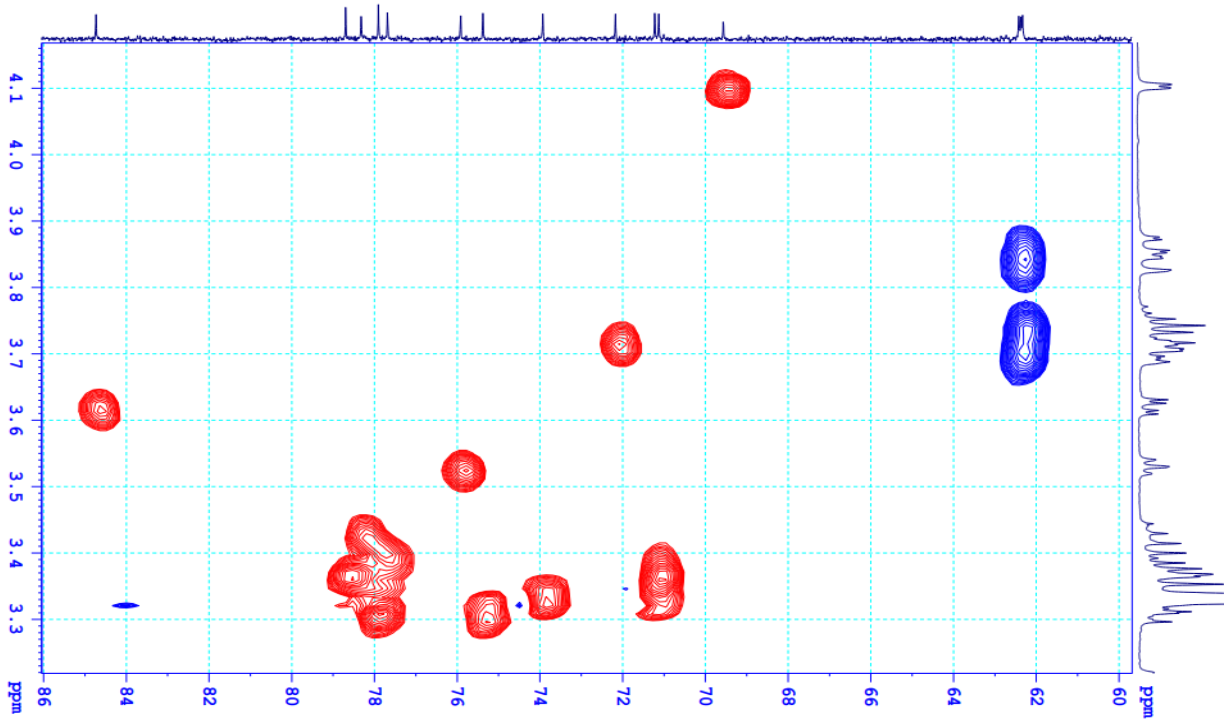

Figure S13. Extended HSQC spectrum of compound **1**

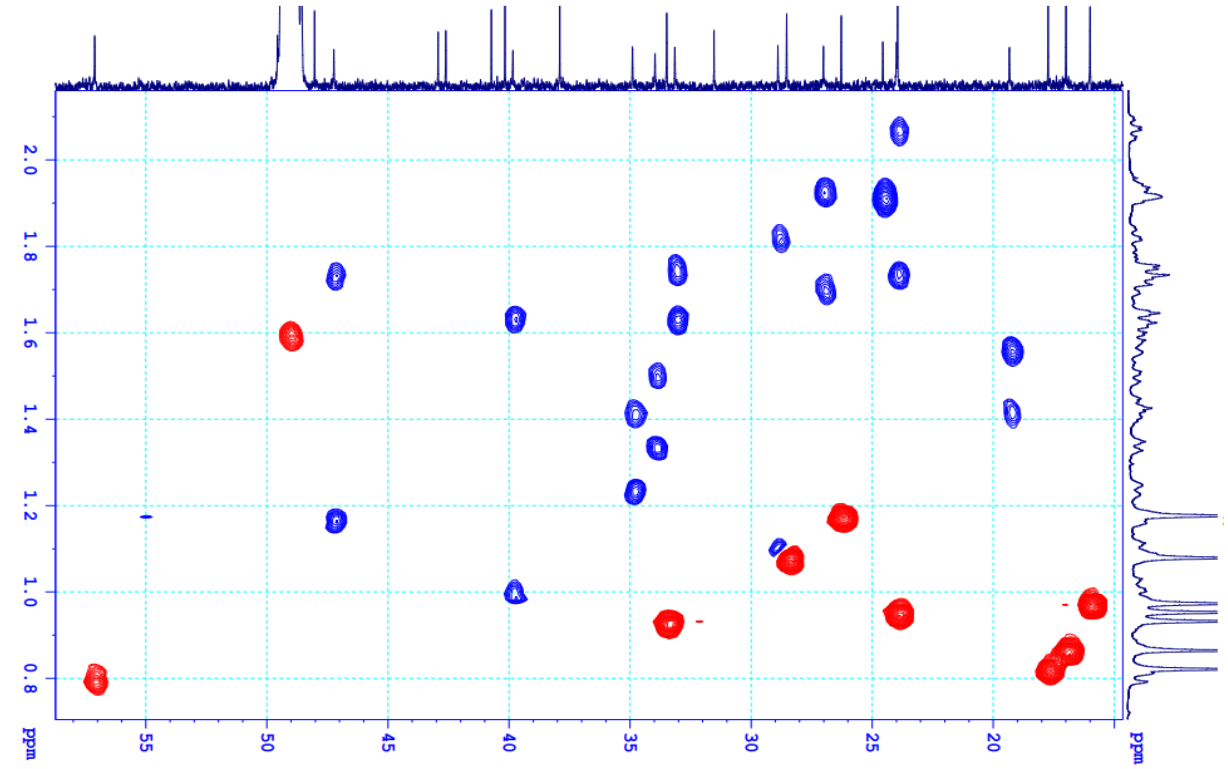

Figure S14. Extended HSQC spectrum of compound **1**

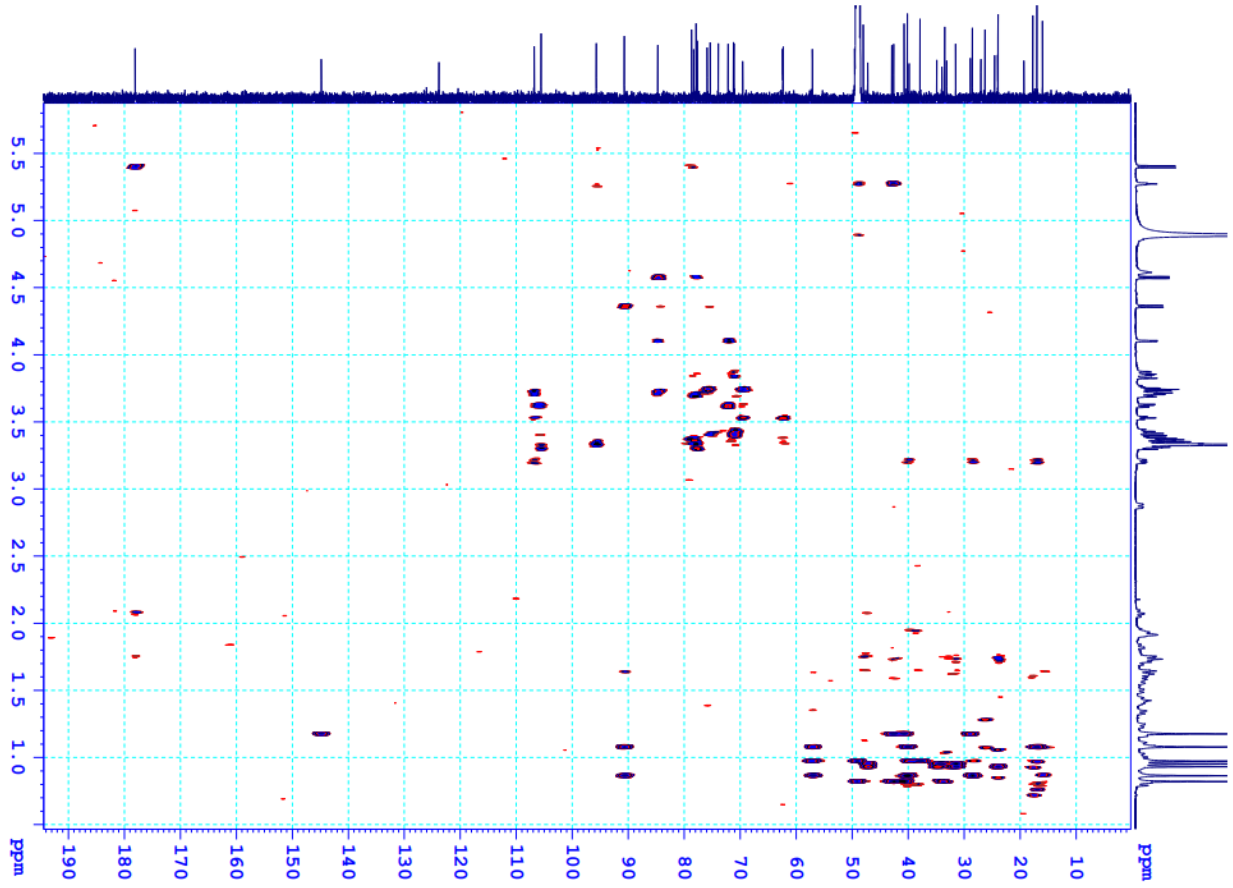

Figure S15. HMBC spectrum of compound **1**

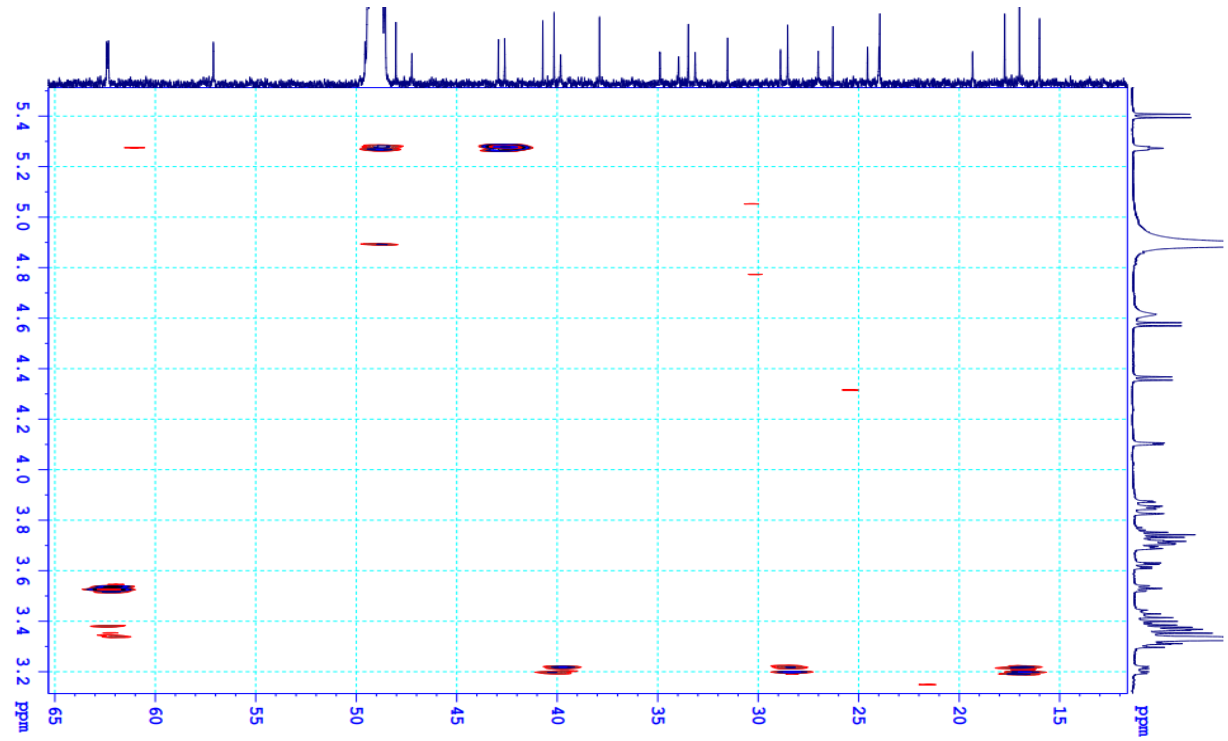

Figure S16. Extended HMBC spectrum of compound **1**

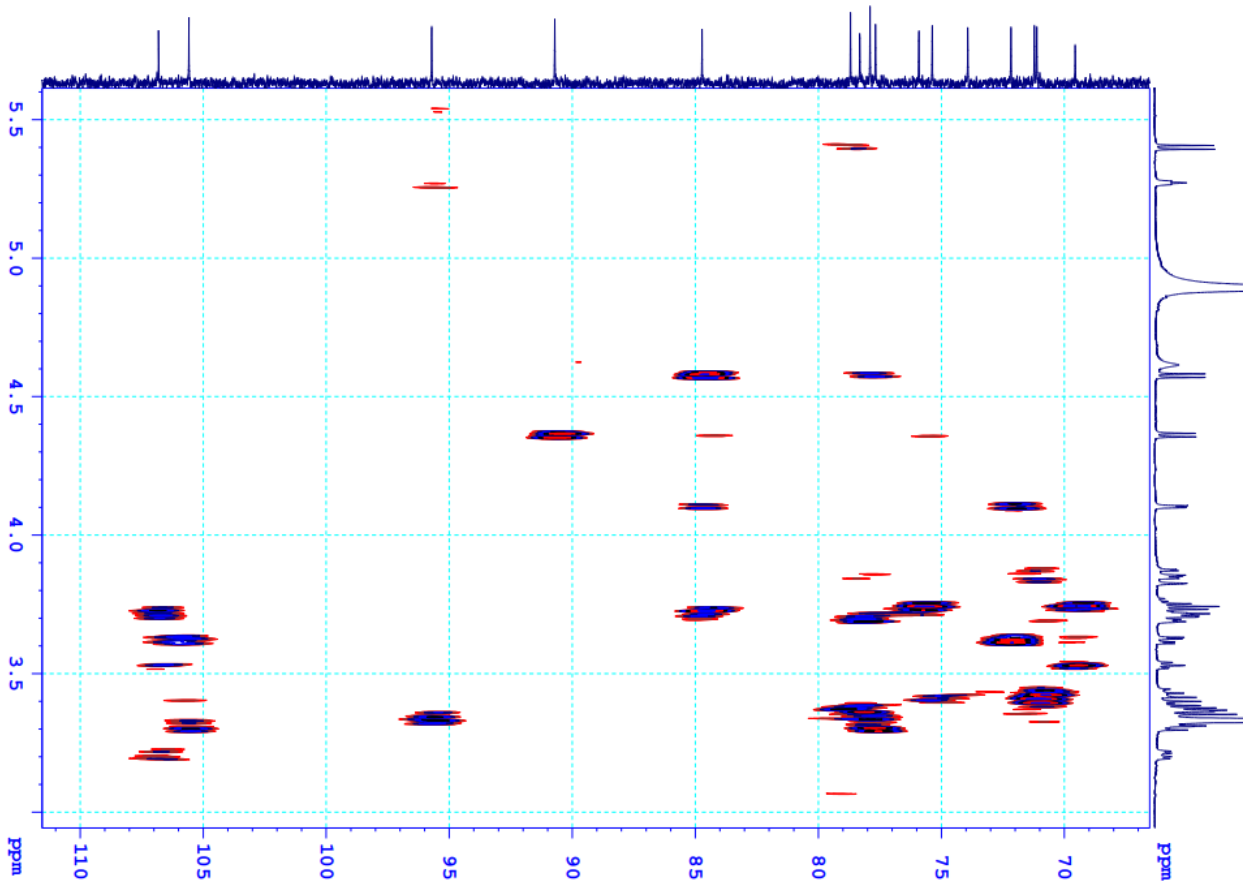

Figure S17. Extended HMBC spectrum of compound **1**

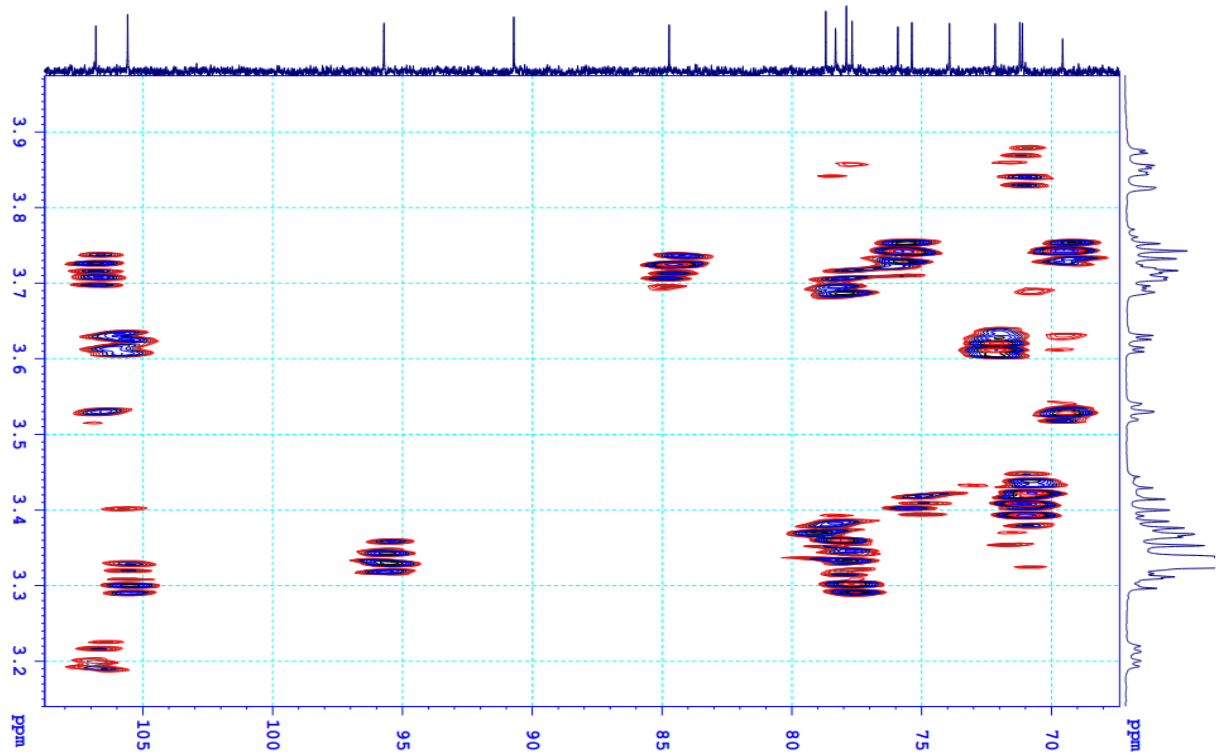

Figure S18. Extended HMBC spectrum of compound **1**

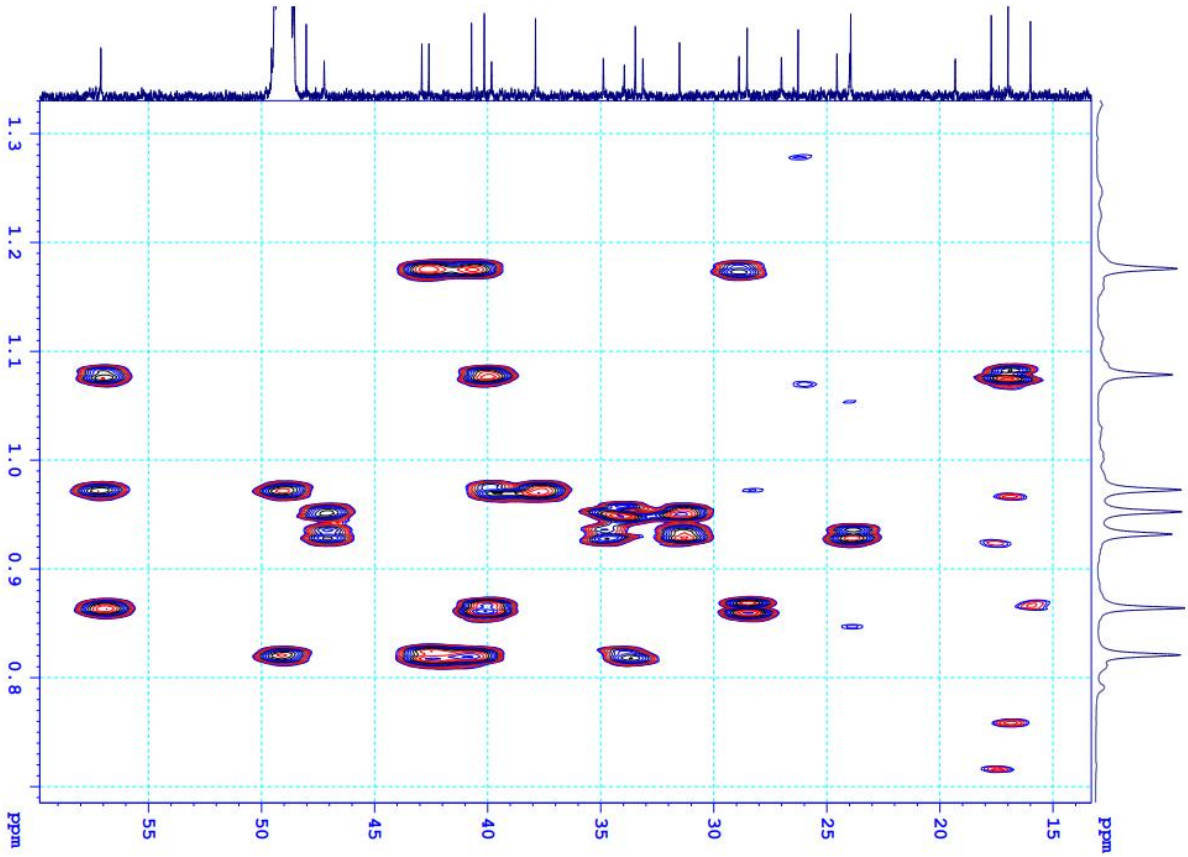

Figure S19. Extended HMBC spectrum of compound **1**

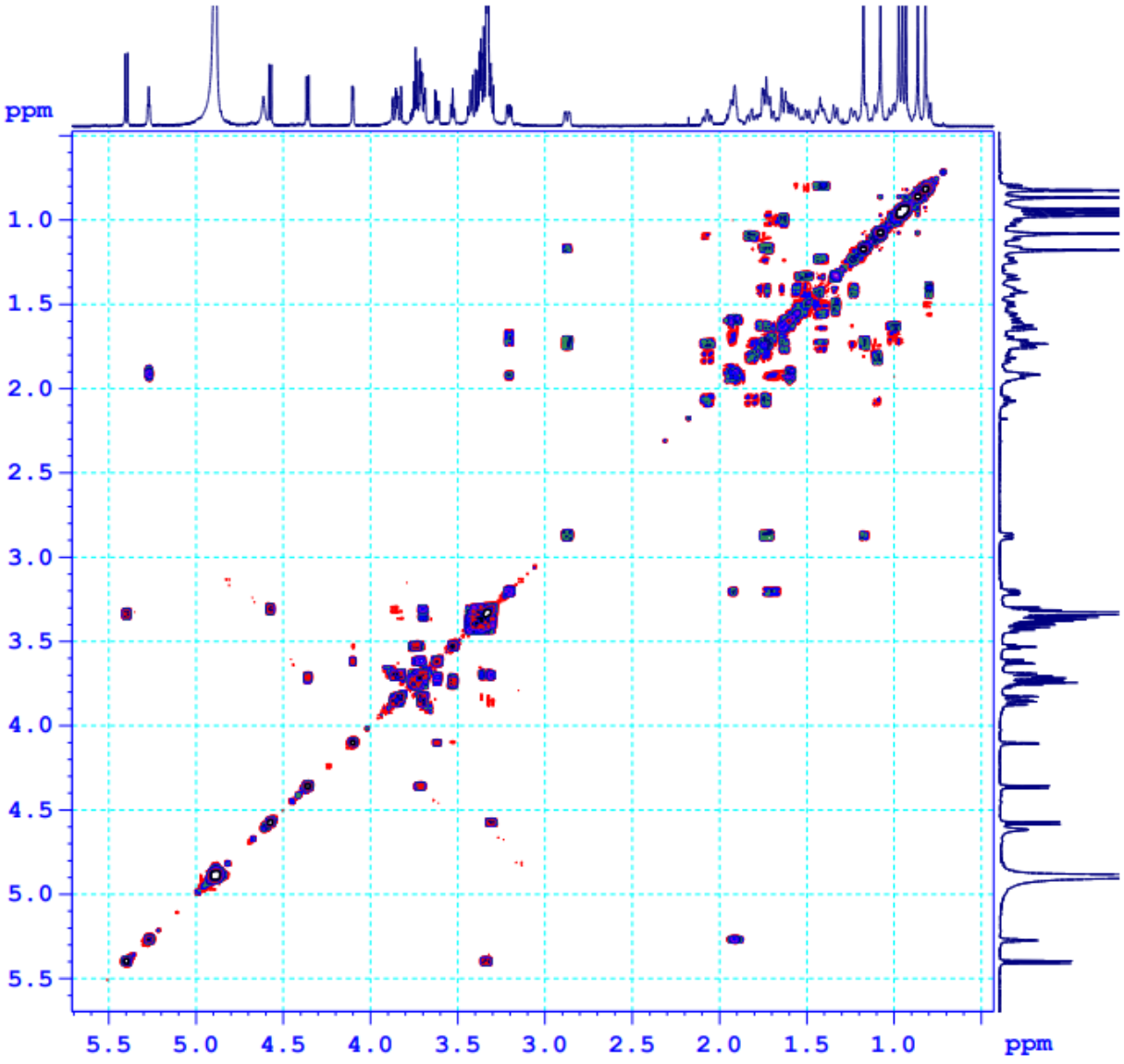

Figure S20. ^{1}H-^{1}H COSY spectrum of compound **1**

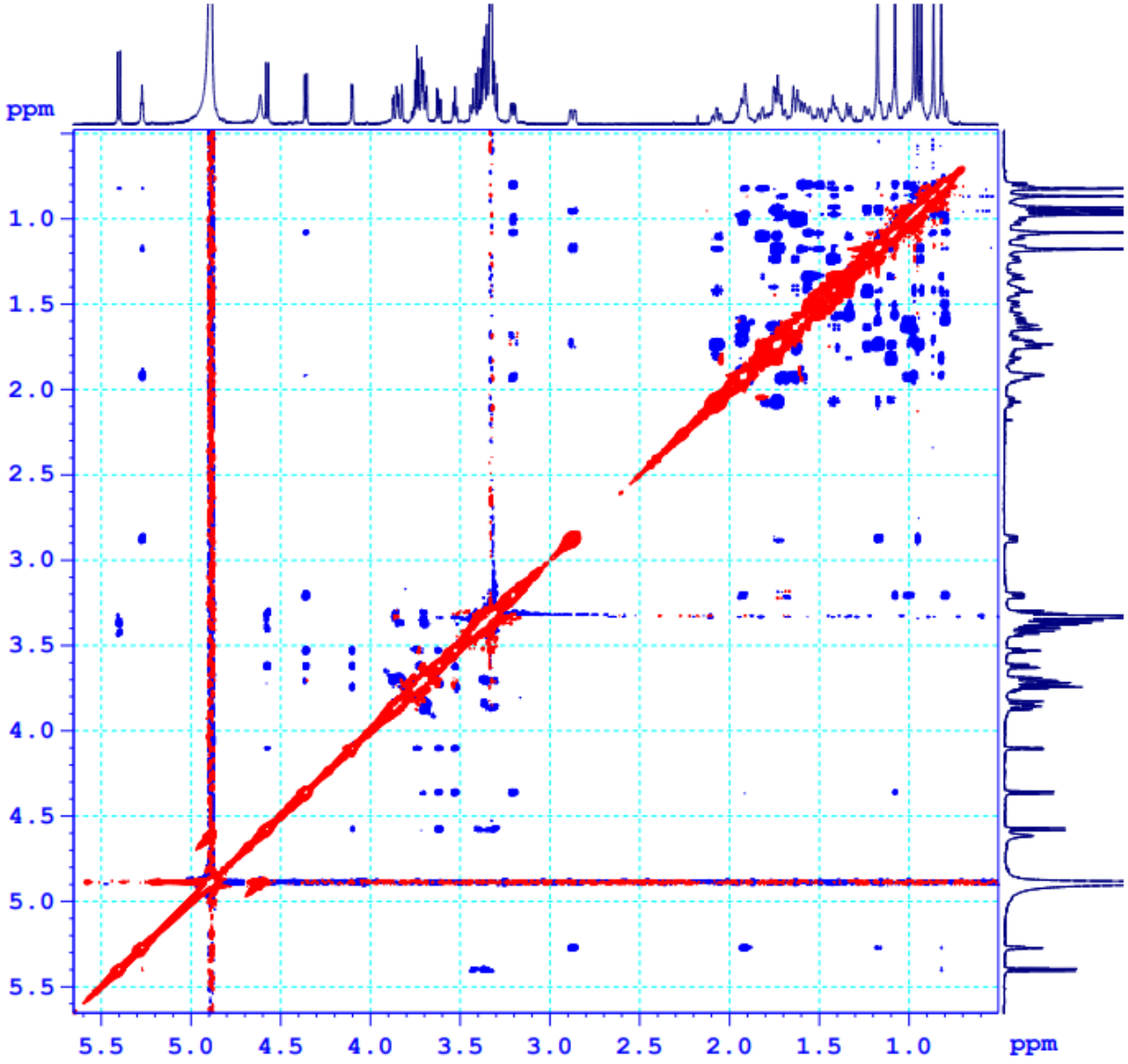

Figure S21. NOESY spectrum of compound **1**

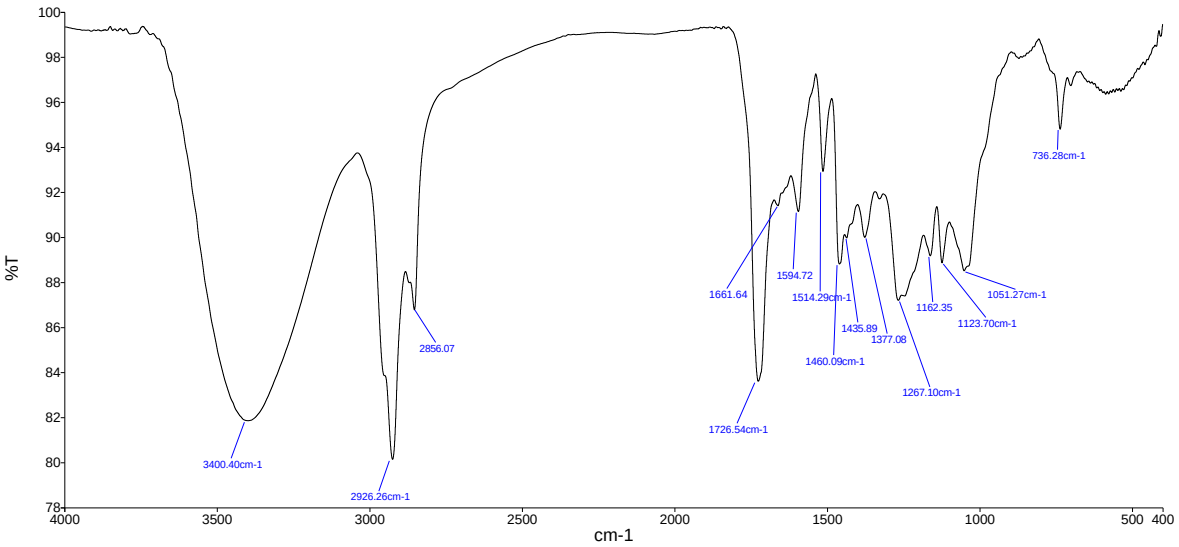

Figure S22. IR spectrum of compound **2**

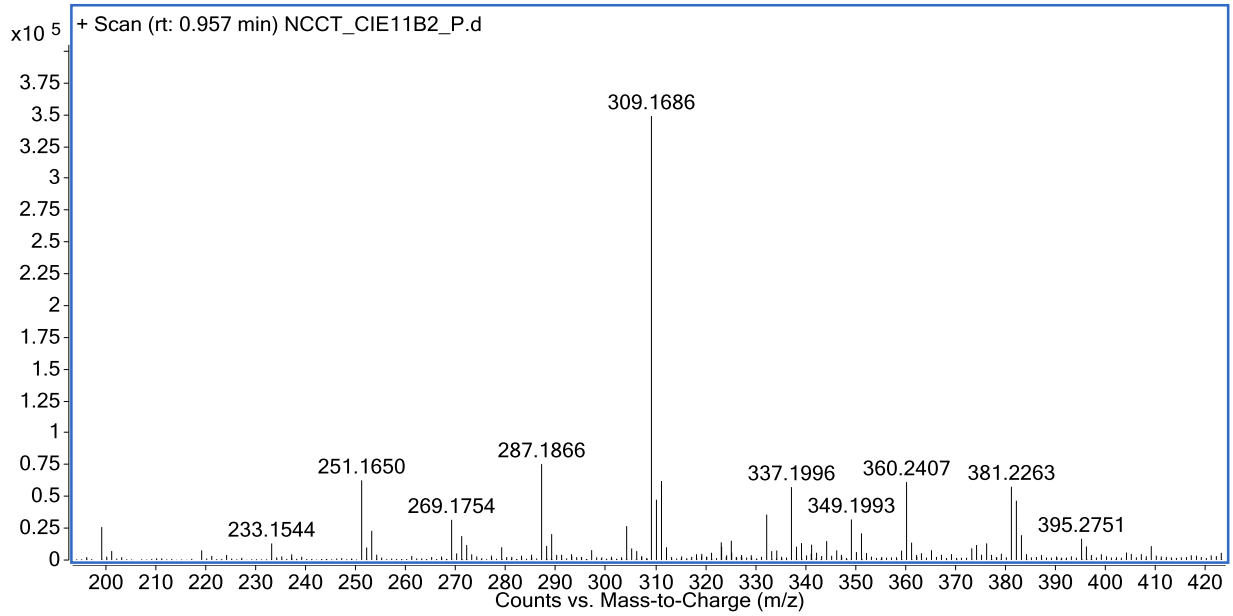

Figure S23. HR-ESI-MS of compound **2**

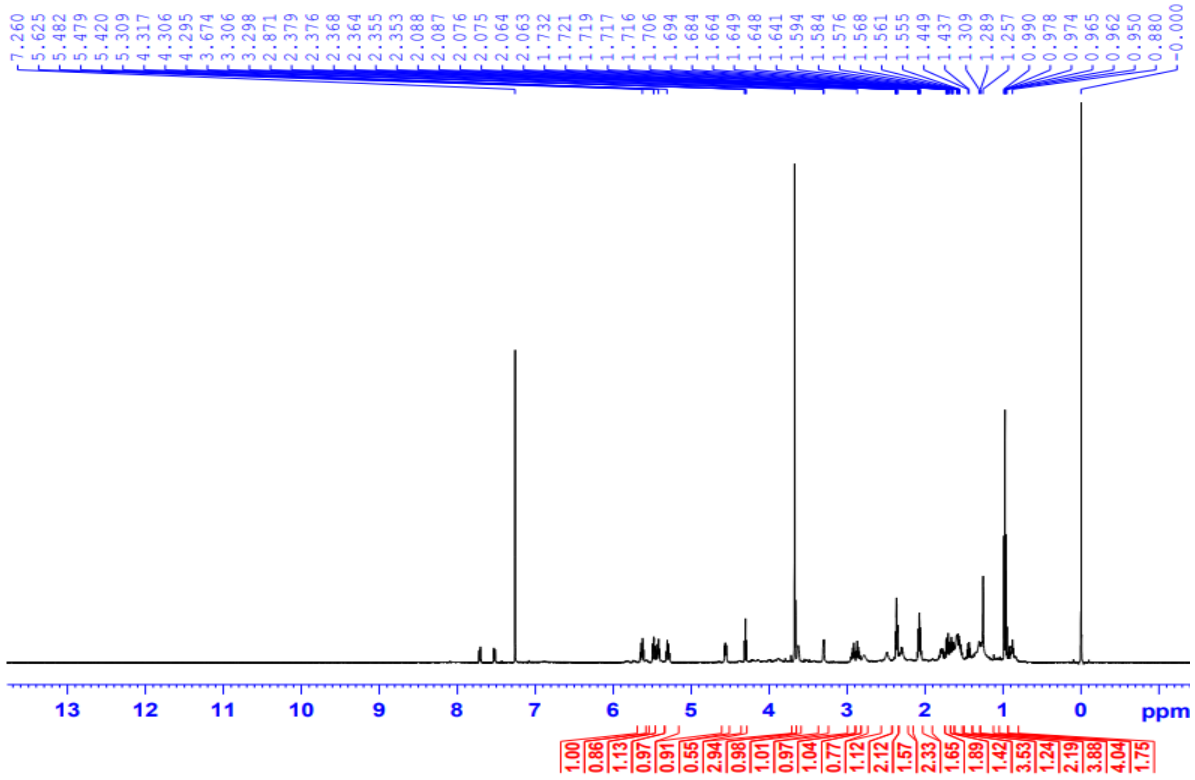

Figure S24. ^{1}H-NMR spectrum of compound **2**

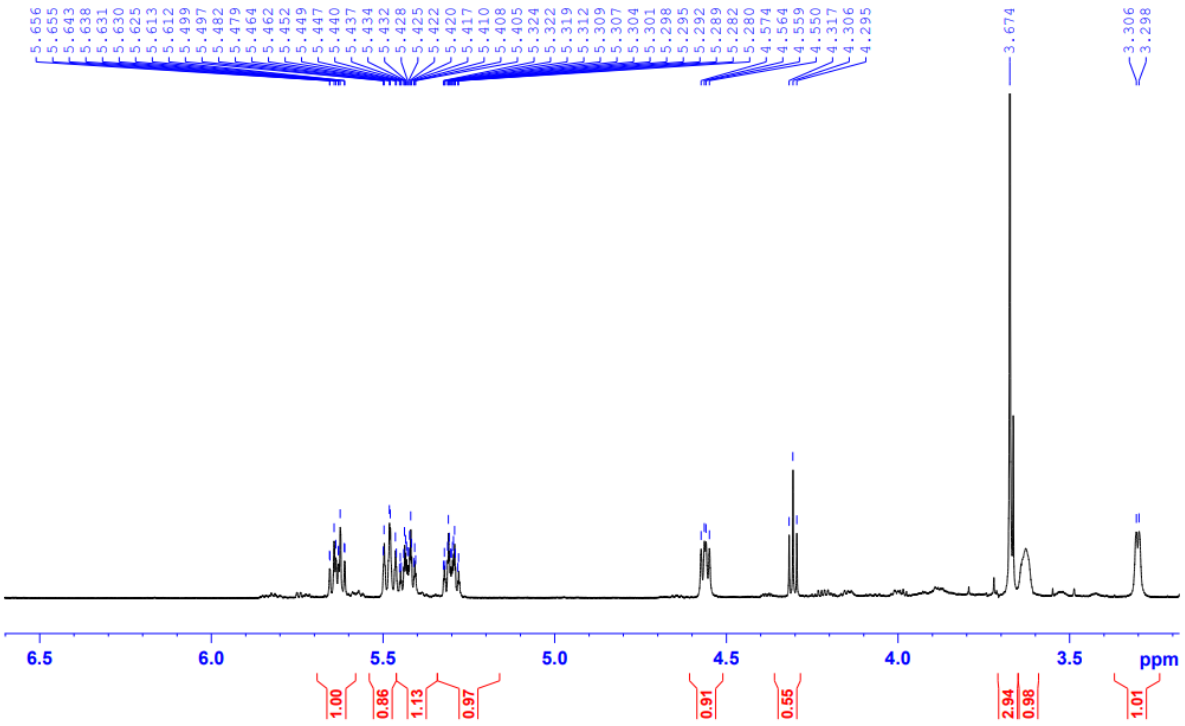

Figure S25. Extended ^{1}H-NMR spectrum of compound **2**

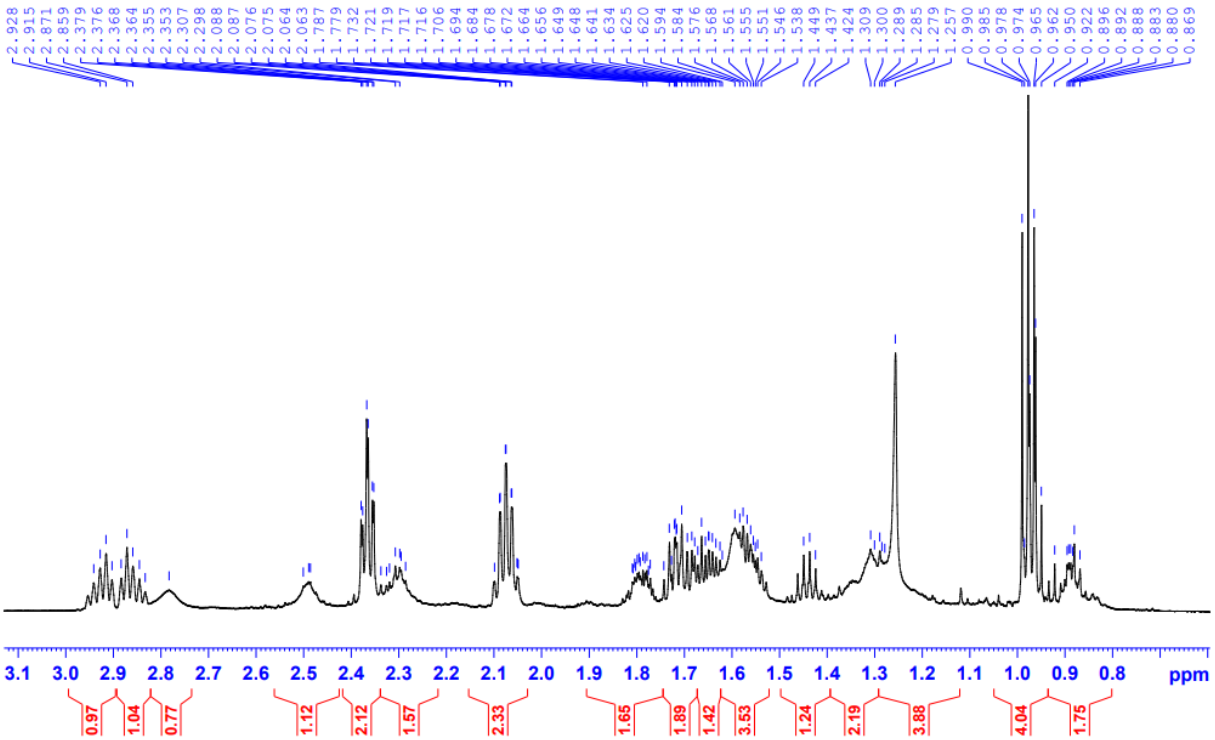

Figure S26. Extended ^{1}H-NMR spectrum of compound **2**

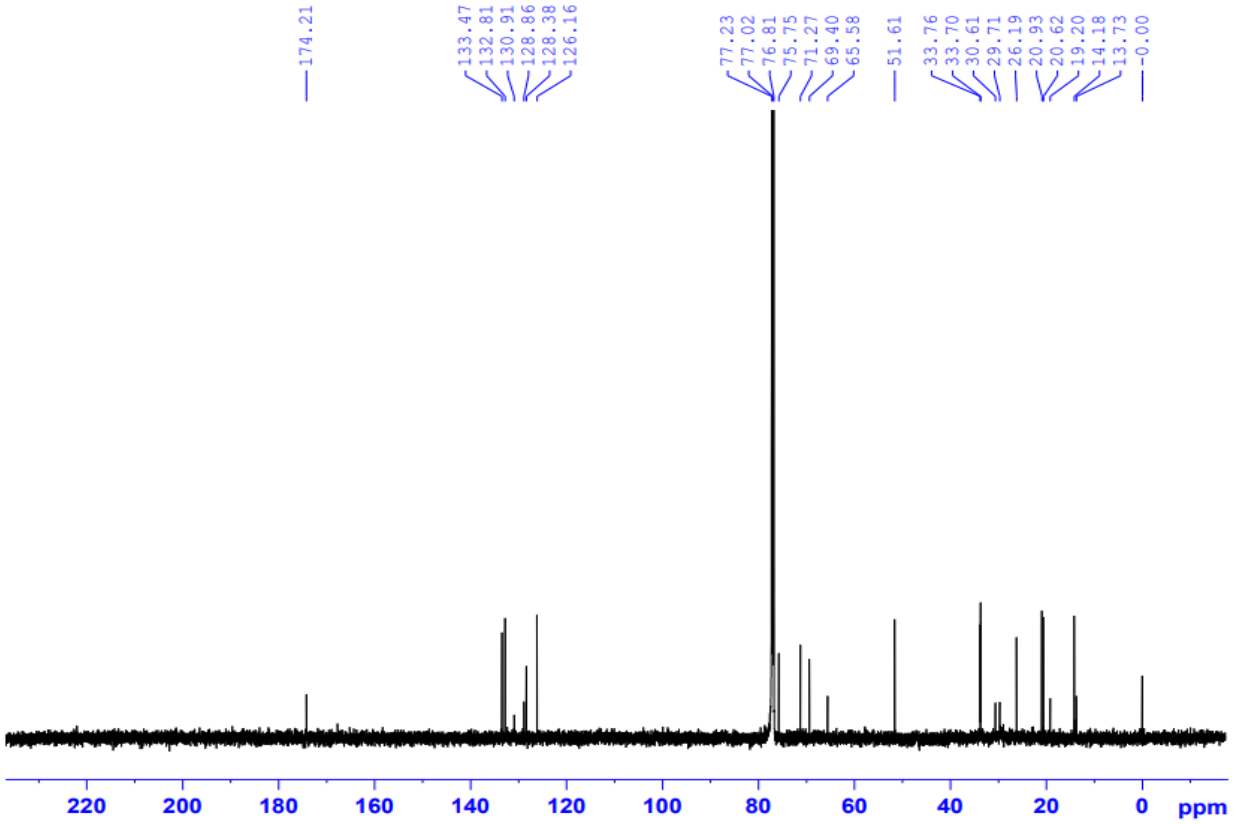

Figure S27. ^{13}C-NMR spectrum of compound **2**

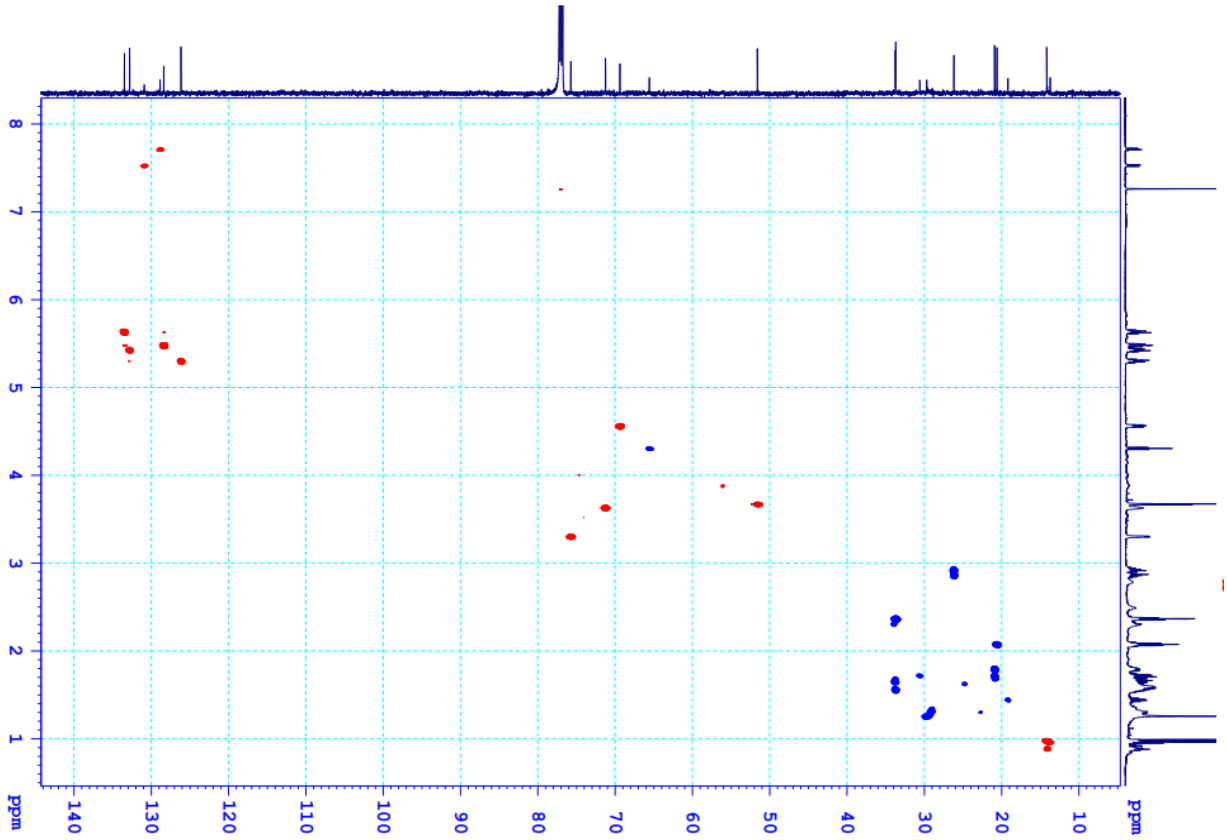

Figure S28. HSQC spectrum of compound **2**

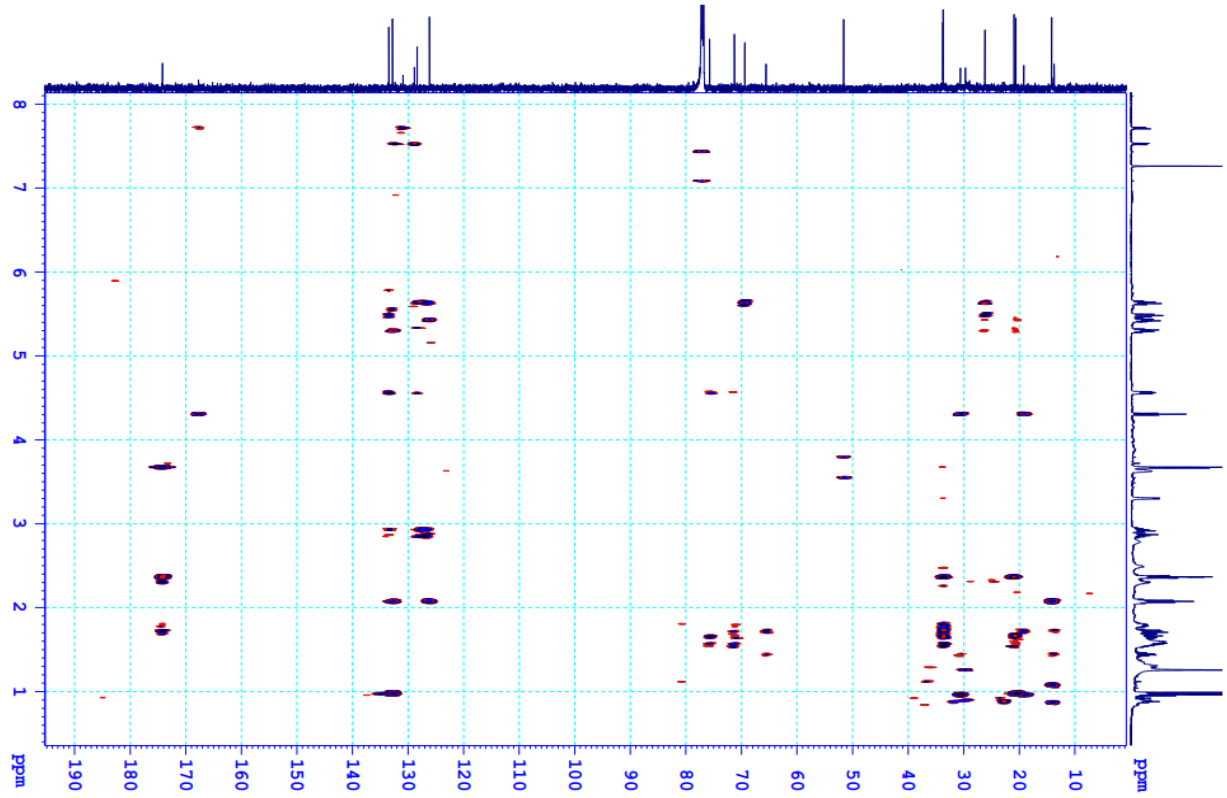

Figure S29. HMBC spectrum of compound **2**

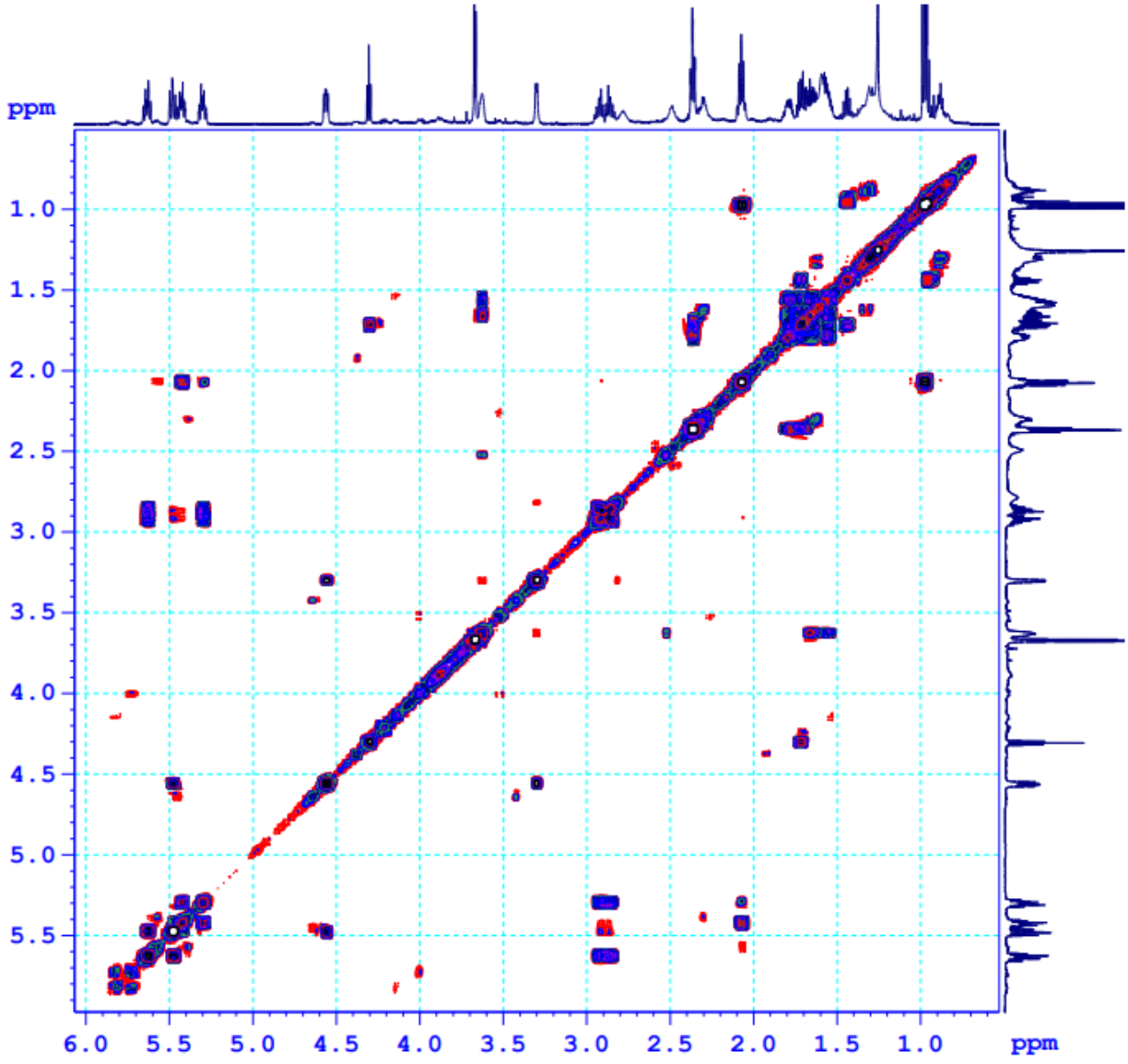

Figure S30. COSY spectrum of compound **2**

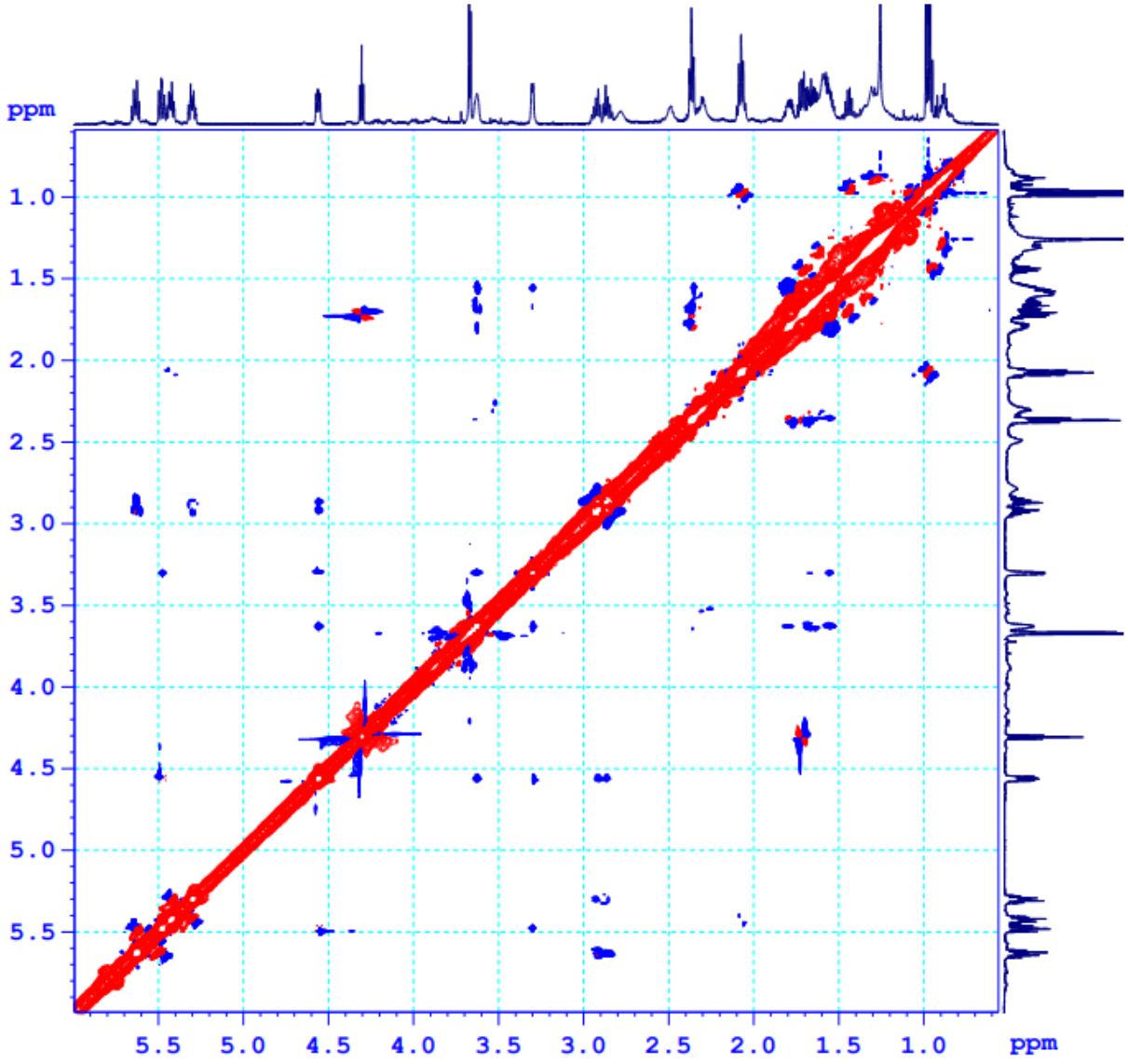

Figure S31. NOESY spectrum of compound **2**

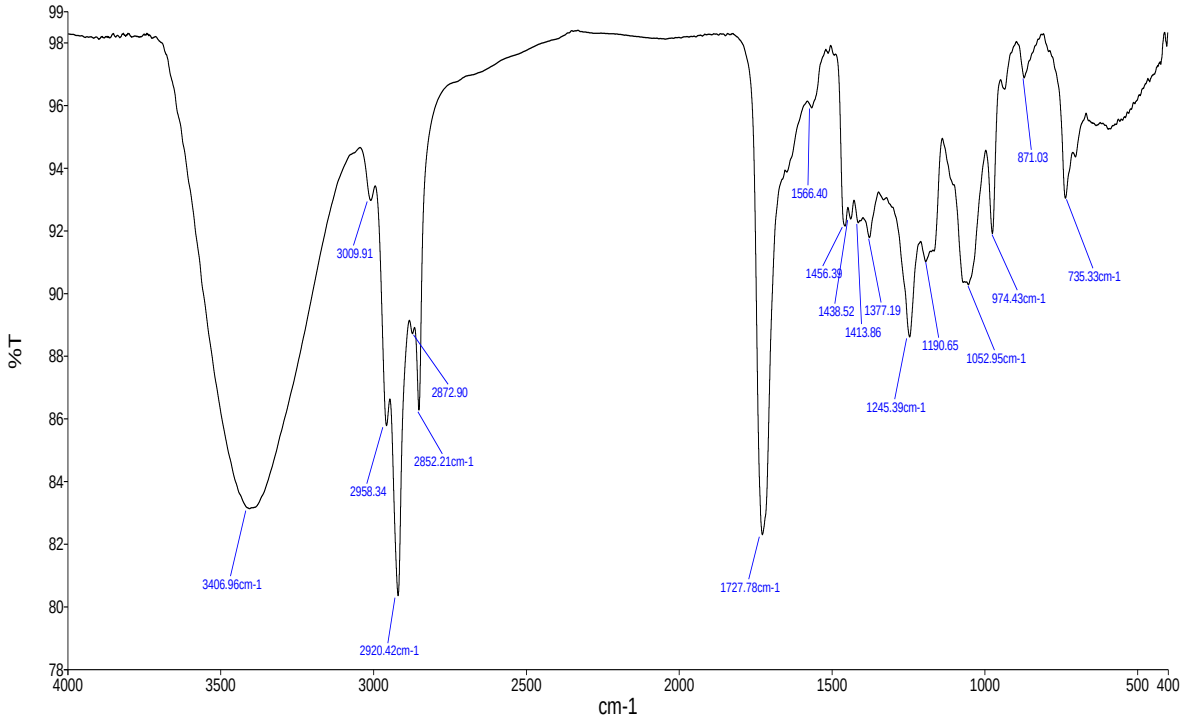

Figure S32. IR spectrum of compound **3**

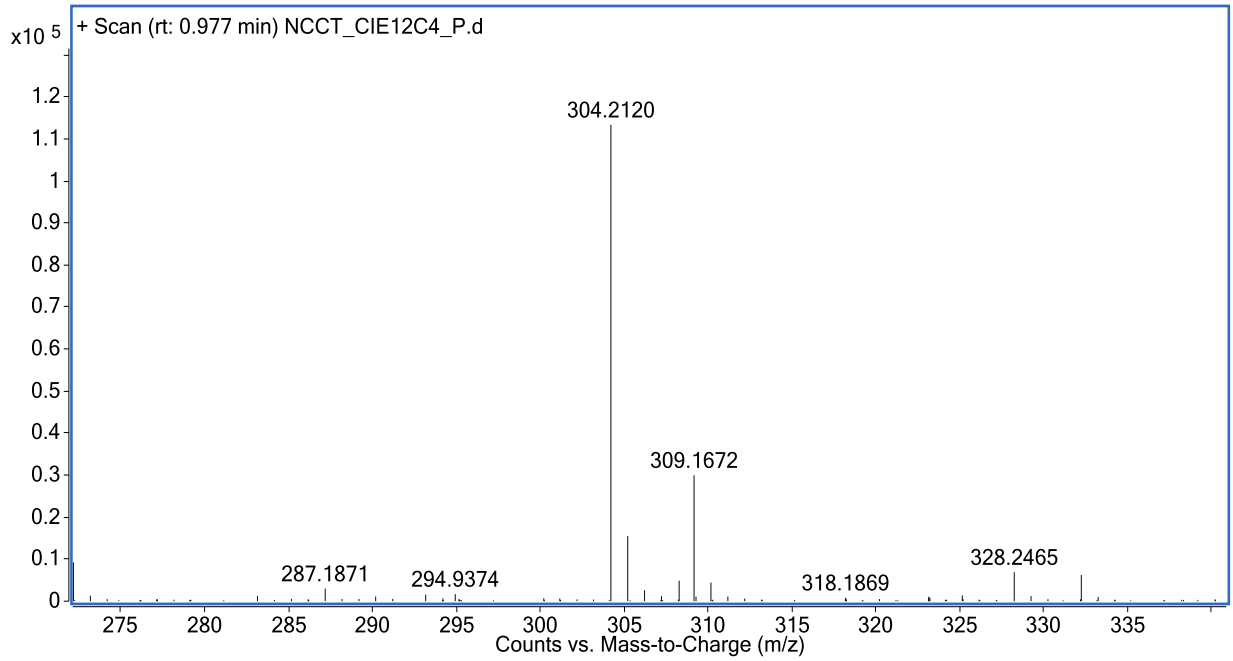

Figure S33. HRESIMS spectrum of compound **3**

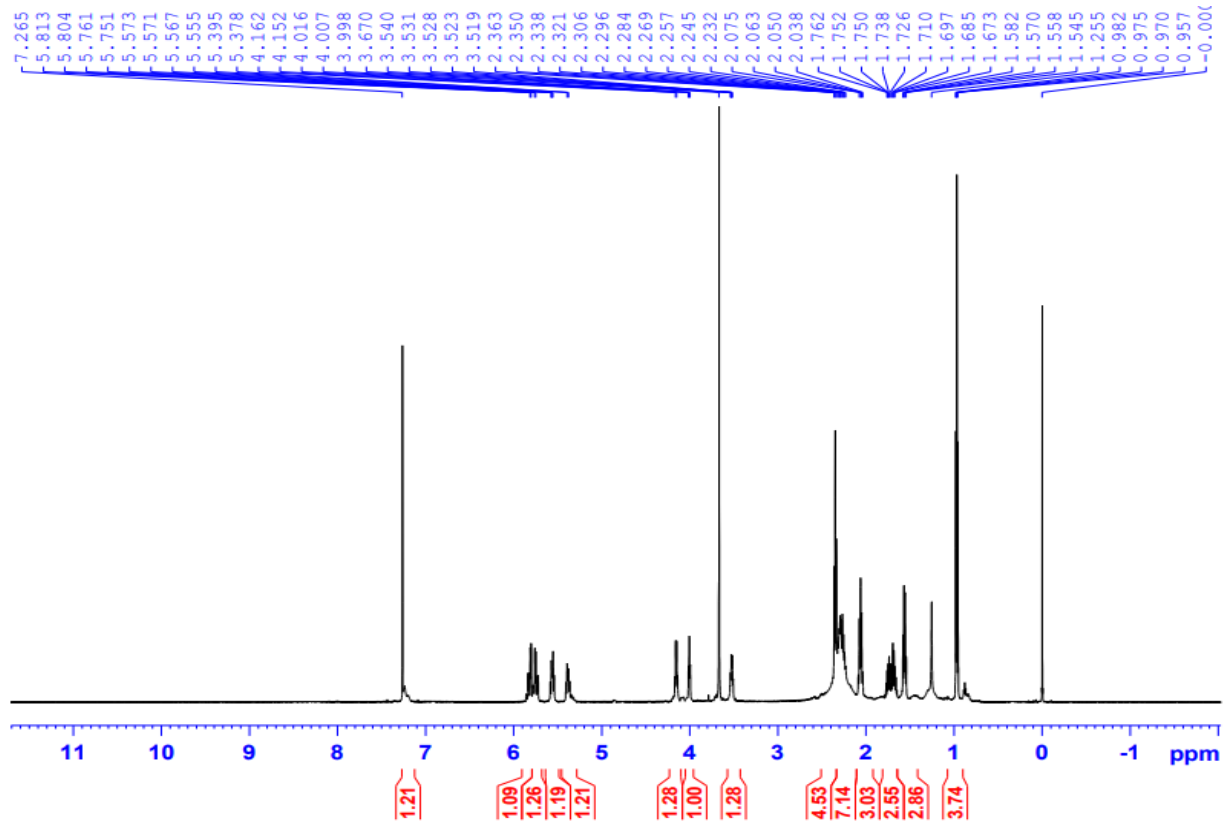

Figure S34. ^{1}H NMR spectrum of compound **3**

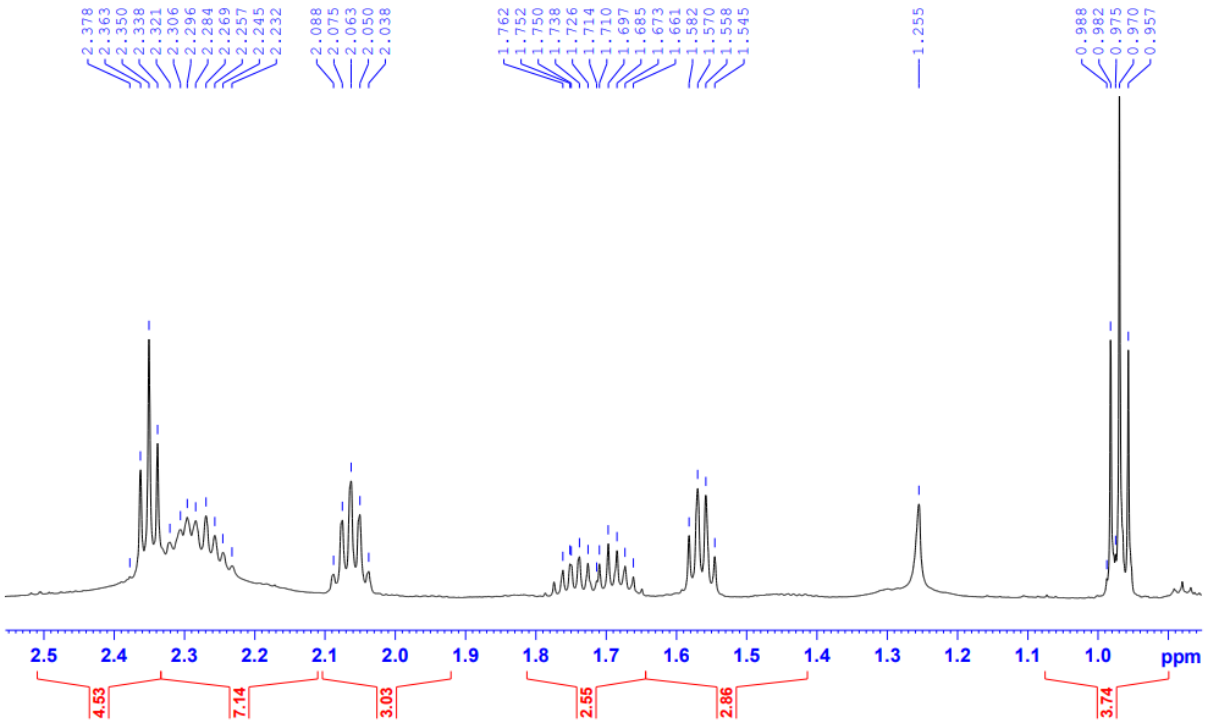

Figure S35. Extended ^{1}H NMR spectrum of compound **3**

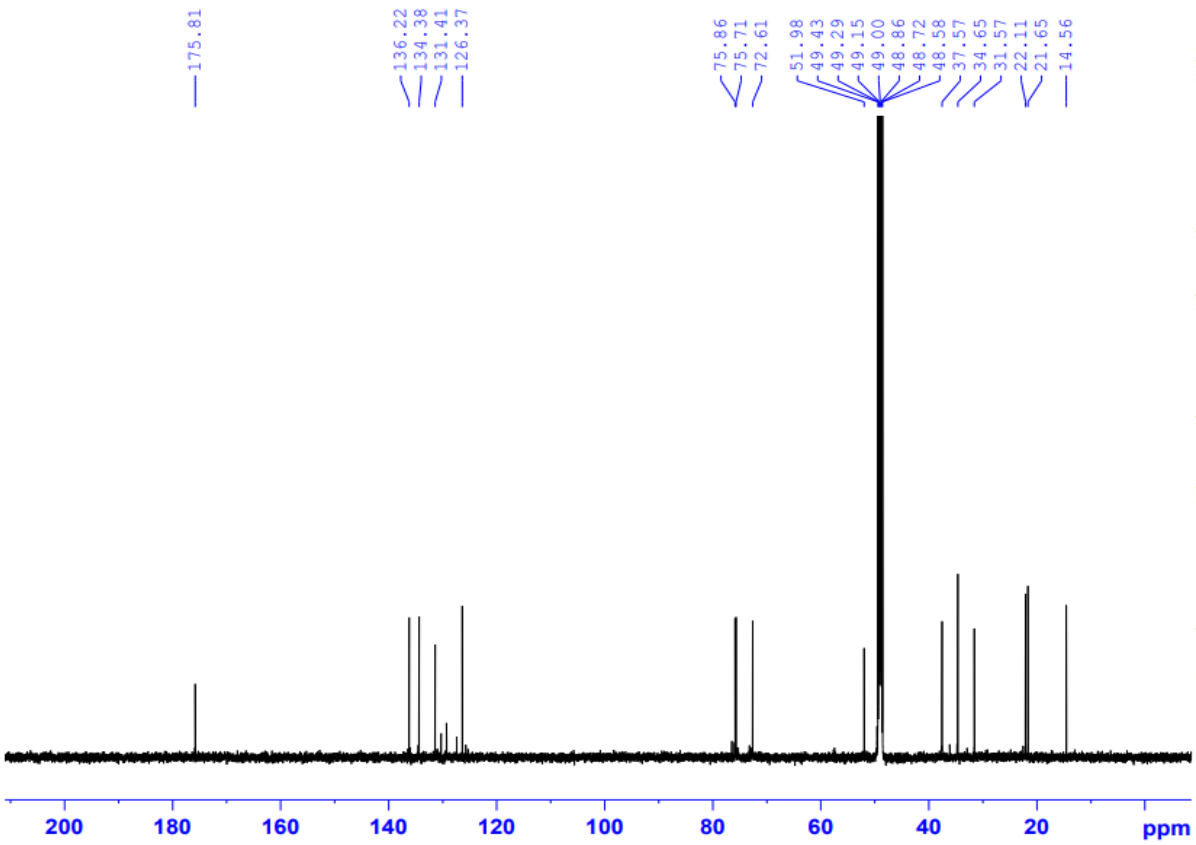

Figure S36. ^{13}C NMR spectrum of compound **3**

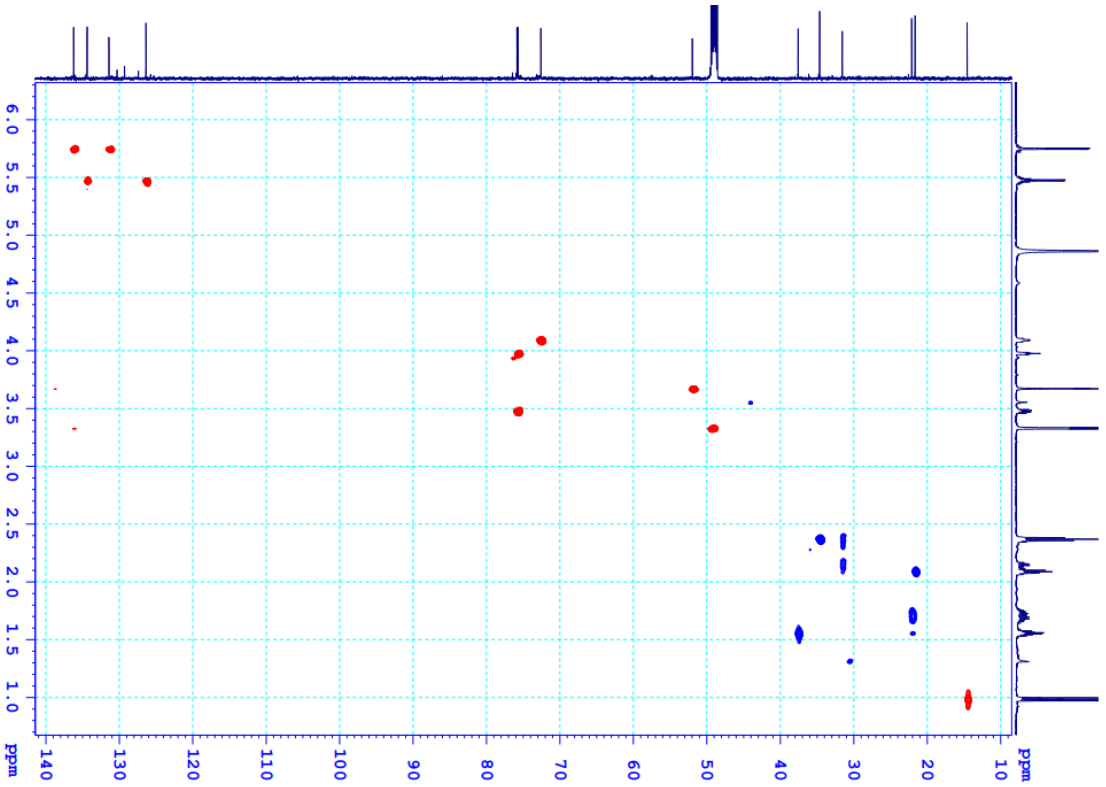

Figure S37. HSQC spectrum of compound **3**

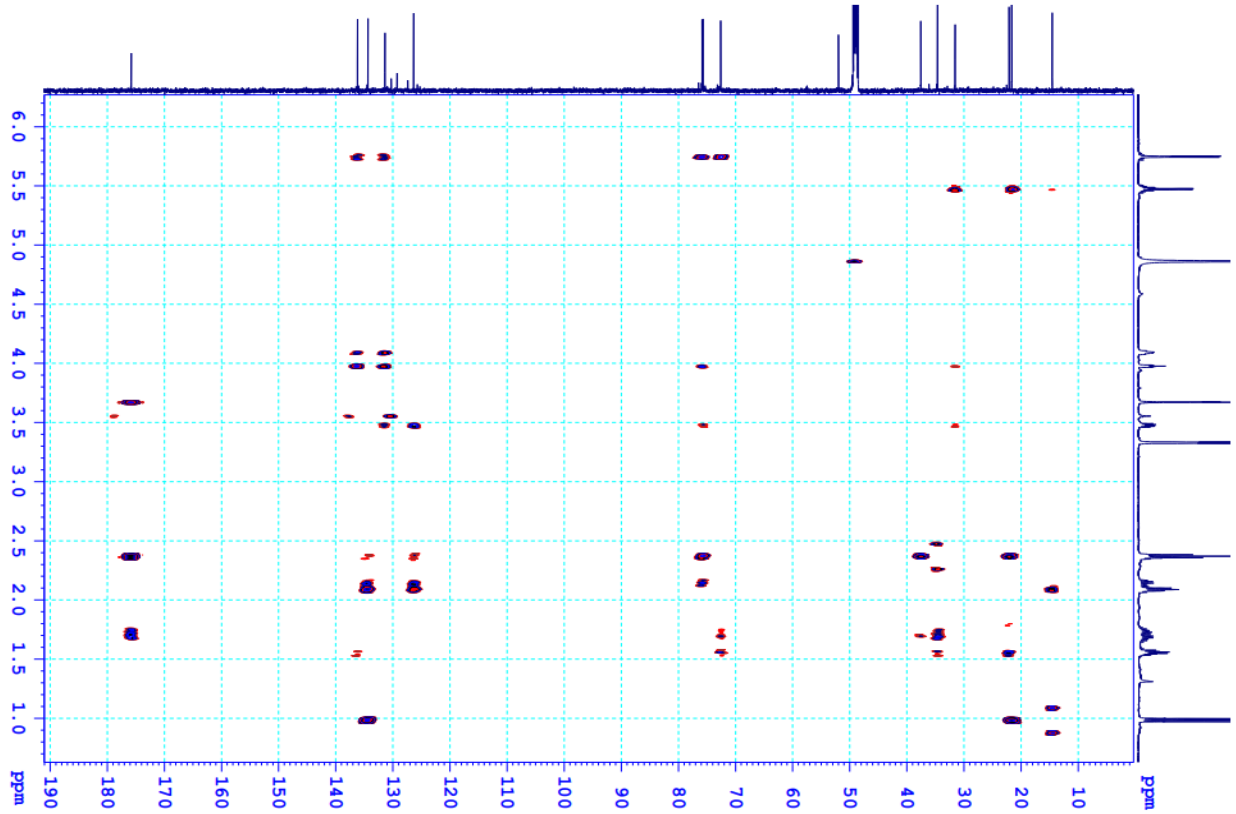

Figure S38. HMBC spectrum of compound **3**

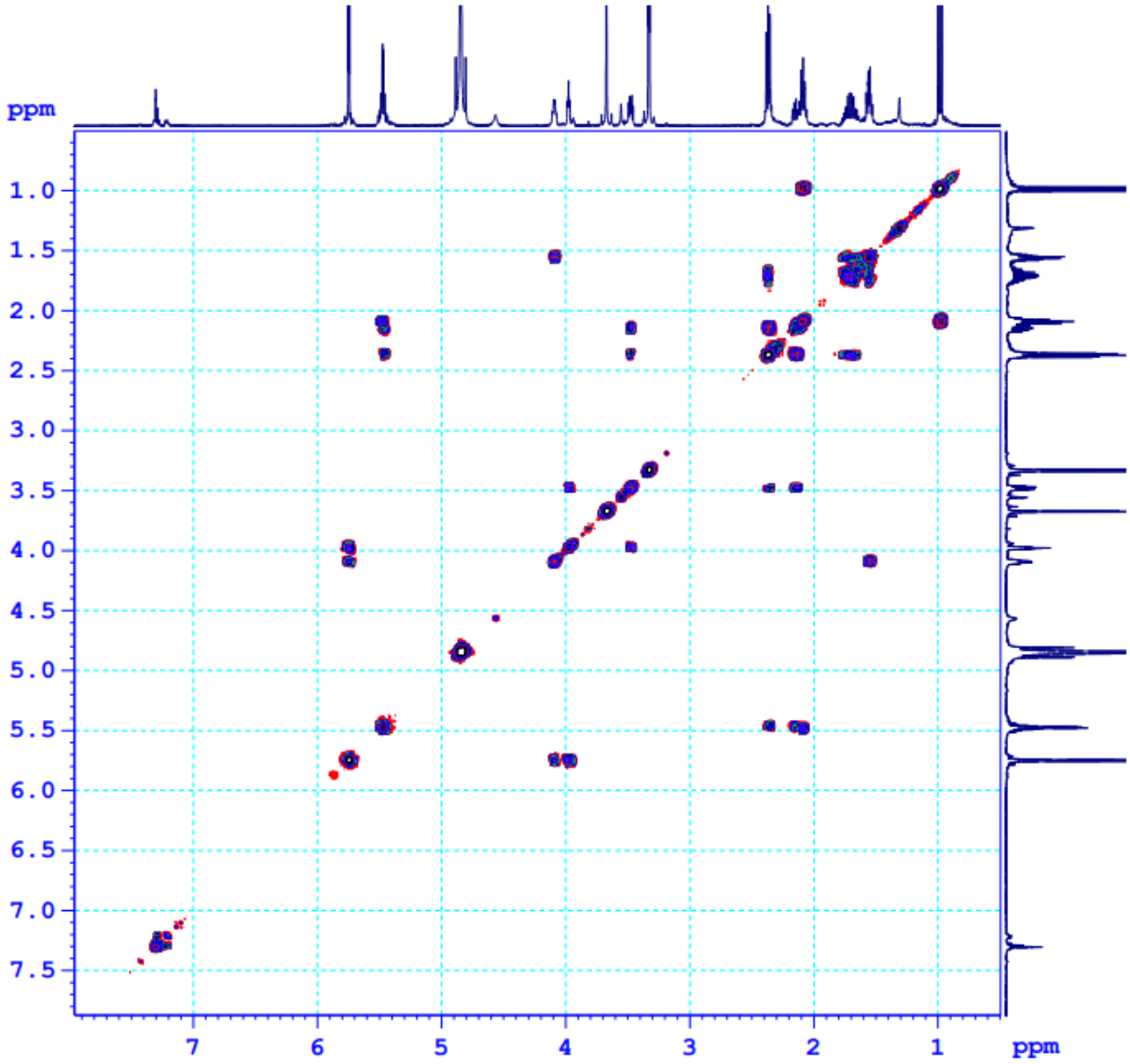

Figure S39. COSY spectrum of compound **3**

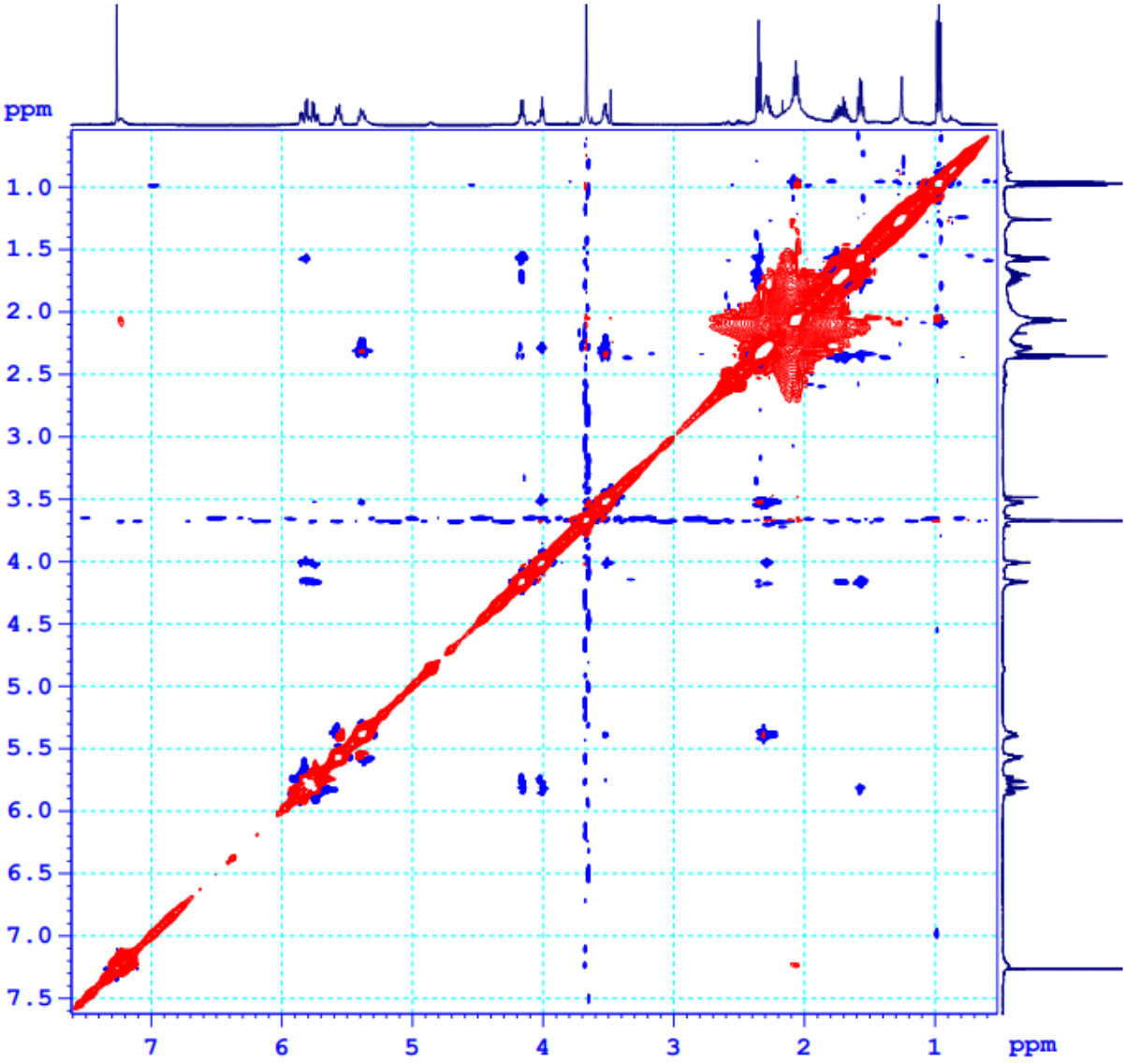

Figure S40. NOESY spectrum of compound **3**

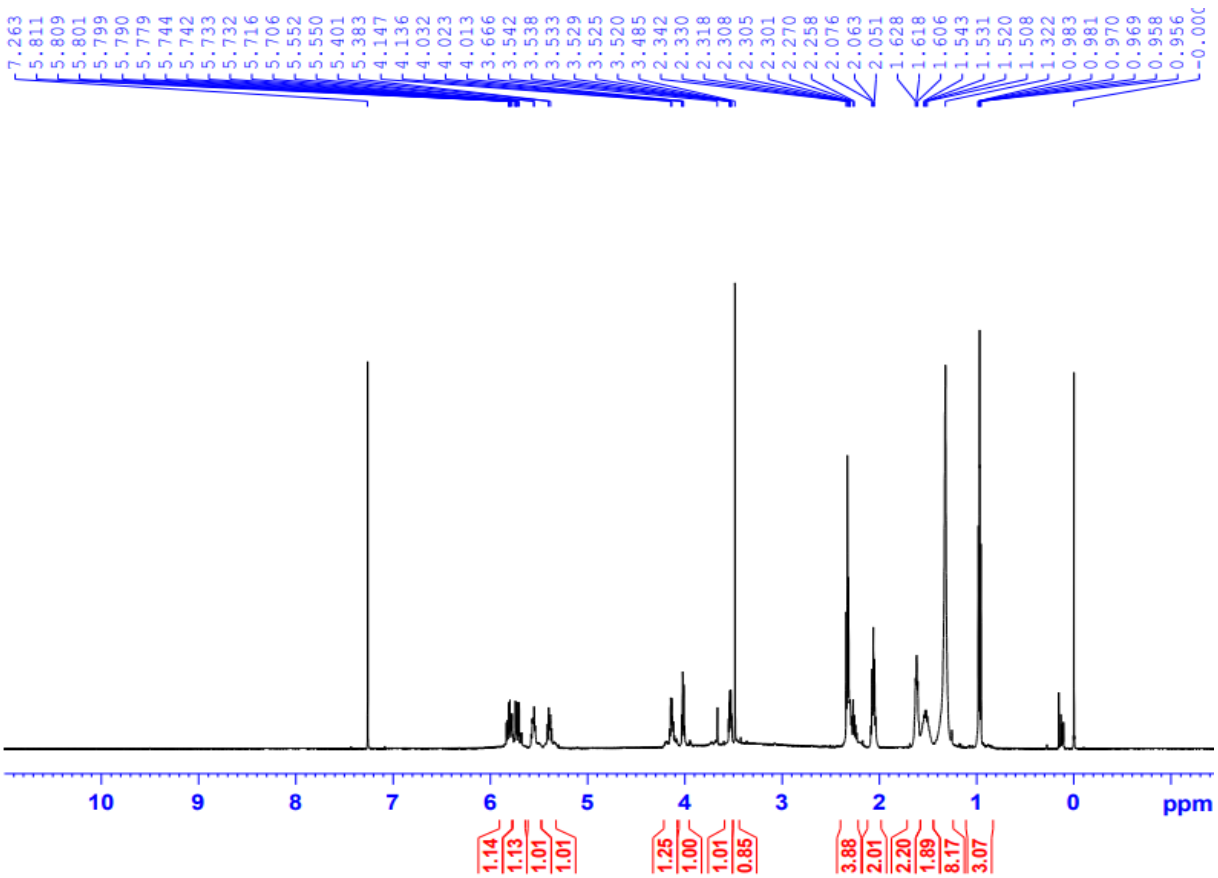

Figure S41. ^{1}H NMR spectrum of compound **4**

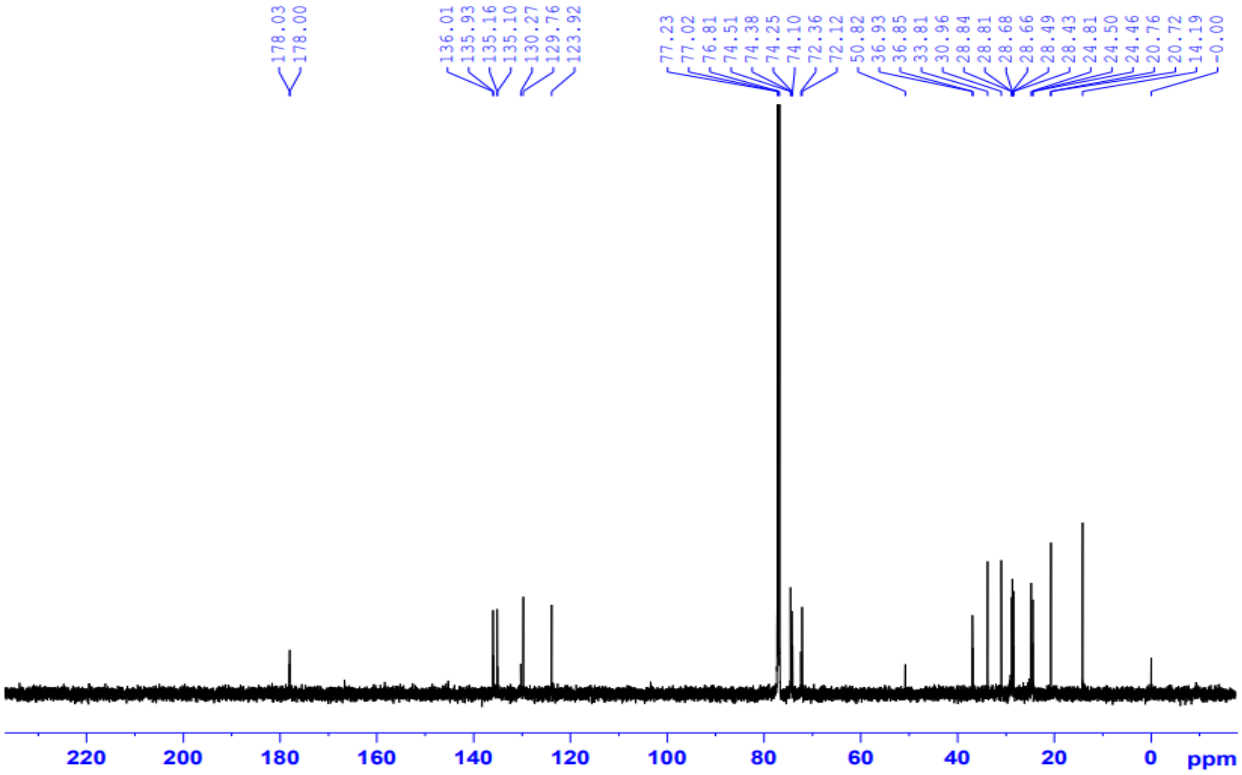

Figure S42. ^{13}C NMR spectrum of compound **4**

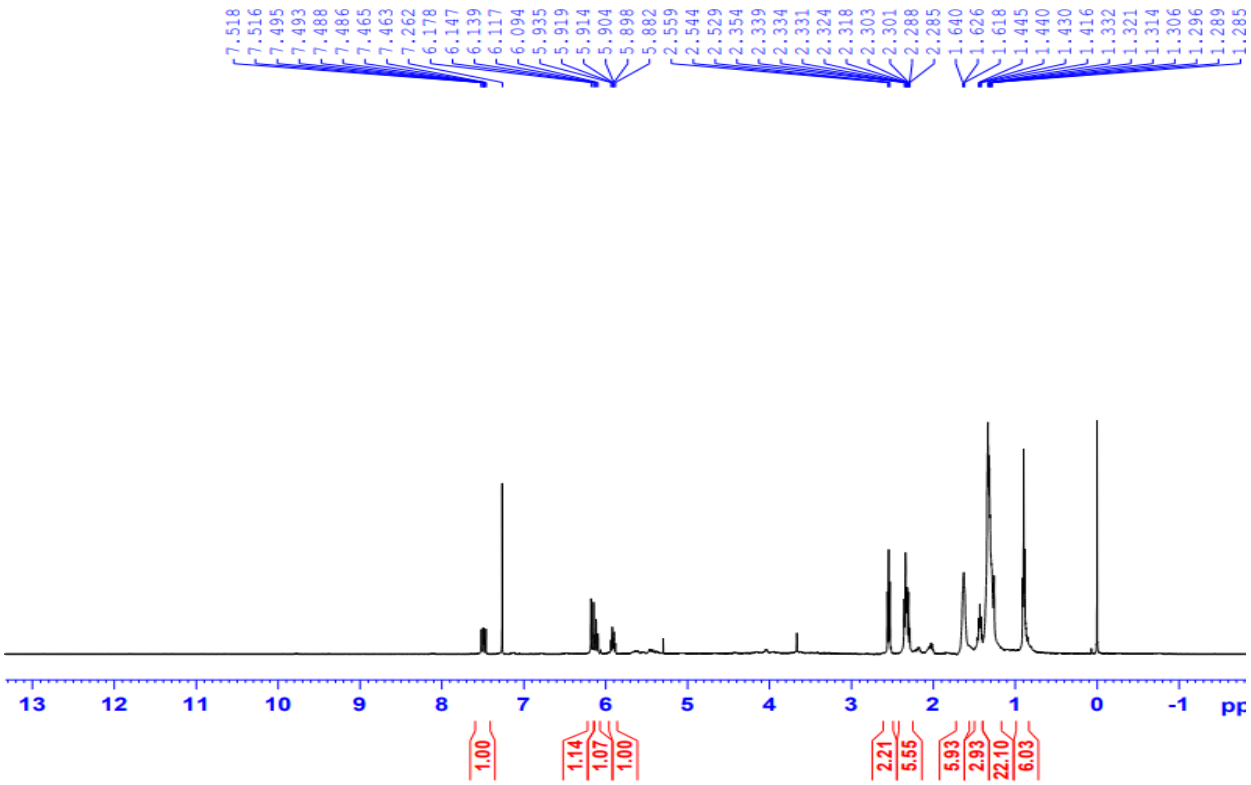

Figure S43. ^{1}H NMR spectrum of compound **5**

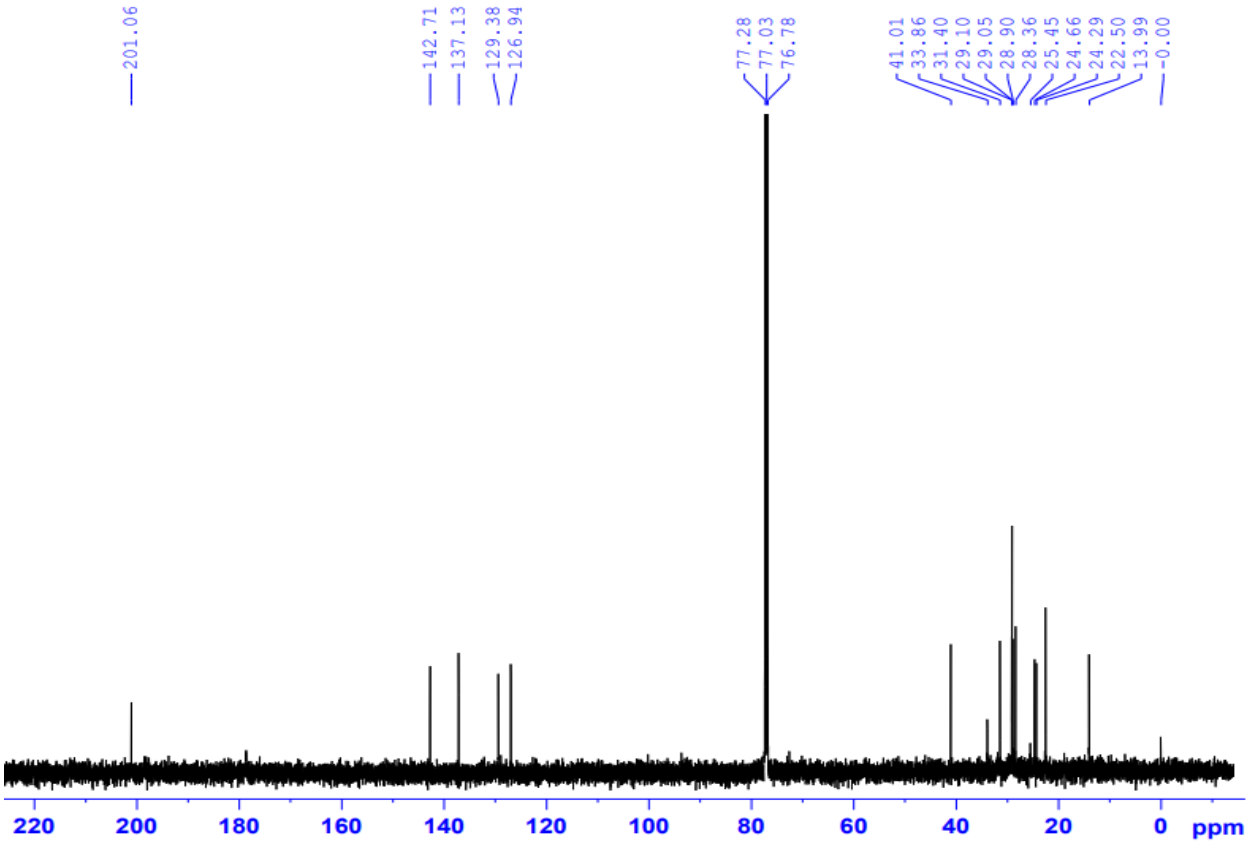

Figure S44. ^{13}C NMR spectrum of compound **5**

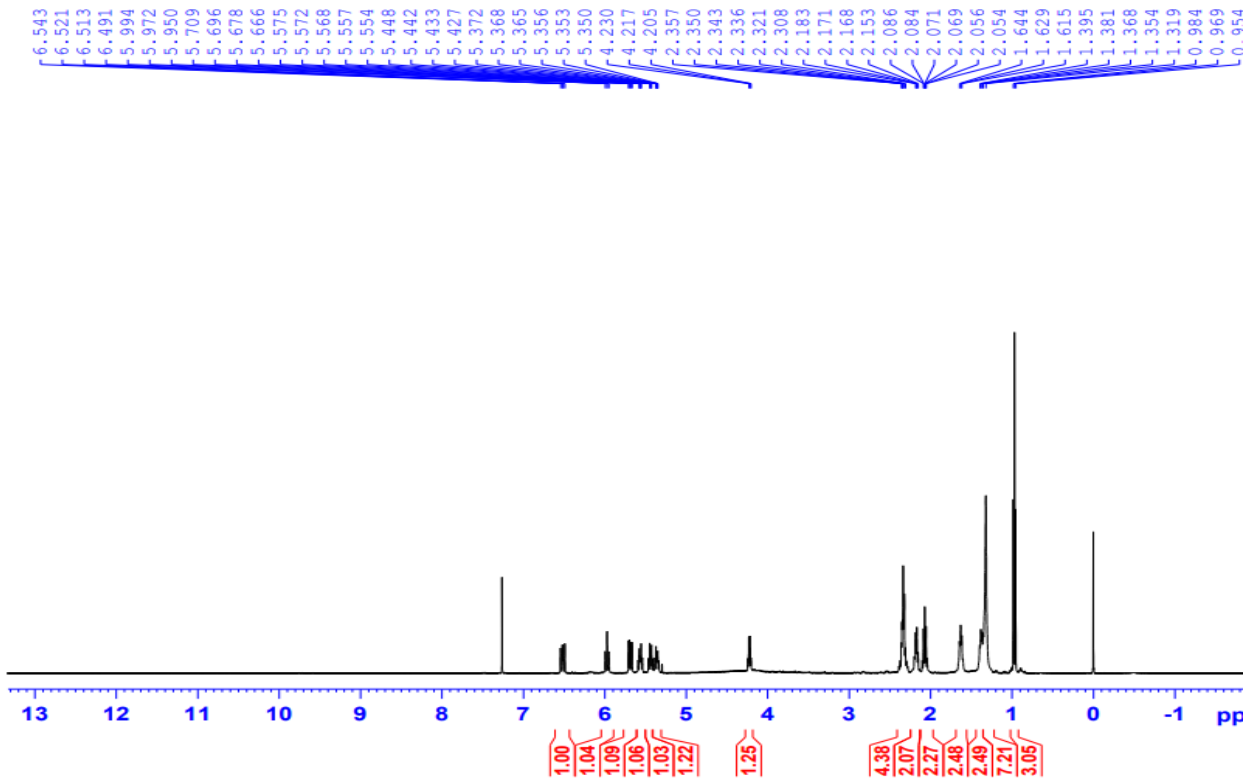

Figure S45. ^{1}H NMR spectrum of compound **6**

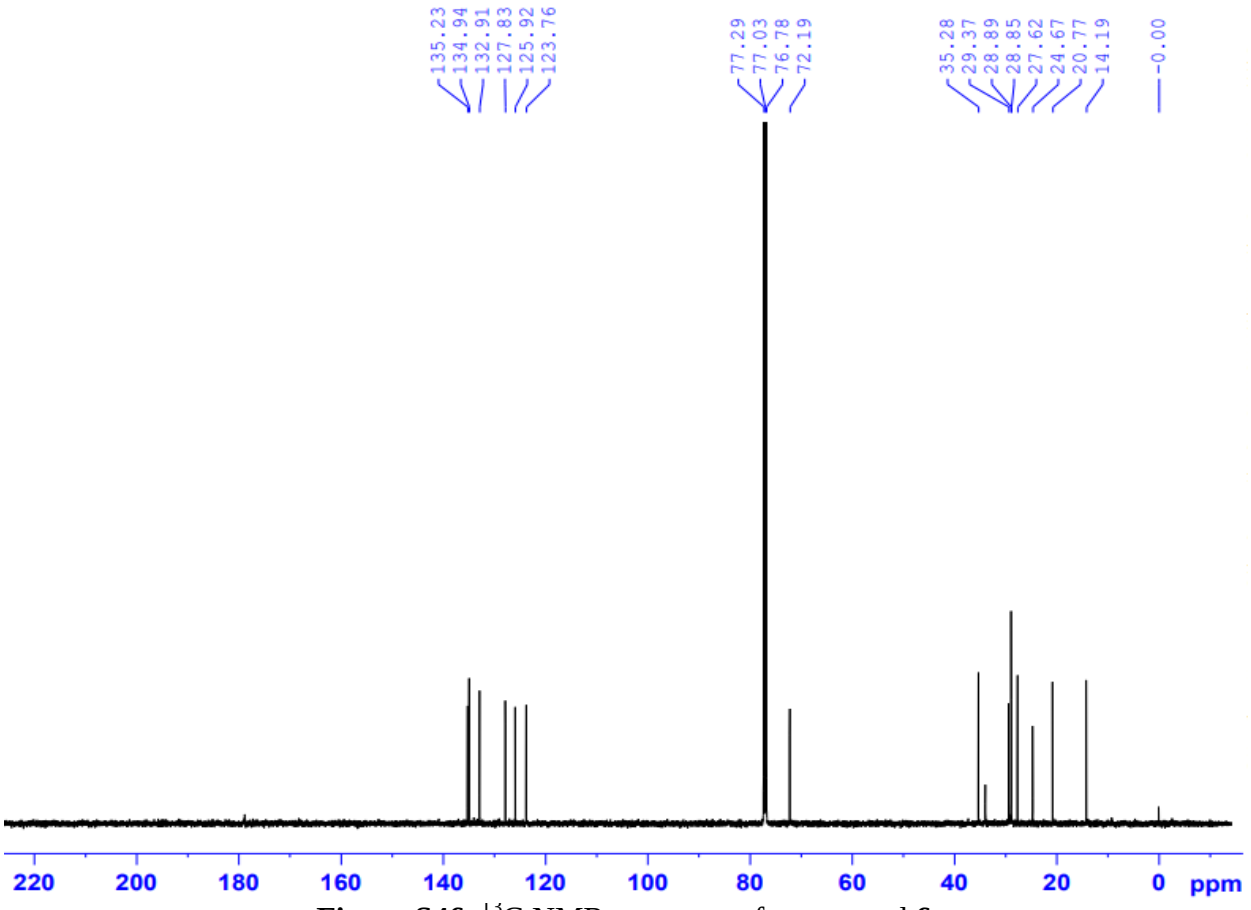

Figure S46. ^{13}C NMR spectrum of compound **6**

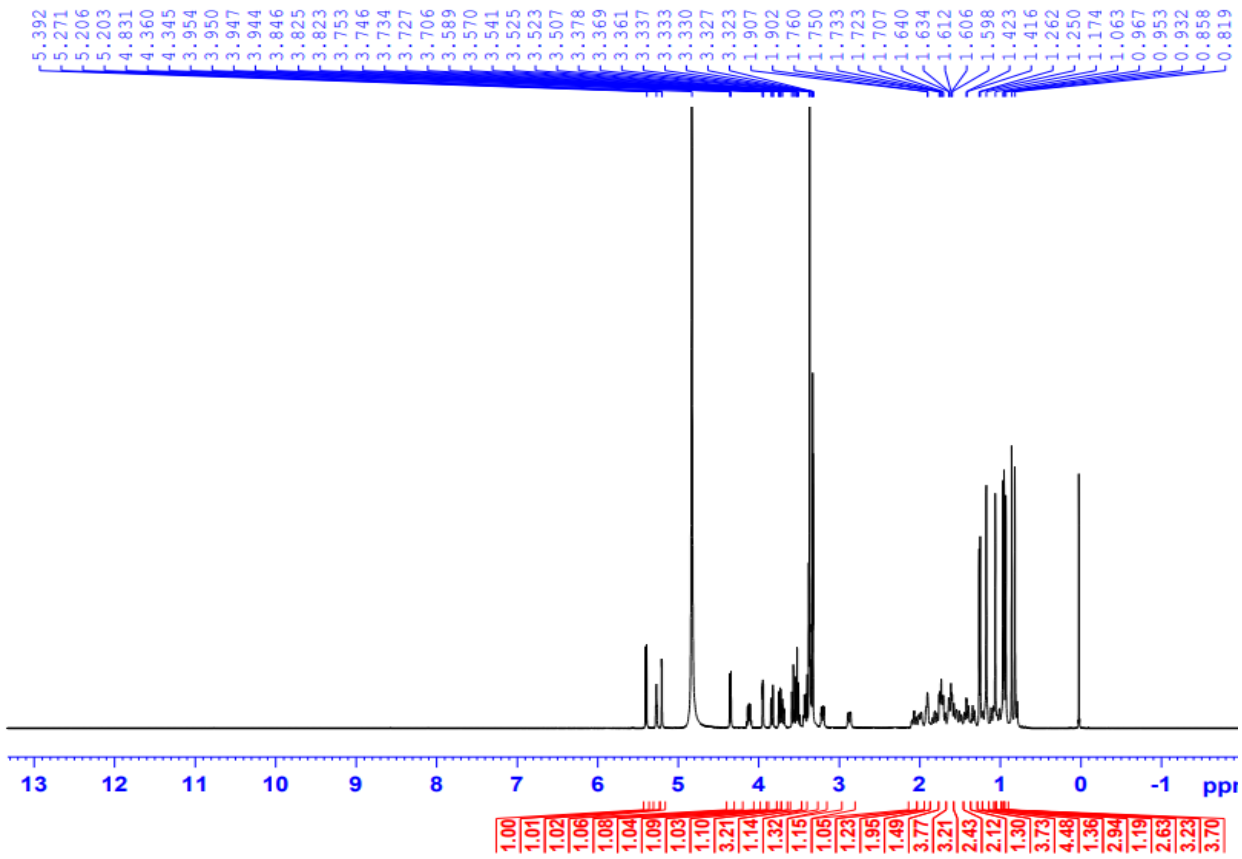

Figure S47. ^{1}H NMR spectrum of compound **7**

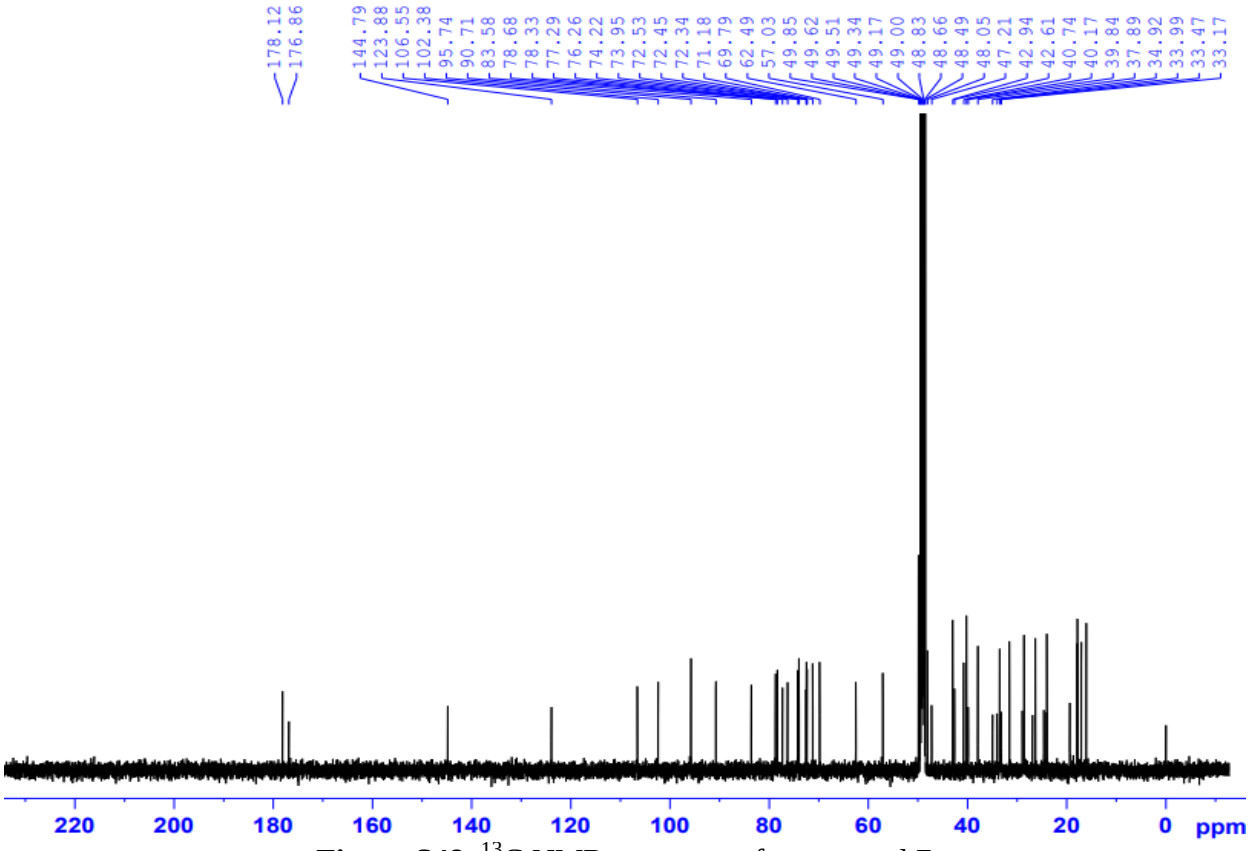

Figure S48. ^{13}C NMR spectrum of compound **7**

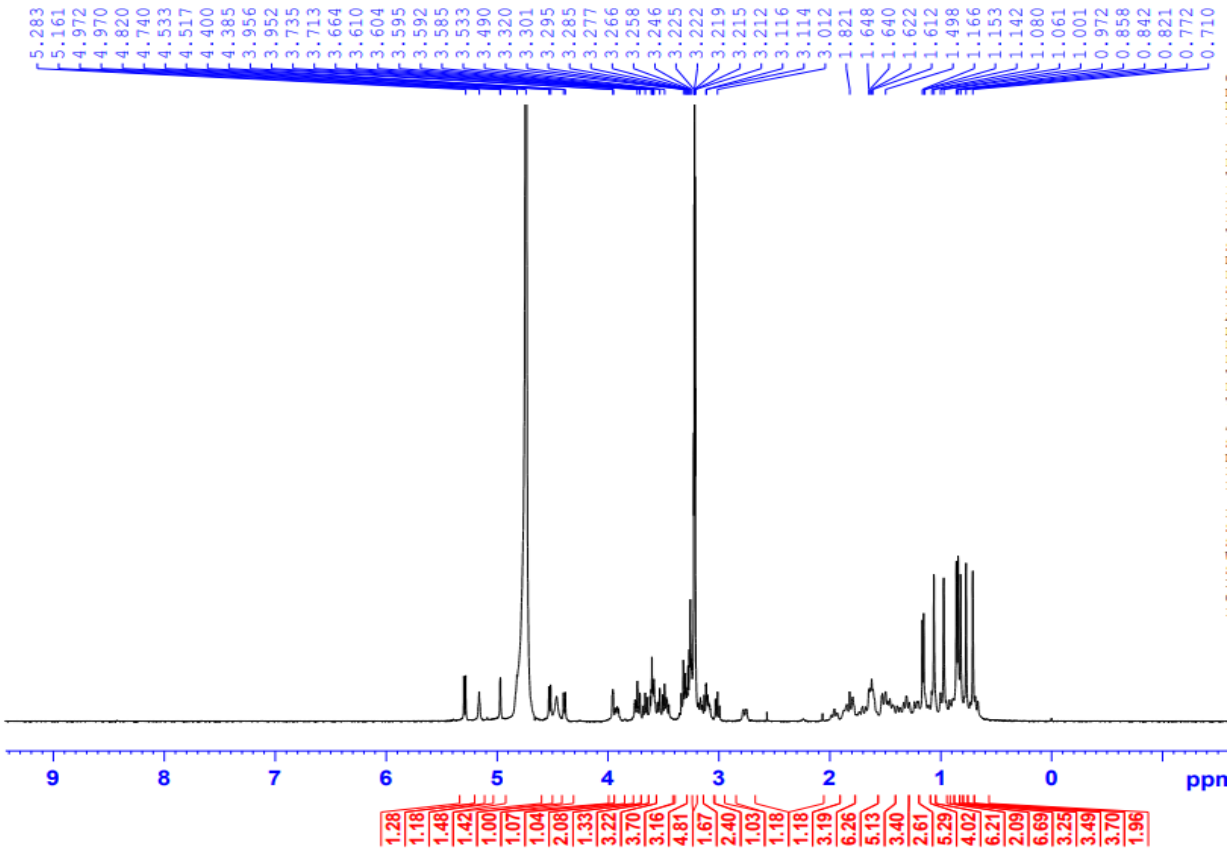

Figure S49. ^{1}H NMR spectrum of compound **8**

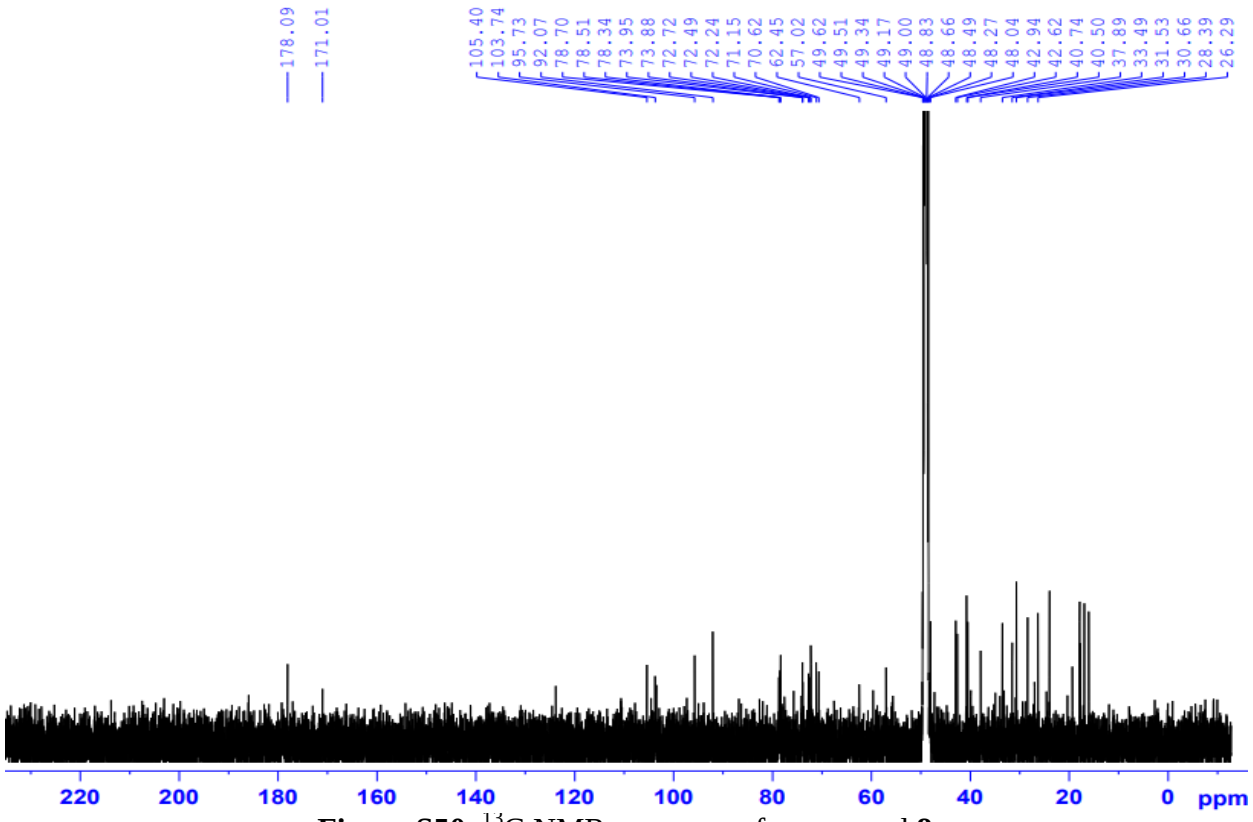

Figure S50. ^{13}C NMR spectrum of compound **8**

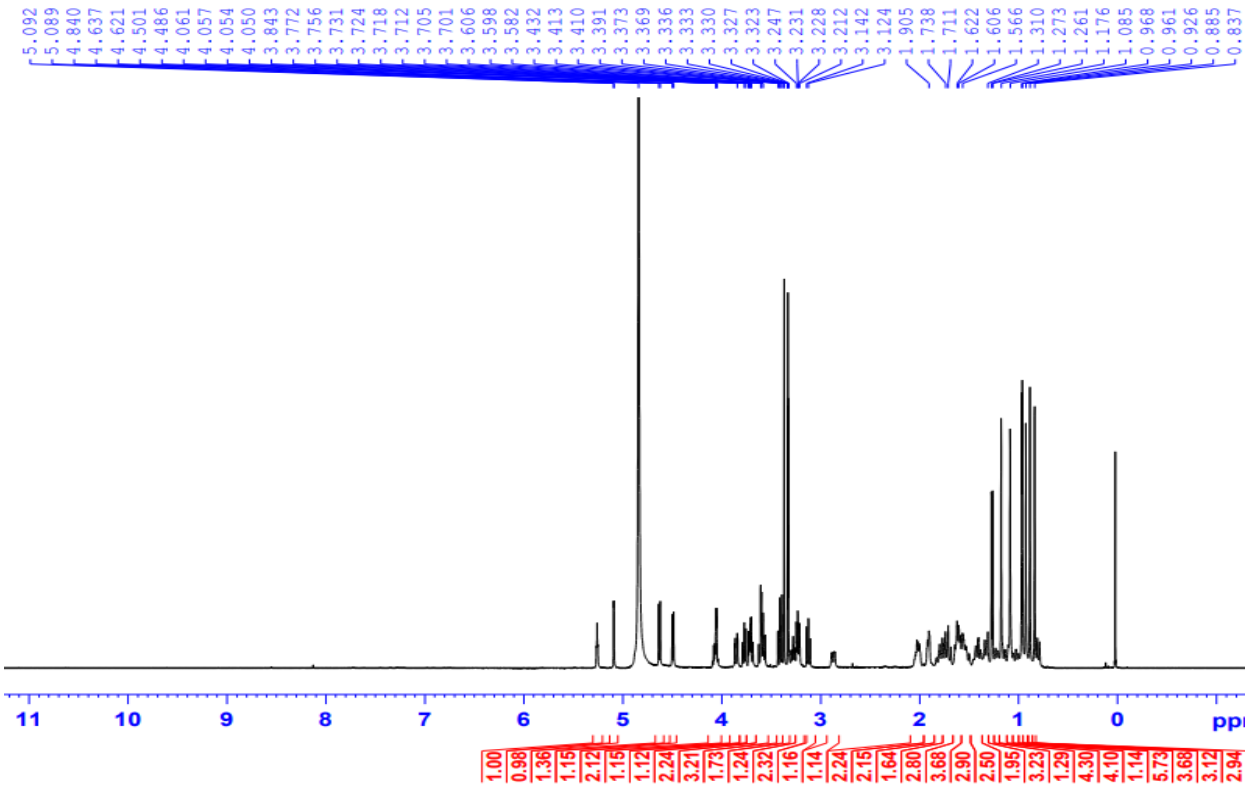

Figure S51. ^{1}H NMR spectrum of compound **9**

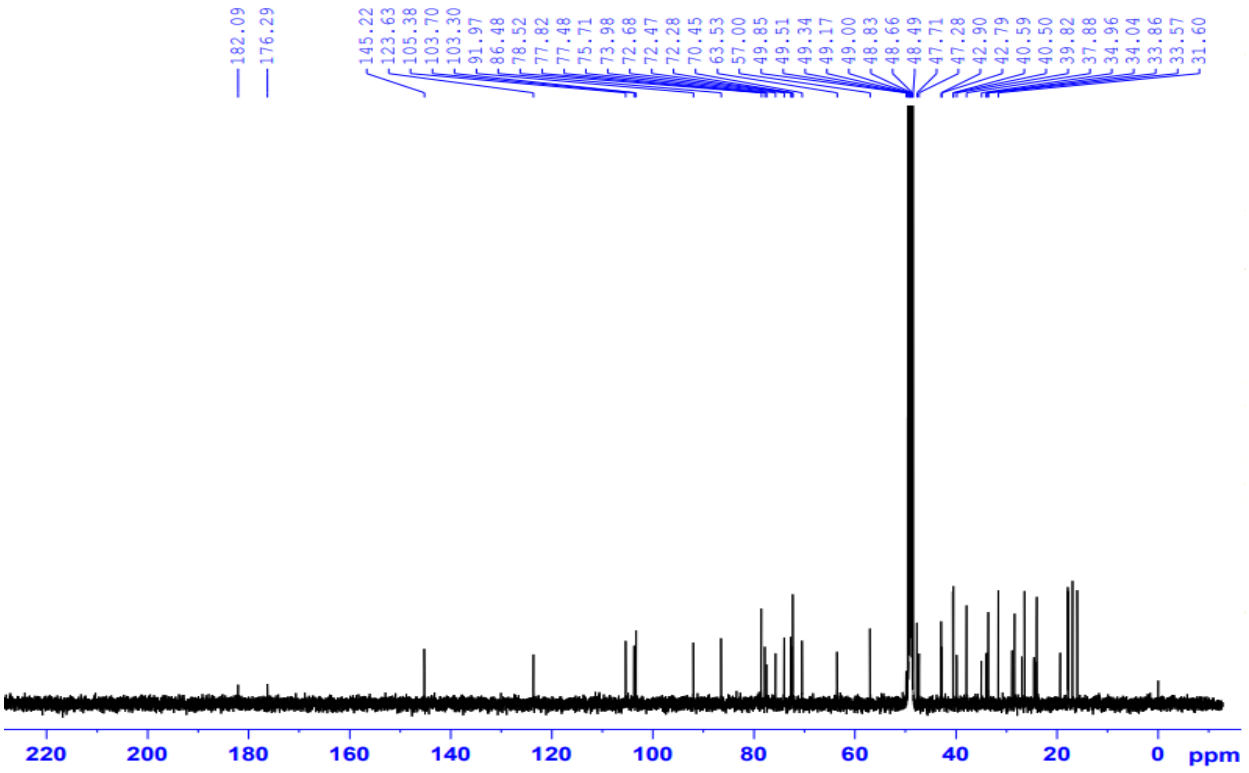

Figure S52. ^{13}C NMR spectrum of compound **9**

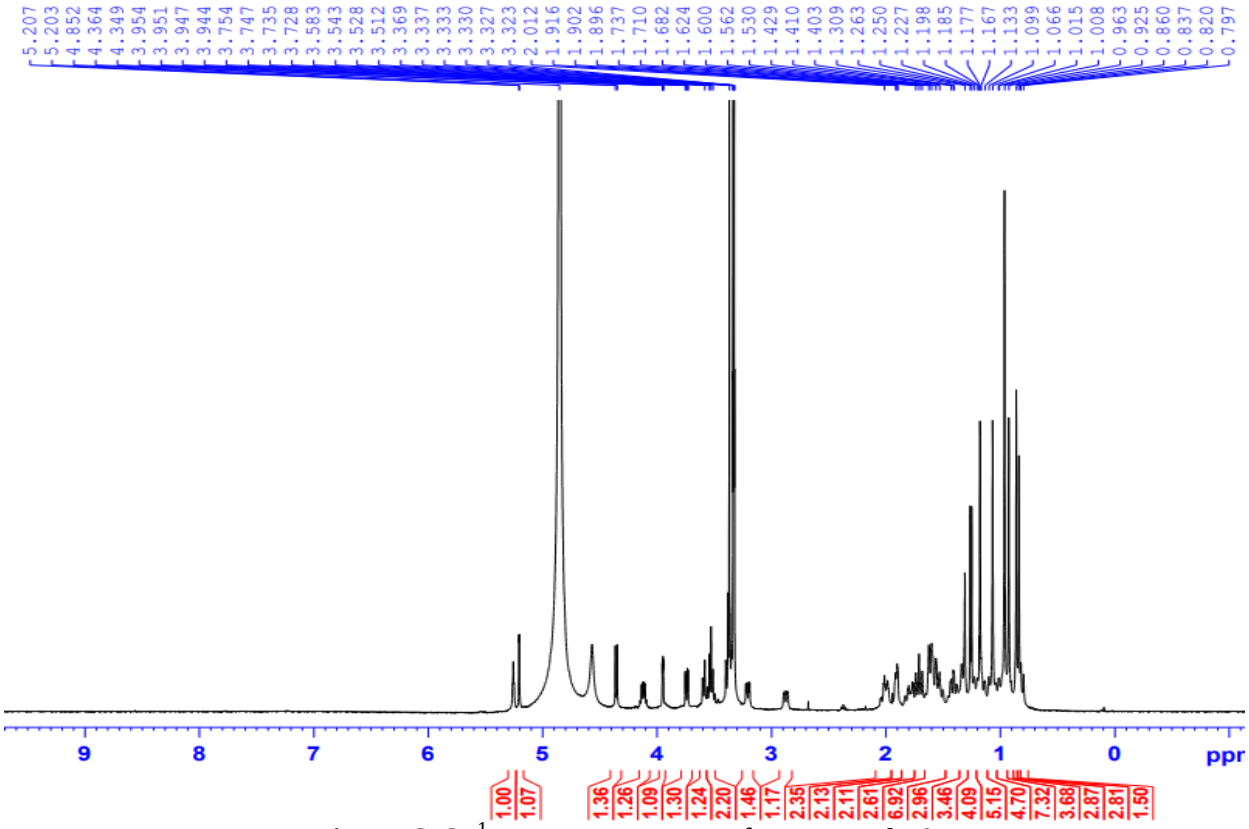

Figure S53. ^{1}H NMR spectrum of compound **10**

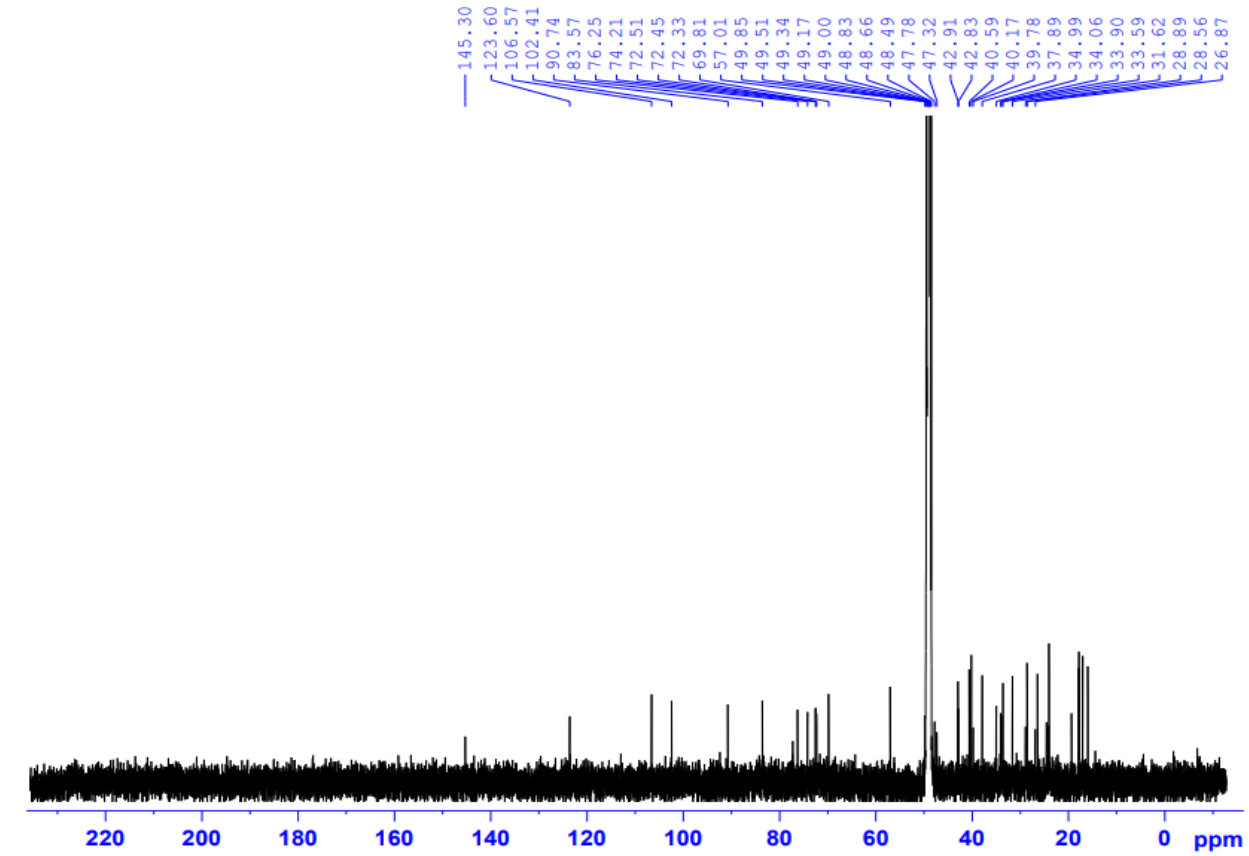

Figure S54. ^{13}C NMR spectrum of compound **10**

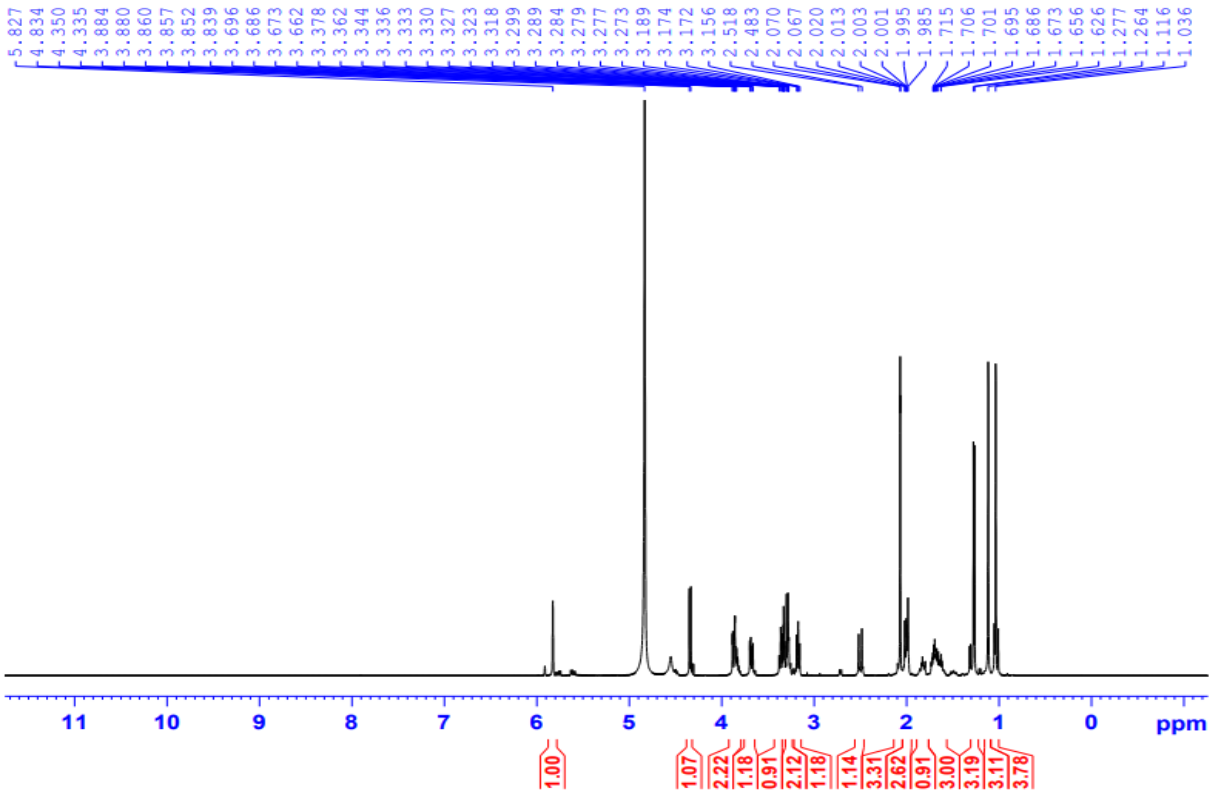

Figure S55. ^{1}H NMR spectrum of compound **11**

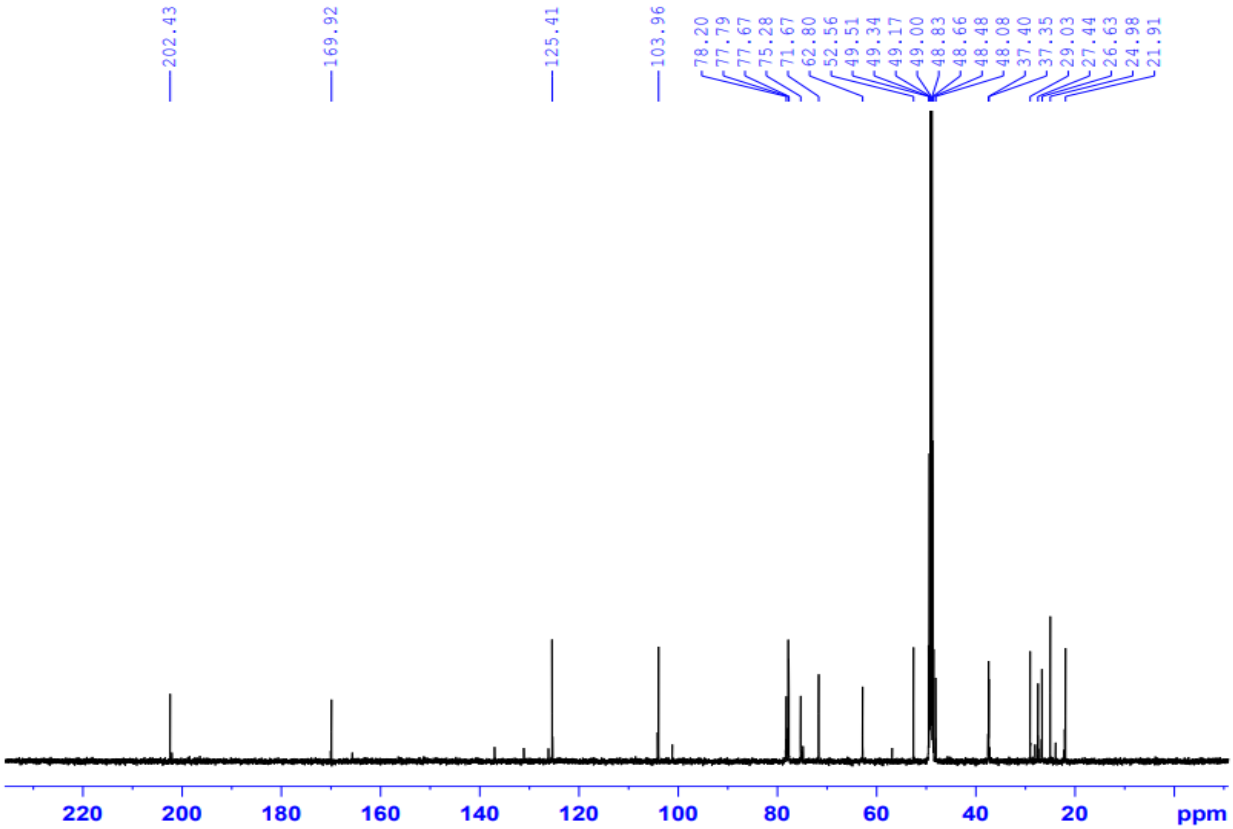

Figure S56. ^{13}C NMR spectrum of compound **11**

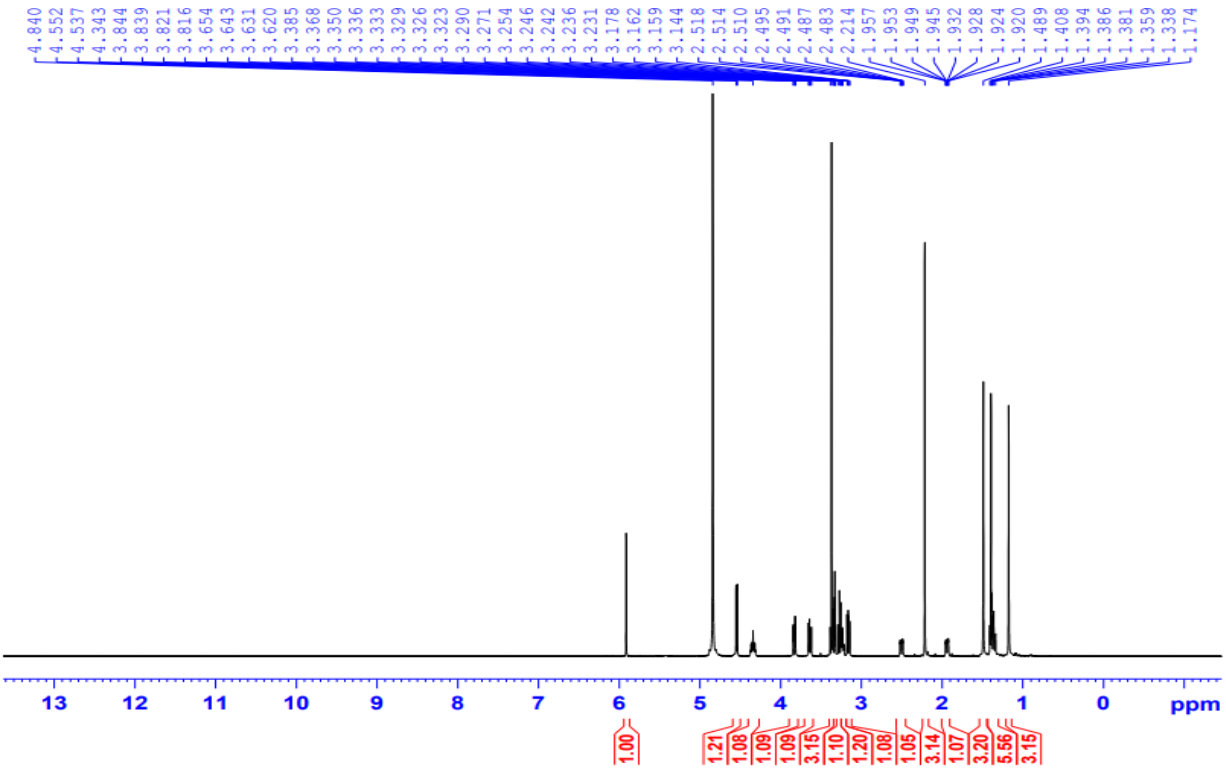

Figure S57. ^{1}H NMR spectrum of compound **12**

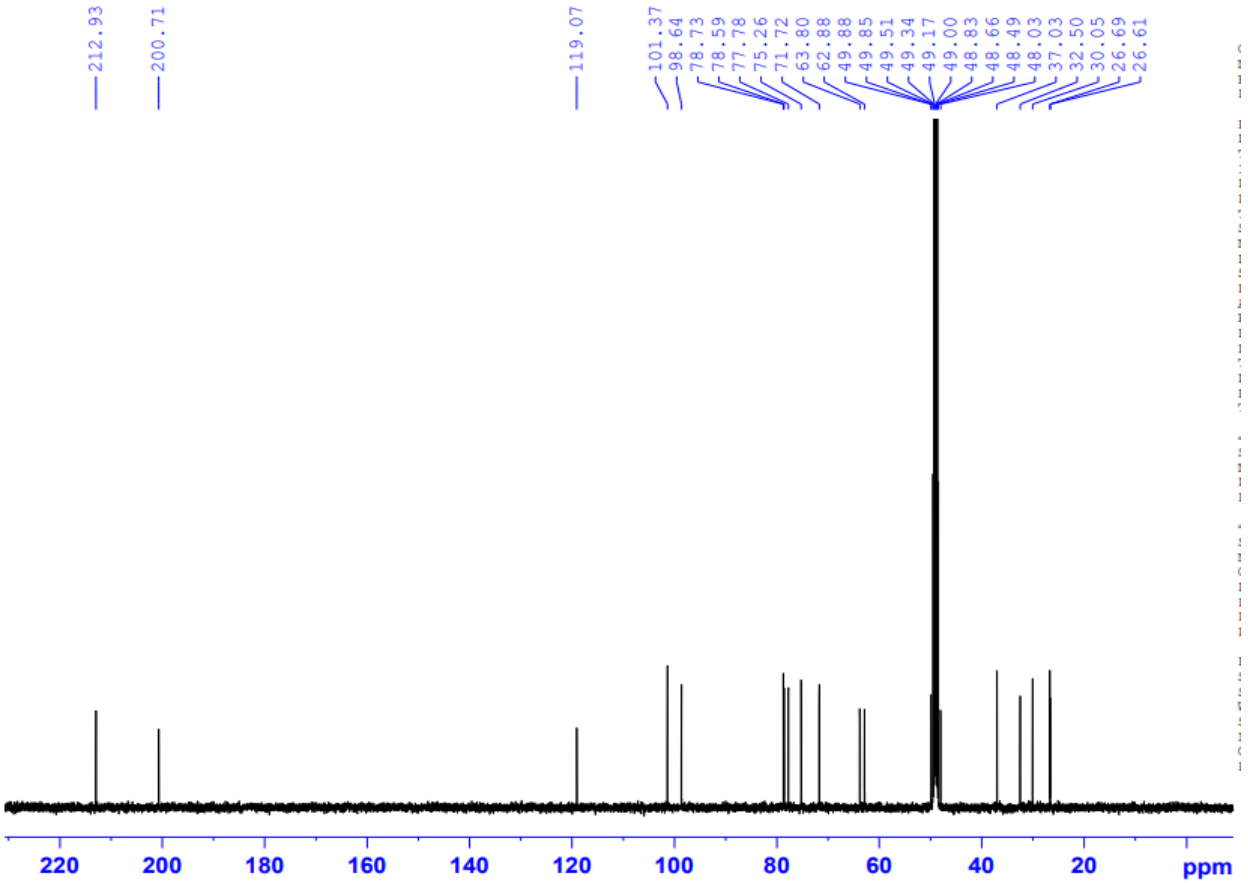

Figure S58. ^{13}C NMR spectrum of compound **12**

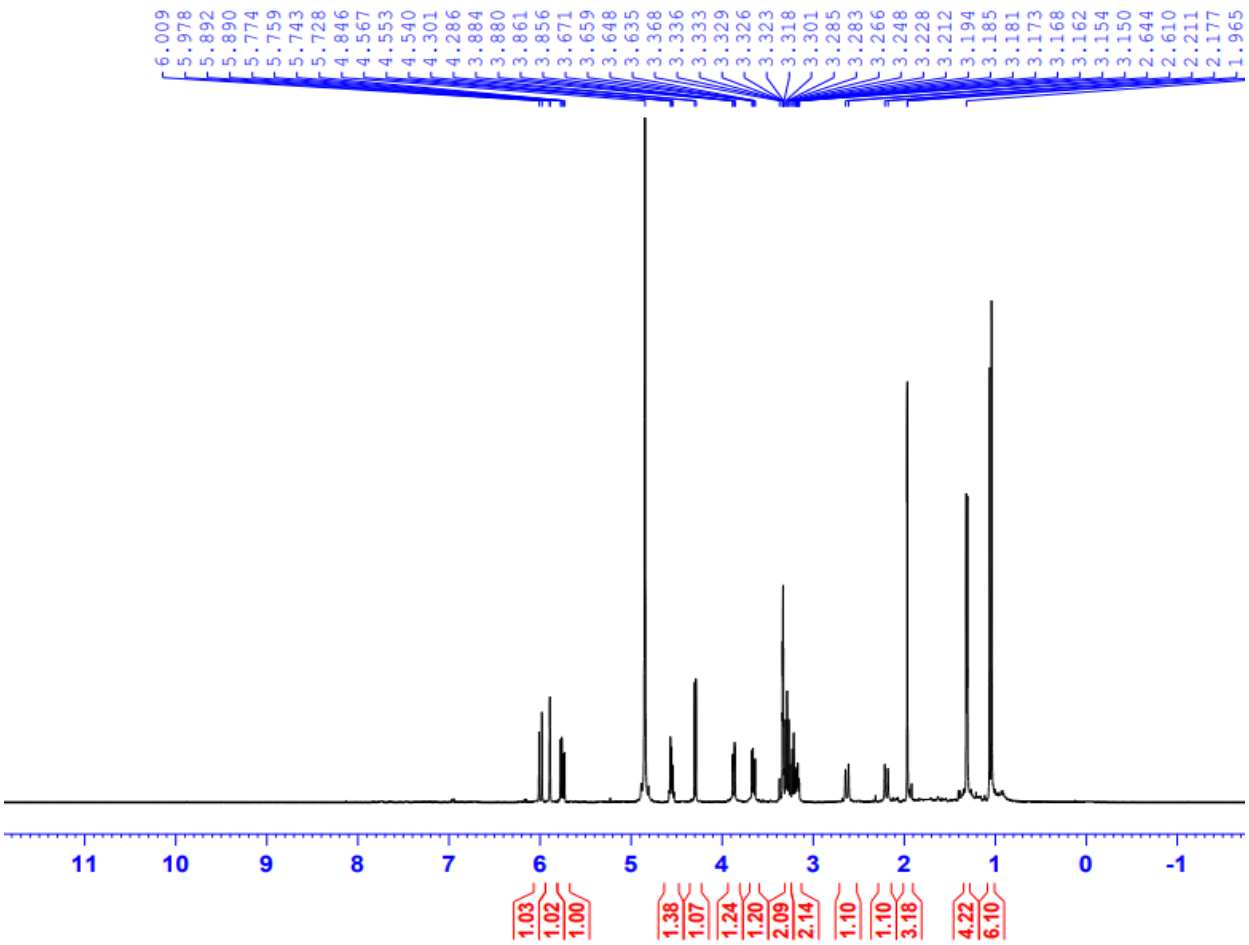

Figure S59. ^{1}H NMR spectrum of compound **13**

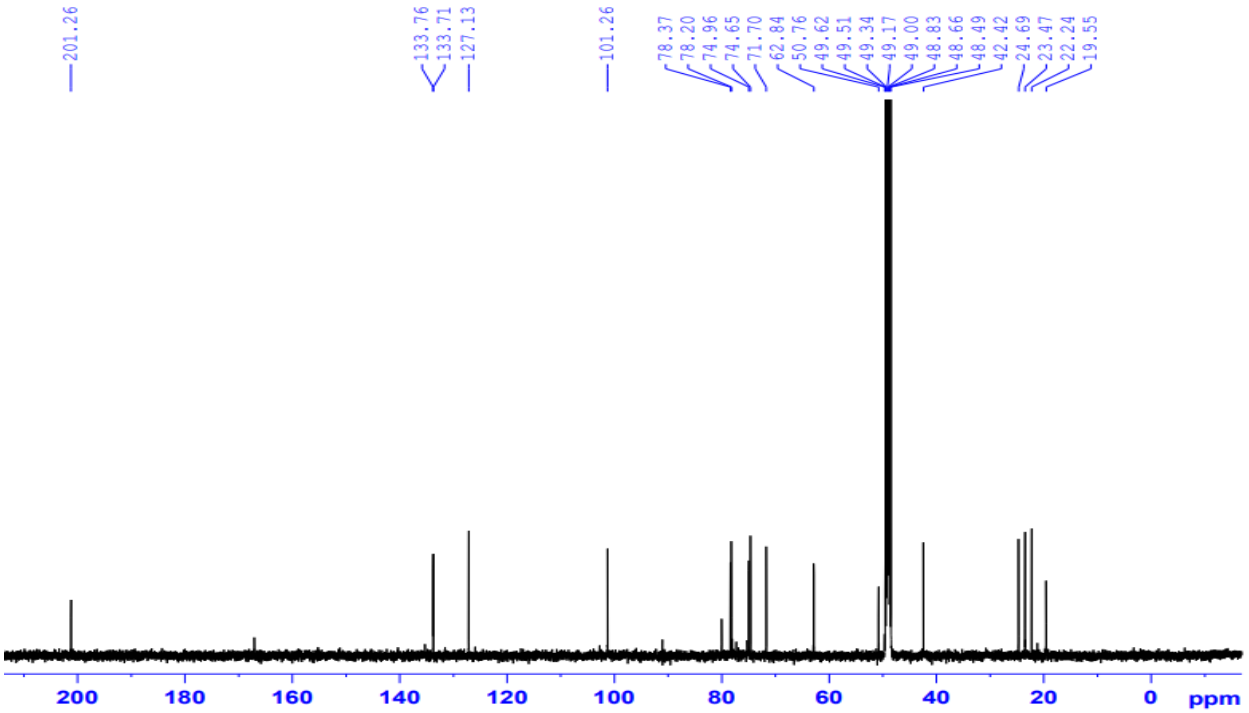

Figure S60. ^{13}C NMR spectrum of compound **13**

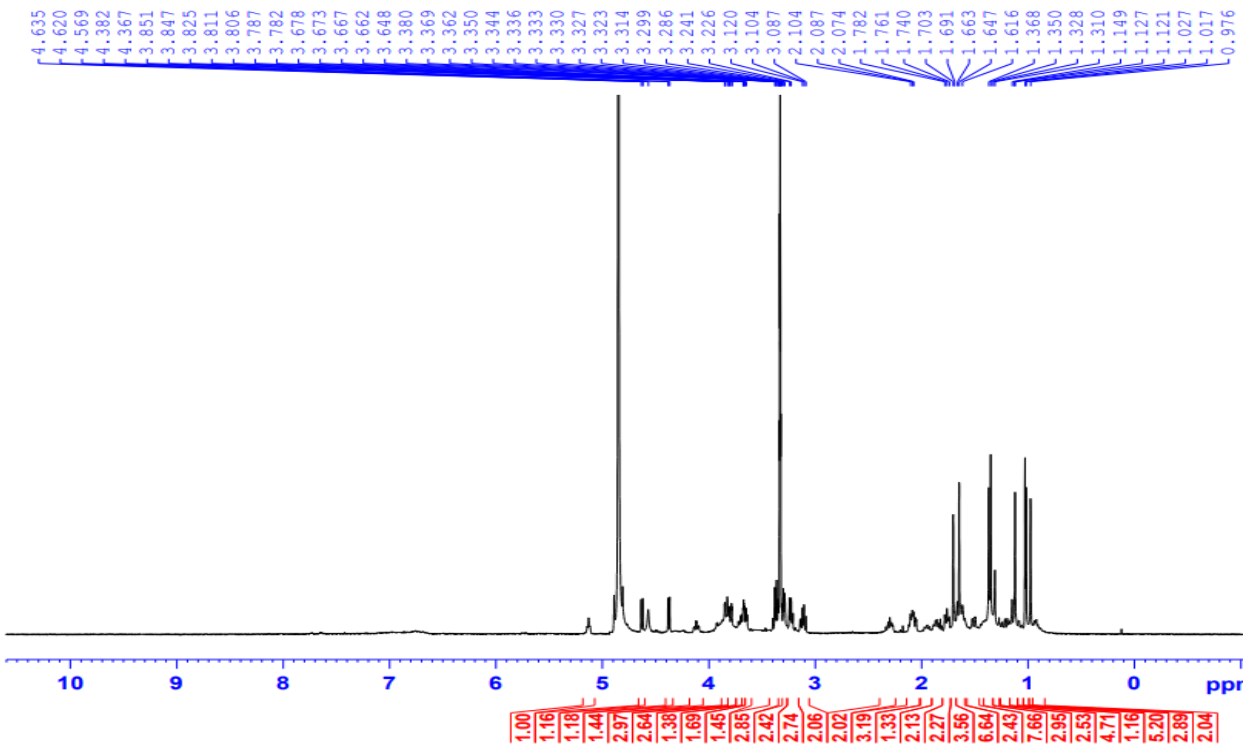

Figure S61. ^{1}H NMR spectrum of compound **14**

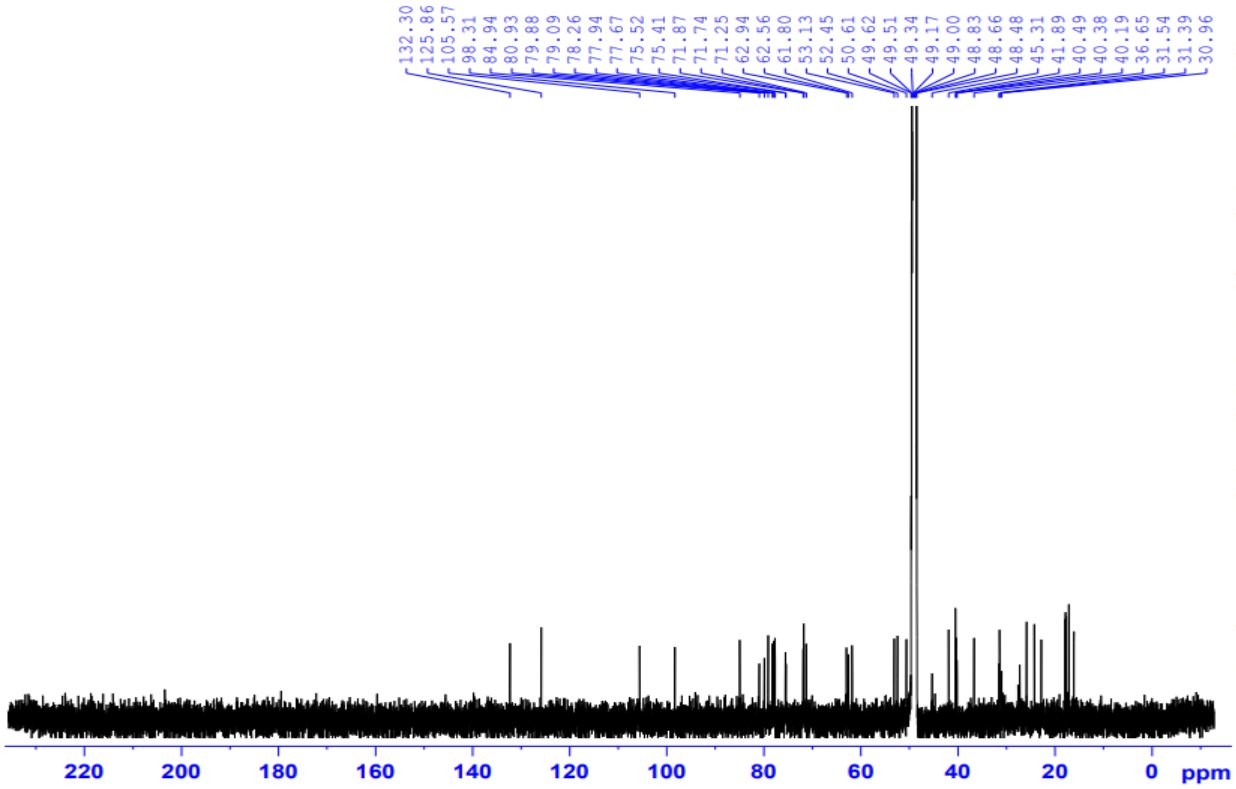

Figure S62. ^{13}C NMR spectrum of compound **14**

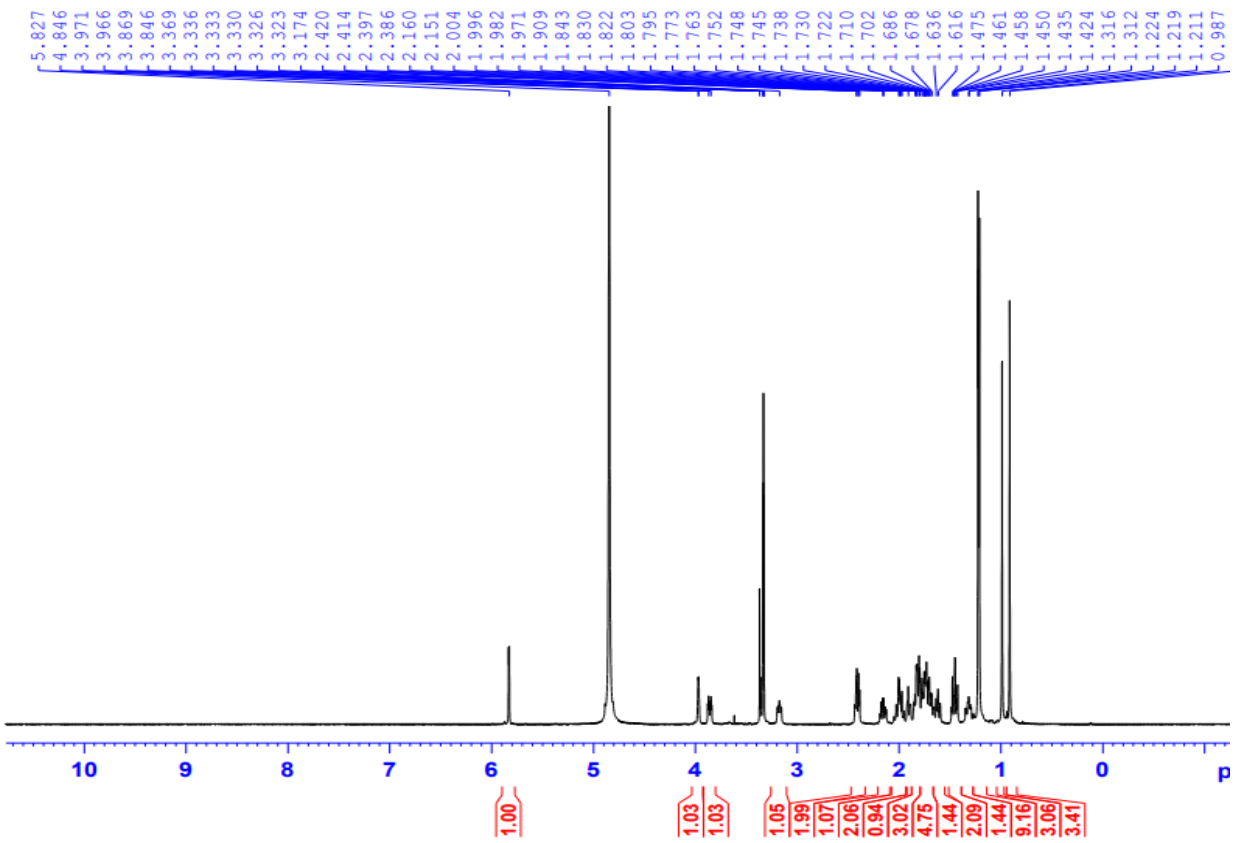

Figure S63. ^{1}H NMR spectrum of compound **15**

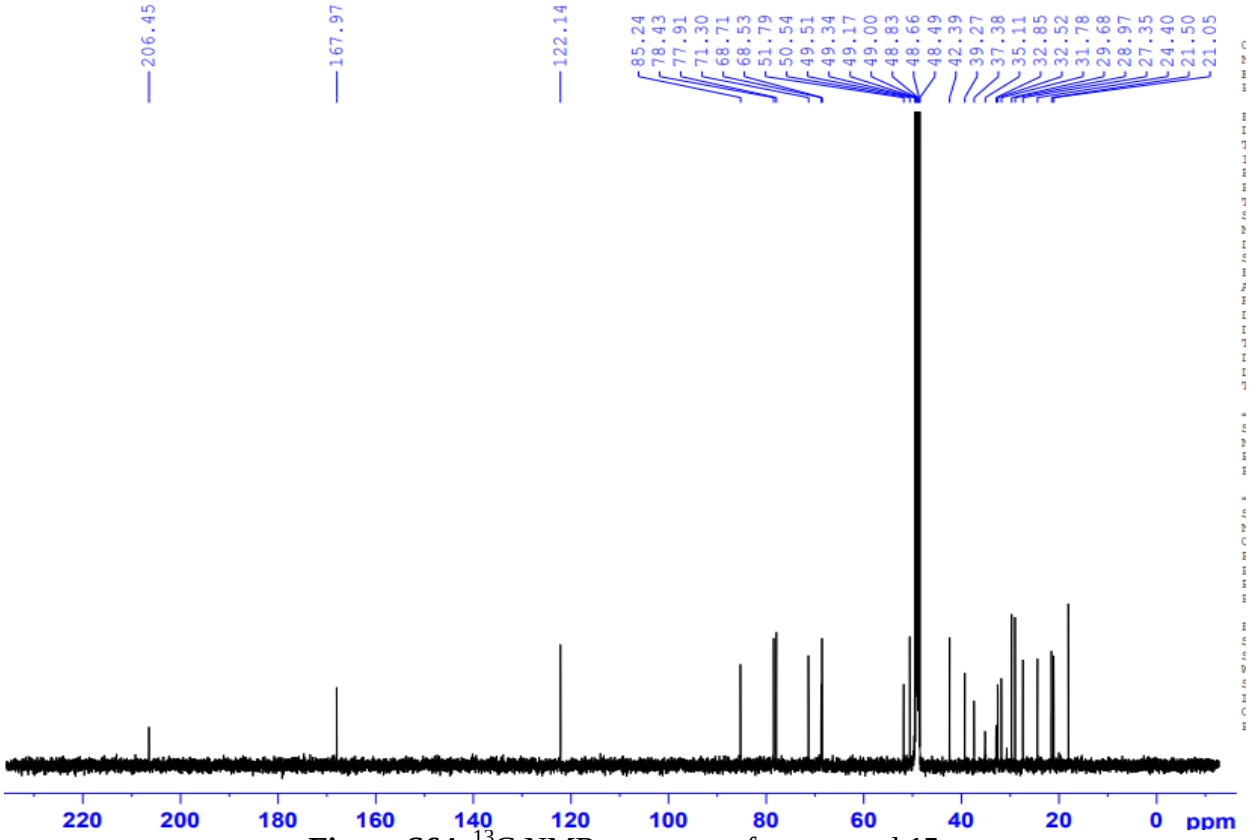

Figure S64. ^{13}C NMR spectrum of compound **15**

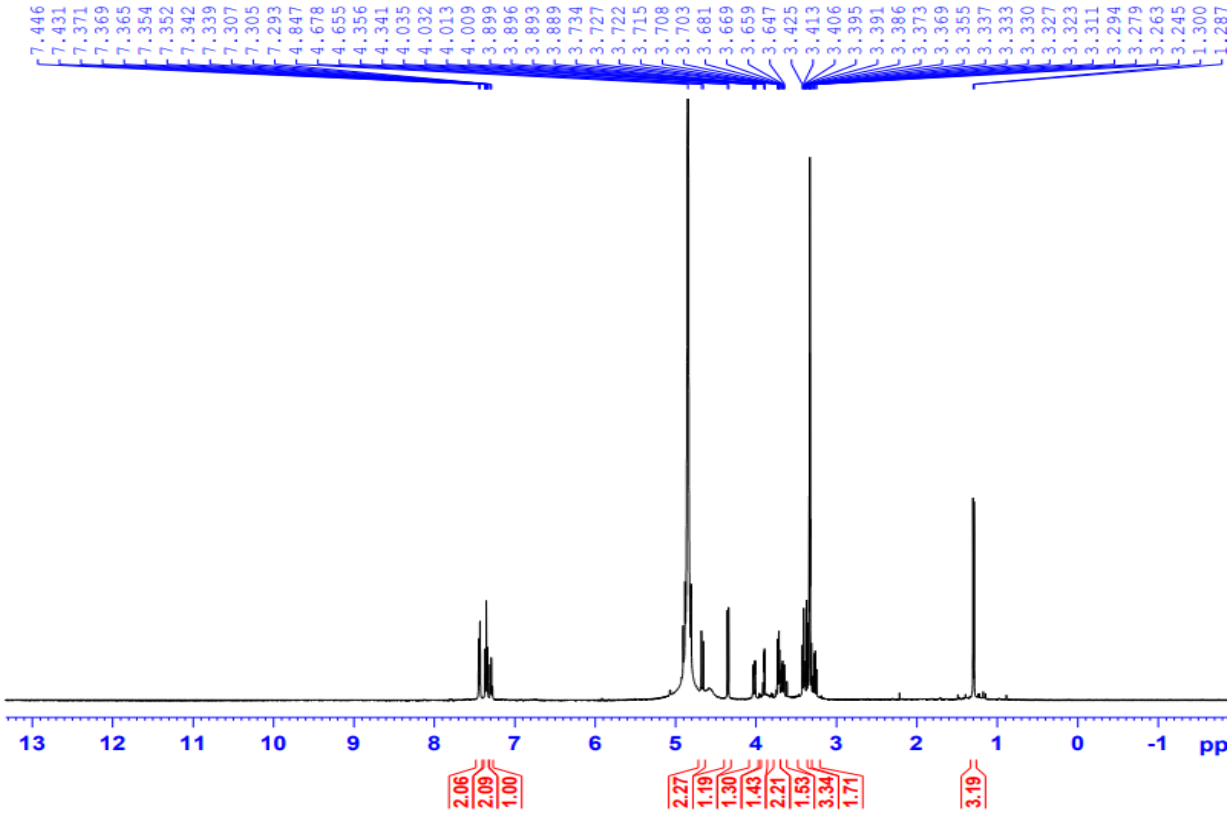

Figure S65. ^{1}H NMR spectrum of compound **16**

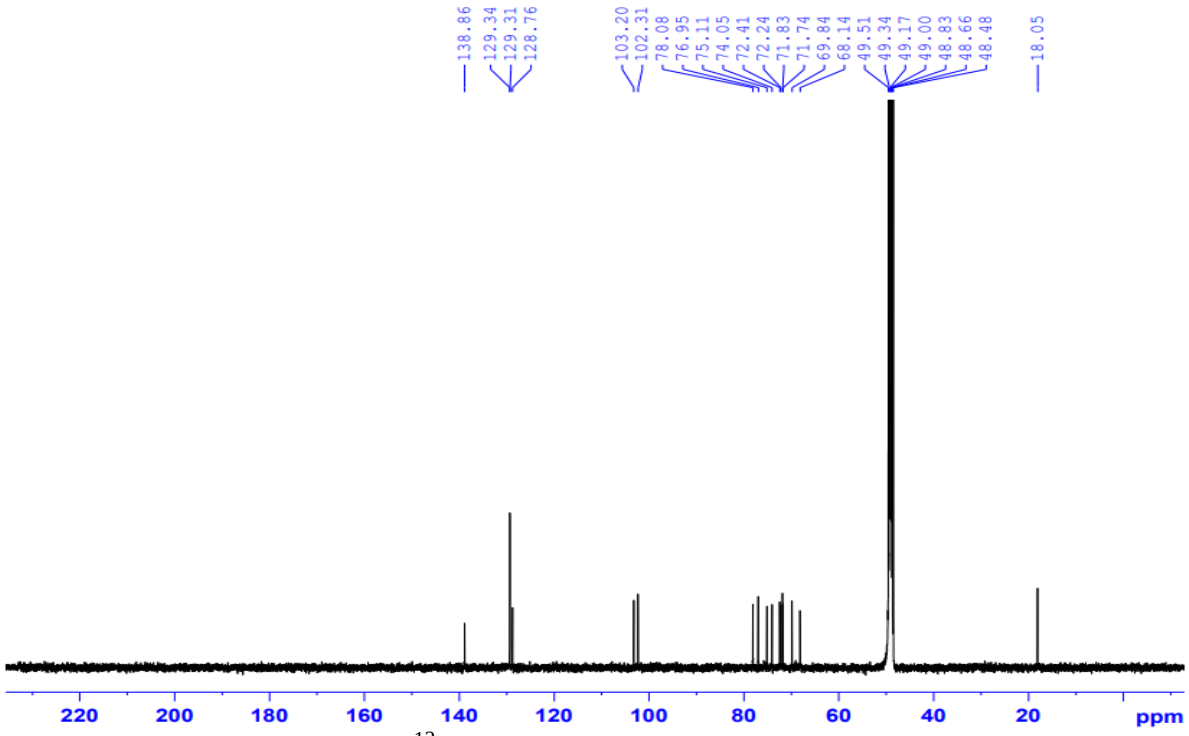

Figure S66. ^{13}C NMR spectrum of compound **16**